Fall 2011

Multiobjective simulation and optimization of an occupied university building

Héctor Jesús Uribe
University of Iowa

Recommended Citation

Uribe, Héctor Jesús. "Multiobjective simulation and optimization of an occupied university building." MS (Master of Science) thesis, University of Iowa, 2011.
https://doi.org/10.17077/etd.v37kdr1c

MULTIOBJECTIVE SIMULATION AND OPTIMIZATION OF AN OCCUPIED

UNIVERSITY BUILDING

by

Héctor Jesús Uribe

A thesis submitted in partial fulfilment of the
requirements for the Master of Science
degree in Mechanical Engineering
in the Graduate College of
The University of Iowa

December 2011

Thesis Supervisor: Professor Andrew Kusiak

Graduate College
The University of Iowa
Iowa City, Iowa

CERTIFICATE OF APPROVAL

_____

MASTER'S THESIS

_____

This is to certify that the Master's thesis of

Héctor Jesús Uribe

has been approved by the Examining Committee
for the thesis requirement for the Master of Science
degree in Mechanical Engineering at the December 2011 graduation.

Thesis Committee: _____
                    Andrew Kusiak, Thesis Supervisor

                    _____
                    Albert Ratner

                    _____
                    Pablo Carrica

                    _____
                    Pavlo A. Krokhmal

To My Parents and Family

A person who never made a mistake never tried anything new.

Albert Einstein

ACKNOWLEDGEMENTS

ABSTRACT

In the past decade, building simulation and optimization techniques have gained momentum in the modeling of energy performance due to economic and environmental pressure to make facilities more efficient. The complexity of their multivariate non-linear systems have posed challenges for modeling and performance optimization.

Building simulation tools have evolved over the years, increasing their capabilities to handle advanced approaches that integrate multiple aspects. Currently, these tools are widely accepted for building energy assessments with eQUEST being the most recognized simulation program in use. It has been validated in the public domain through its long history.

Computational Intelligence (CI) techniques have been an emerging area of study providing powerful tools for predicting and optimizing complex systems. These techniques are concerned with the discovery of structures in data and recognition of patterns. They also embrace nature-inspired paradigms such as evolutionary computation and particle swarm intelligence. The recent advances in information technology and systems have enabled collection and processing of larger volumes of data.

The contribution of the research reported in this thesis is the implementation of a hybrid model using eQUEST and particle swarm intelligence to replicate the current baseline energy performance of a fully occupied university facility and to optimize it in order to generate potential energy savings while maintaining comfortable indoor temperature. Another major contribution is demonstrating the accuracy of a hybrid energy savings model accomplished by modifying discharge air temperature and supply fan static pressure set point of the air handling unit.

TABLE OF CONTENTS

LIST OF TABLES

LIST OF FIGURES

x

CHAPTER 1

INTRODUCTION

The building industry is critical to the economy and to people's lives. Over time, buildings have changed to meet the needs of society, including changes in design, construction strategies, materials, product development and needed skill sets. The building industry, residential and commercial sectors, accounts for forty percent of the total energy consumed in the United States; which is the biggest consumer of energy in the world [23] Energy consumption by country and region is shown in Figure 1.1.
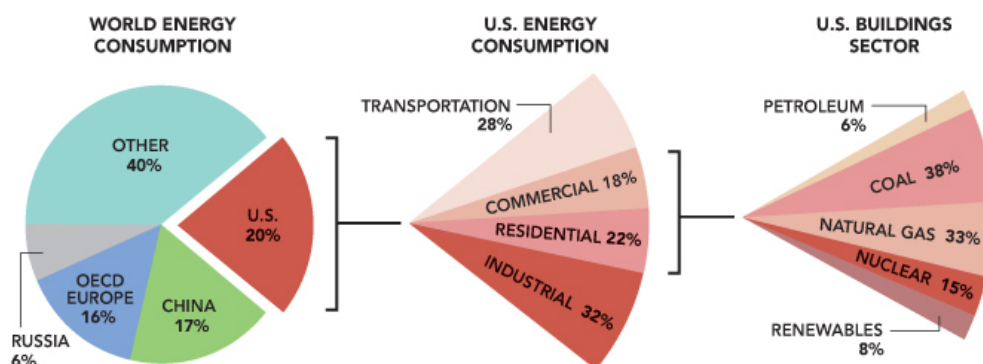
Figure 1.1 World primary energy consumption by country/region

Over the recent years, businesses, industry and government organizations have been under tremendous economic and environmental pressure to make their facilities and systems more energy efficient minimizing their negative impact on the environment. State of the art building management systems and tools, have become essential in the monitoring and optimization of energy consumption, where space heating, space cooling and lighting are the top three end uses. They represent close to half of the building energy consumption [39, 23].

Space heating and cooling belong to the heating, ventilating and air conditioning system (HVAC) that provides building thermal comfort and air quality. According to the Department of Energy (DOE), HVAC systems account for nearly one third of the total energy consumed in a building in the United States [52]. The understanding of these multidimensional and non-linear systems allows the implementation of modeling and optimization energy conservation techniques. It is important to emphasize that building thermal comfort and air quality should not be compromised in achievieng energy savings.

1.1. Literature Review

Energy consumption and indoor thermal comfort are two fundamental yet conflicting objectives of building design. Finding a facility that takes full advantage of this situation while satisfying both of these objectives has been a challenge for engineers due to the number of parameter and strategies involved. Over time, classical rule of thumb have emerged from trial and error processes in order to find optimal solutions to this problem. However, in order to significantly reduce energy consumption within a facility while maintaining comfortable indoor air temperature, more advanced techniques such as evolutionary computation are required [11]

Multiobjective optimization using genetic algorithms, neural networks and the software simulation model TRNSYS was studied by Magnier et al [45]. The research explored the optimization of thermal comfort and energy consumption in a single residence. Fong et al proposed a simulation-optimization approach using evolutionary programming and TRNSYS. They devised a reset scheme of chilled water discharge air temperatures of the HVAC in a subway station to provide cooling [42]. Zhang et al [78] proposed a physics-based supervisory control strategy to minimize the net external

energy consumption under a series of constraints. The reliability of their physics-based models was based on the basic assumptions made. Detailed simulation models often involve high computational cost and extensive memory resources due to their complexity, which makes them difficult to use in real online applications [64]

Wang et al [77] presented a simple yet accurate model for cooling coil unit and achieved improved real time control and optimization. Cumali et al [80] modeled the HVAC system as an optimization problem based on the fundamental principles of laws of energy, mass and heat tranfer. Turrin et al [54], integrated parametric modeling with other computational techniques, based on the complexity of exploring the solution space of the model. Yu et al [76] developed dynamic models for both dry and wet cooling coils using the mass balance and energy equations. Henze et al [27] modeled a building using TRNSYS and proposed a model prediction strategy to control active and passive building thermal storage inventory in real time. Zhu applied eQUEST to evaluate different energy conservation alternatives [79]. No data-driven approaches for optimization were studied as part of his research.

Unlike real-time building systems, computational simulation programs present some restrictions. The change in the information occurs in more elongated periods of time and the response of the model is not as dynamic as it is in reality for handling high frequency disturbance to the system. Nonetheless, the response of the simulation model is fast enough to reproduce, in a precise manner, the performance of the existing facility. Because of the non-linear nature of HVAC systems in buildings, data-driven techniques derived with data-mining algorithms make optimization of the process feasible without detail physical knowledge [5].

There is limited information regarding hybrid models for energy optimization in the literature. Simulation tools such as TRNSYS [56], HVACSIM+ [20] and SIMBAD [18] have been explored. No models involving eQUEST and particle swarm optimization for a fully occupied facility were found in the literature reviewed.

1.2. Simulation and Optimization of HVAC Systems

Computational intelligence provides a powerful tool for HVAC systems optimization creating and adaptive mechanism that enables and facilitates intelligent decision-making actions. Some of these powerful tools include neural networks [26, 53], evolutionary computation [37, 17], swarm intelligence [38], fuzzy system [43] genetic algorithms [61] among others [10]. In recent years many researchers have focused their attention in HVAC modeling, control and optimization [1].

The prediction of heating, ventilating and air-conditioning loads has been crucial in the implementation of data-driven approaches, especially for loads occurring during peak hours [49]. The use of accurate predictive models derived from data-mining algorithms usings historical building data information has been demonstrated to be and economical possibility to minize energy consumption while maintaining corresponding indoor thermal comfort [4].

With the growth in computer capabilities and processing power, computer-based simulation has gained more acceptance as a tool for evaluating building energy use [40, 51]. There are many different types of building simulation tools available for performing energy analysis. However, eQUEST has been proven to be the most widely used and respected building energy analysis program in use today [62]. Since its release in the late 1970's as DOE-2, eQUEST has been widely reviewed and validated in the public domain

[73]. This simulation engine expands and extends DOE-2's capabilities in several important ways, including: interactive operation, dynamic/intelligent defaults, and improvements to numerous long-standing shortcomings of DOE-2 older versions (which limited its use by mainstream designers and building professionals [74]).

Applying multi-objective optimization of HVAC systems and simulation techniques, will allow to meet the goals of this approach and at the same time will avoid the logistical issues of dealing with building managers and tenants for verification. The optimization impact on a building energy consumption and indoor thermal comfort will be known before any implementation is undertaken.
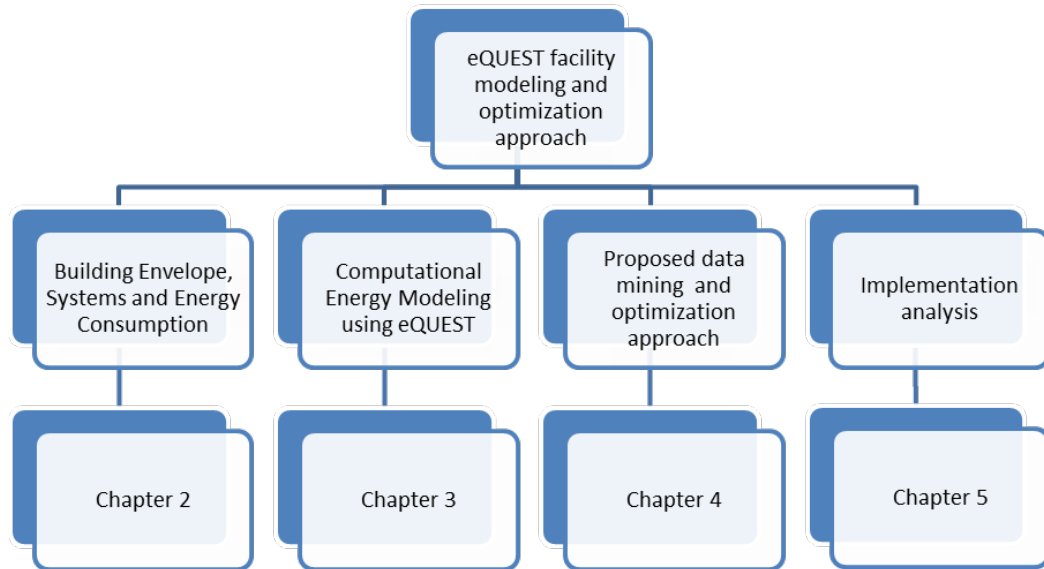
Figure 1.2 Thesis structure

The structure of the thesis is presented in figure 1.2. In Chapter 2 a detailed explanation of the systems enclosed in a fully functional occupied facility is introduced. The size of the building, acitivities performed and hours of operation are presented to better understand its annual energy consumption. An energy assessment is done using a

seven-year average utility bill and compared to facilities with the same characteristics in the Midwest using the Commercial Building Energy Consumption Survey (CBECS). The energy consumption is analysied more in detail by separating it up into its three main contributors – electricity, steam and chilled water – to assess energy trends. Variations and fluctuations in the utiliy bill are analyzed and explained. This research is focused on energy savings for the summer season as well as its impact in the annual utility bill.

Chapter 3 discusses the use of energy simulation tools and their importance in energy conservation strategies. Selection of eQUEST and pre-work to create floor plans using AutoCAD are presented. Simulation results are obtained and compared versus actual seven-year average utility data. The accuracy of the simulation model is established. Results of the energy model include an overall summary of the total systems energy consumption. A further division of energy associated to the HVAC sytem is performed.

Chapter 4 presents the proposed data-mining and optimization approach applied to the existing HVAC system. A predictive model of energy consumption and room temperature are generated using a dynamic neural network (DNN) algorithm. The accuracy of the model is established. The model is optimized using particle swarm optimization (PSO). Optimized set points for the HVAC system discharge air temperature and supply air static pressure are obtained. Energy savings from the optimization model are obtained for the summer season.

Chapter 5 implements optimized set points from the PSO algorithm, Chapter 4, into the simulation model, Chapter 3, during the summer season. An energy assessment of the results obtained is performed. A group of zones are selected from each floor to

verify indoor zone temperatures before and after optimization and compared versus actual values from the Johnson Controls Metasys building automation system.

Chapter 6 summarizes concepts and results presented in this document and provides future research opportunities.

CHAPTER 2

BUILDING ENVELOPE, SYSTEMS AND ENERGY CONSUMPTION

2.1. Introduction

The Blank Honors Center (BHC), named for one of the families that made its construction possible, houses the Honors Program and the Belin-Blank International Center for Gifted Education and Talent Development at the University of Iowa. Together they make the BHC into the world's only building exclusively for talented-and-gifted student's education in every step of the way from pre-kindergarten through college [70]. The BHC is a classroom and office facility, built in 2003, and is approximately 61,793 square foot. It is located east of the Iowa River on the corner of Bloomington Street and the Cleary Walkway in Iowa City, Iowa, as shown in figure 2.1.
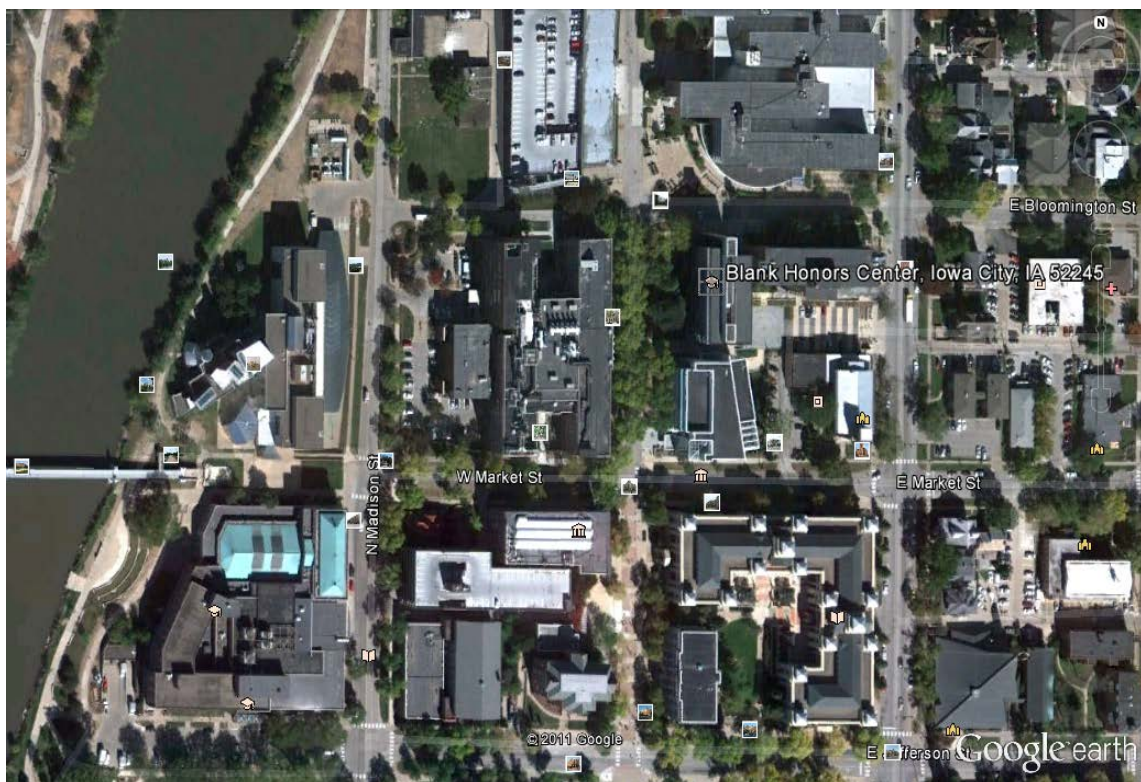
Figure 2.1 Map Location

This multifunctional building also contains six general assignment classrooms to serve the campus, as well as an atrium on the first and second floors. The programs are segregated vertically throughout the facility with public spaces. The fourth floor features the Honors Staff Center, which includes administrative offices, a comfortable reception area, a small Honors Conference Room, a larger Honors Activity Center, a distance-learning classroom, a workroom, and a staff lunchroom for the building. The fifth and sixth floors highlight the Belin-Blank Center administrative offices, reception area and workrooms.

The third floor transitions between public and program-dedicated floors, and serves the students of the two programs. This level is linked by a skywalk to the Kate Daum Residence Hall, which is the honors house where the honors students live in. This floor features three sizable areas for relaxation, conversation, and individual study plus an open-air sun porch. It includes a news-and-information center, a small kitchen complete with vending machines and free food, a game-and-television room, the Commons for large meetings, a handful of small-group study rooms, a research library, and an instructional technology center known as computer laboratory.

Most of the offices are located to the west, and the larger classrooms and open-offices to the east. Honors most often has the building humming throughout the workweek during the school year, whereas the Belin-Blank Center has the building's many chambers especially busy for weekends and summers.

Floors from first to third have occupancy during their peak hours of about 150 to 170 students, where forth to sixth floors are about fifty people including staff, students and visitors [68].

<u>2.2. Building Envelope</u>

The BHC consists of eight stories, where the lower level is below grade and the remaining floors from first through the penthouse are above grade. A longitudinal west view of the different floors is shown in figure 2.2.
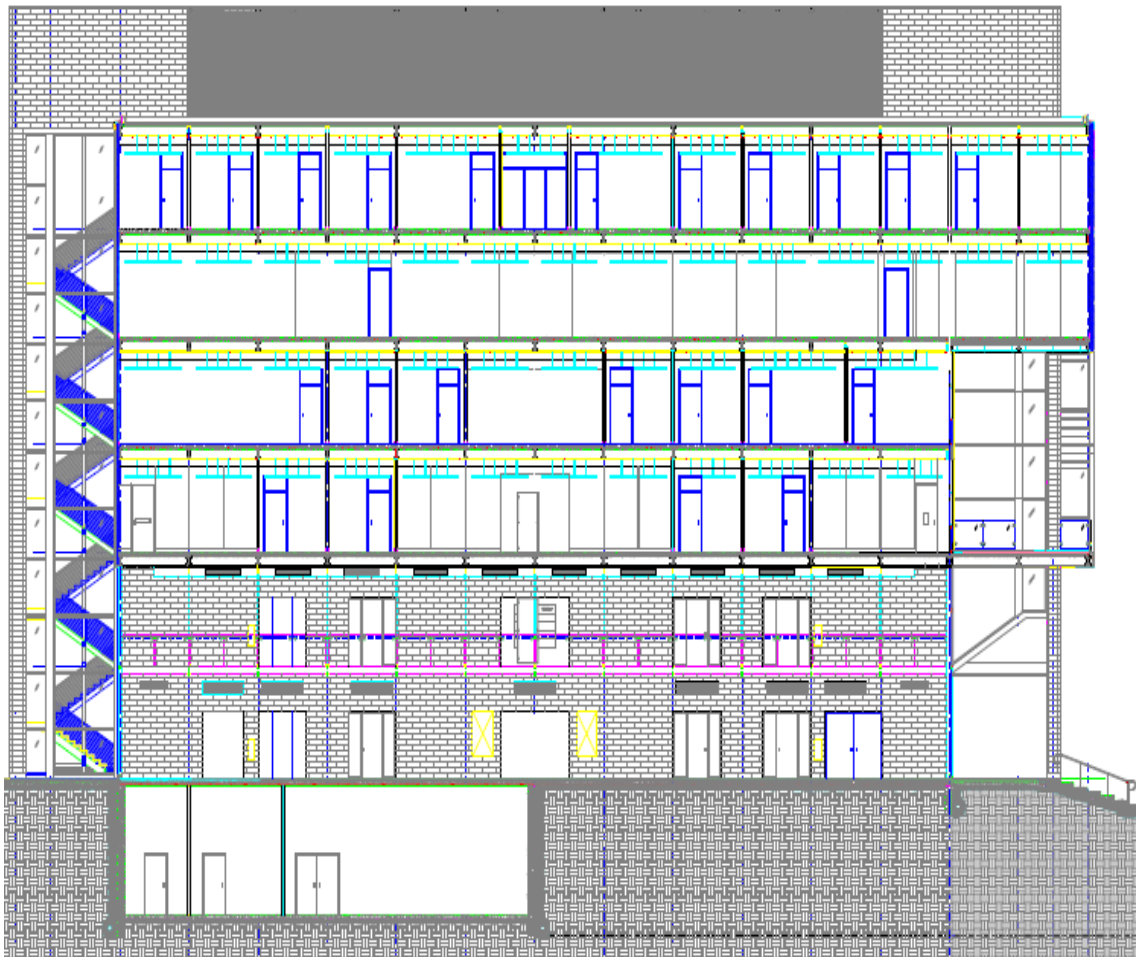
Figure 2.2 West longitudinal view

2.2.1. Envelope Constitution and Characteristics

The lower level provides functional spaces for uses such as storage, mail, maintenance office space, steam/chilled water tunnels and mechanical/electrical areas. It is comprised of two main elements:

1) Foundation walls – a 12 inch cast in place concrete walls with a 2 inch rigid foundation insulation termite barrier board and a waterproof coat to prevent from mold growth.

2) Floor slab – a 5 inch concrete slab on minimum 6 inch porous fill with drain lines.

These elements provide support and accommodate all the structural forms of loading imposed by the interior and exterior environments. The lower level is part of the buildings superstructure [11].

The envelope above grade is constituted as follows on its different faces:

West – consists of a glazed thermal break aluminium curtain wall, which provides natural light throughout the floors within the building. It is designed to resist air and water infiltration, sway induced by wind and seismic forces acting on the building and its own dead load weight forces. There is a double-skin glazing system from third to sixth floor that provides higher protection from the wind as well as reduces solar heat gain from solar rays [68].

North – composed of different types of finishes throughout the different levels to provide structural support, as well as aesthetics to the building. These materials are insulated glass panels, cast masonry unit, 12 inch and 8 inch cast-in-place architectural concrete walls and aluminium wall panels [68].

South – composed of two main types of finishes throughout the different levels. These materials are insulated glass panels and 12 inch and 8 inch cast-in-place

architectural concrete. Adjacent to BHC is Pomerantz Center (PC) which provides shading and protects that side from severe environmental conditions [68].

Roof – consists of a membrane with a minimum of 60 mil thick ethylene propylene diene Monomer (EPDM) non-reinforced sheet. It uses pre-manufactured seam with a minimum width of 5.5 inches. The insulation coefficient of thermal conductance is an R-20 rigid polyisocyanurate with special facers designed for EPDM adhesion. The insulation is attached with mechanical fasteners with caps that lock into screws over metal [69]. Figure 2.3 presents a view of the northwest side of the building.

Figure 2.3 Envelope - Northwest view

East - consists of a glazed thermal break aluminium curtain wall, 12 inch and 8 inch cast-in-place architectural concrete walls and aluminium wall panels. It is also designed with overhangs to protect from the sun rays and to keep comfortable temperatures inside the spaces as shown in figure 2.4. This level is linked by a skywalk to the Kate Daum Residence Hall, to allow access to the students of the honors program to BHC [68].

Figure 2.4 Envelope - East view

2.2.2 Building Infiltration and Fenestration Systems

The original design of the building envelope complies with ASHRAE 90.1 (American Society of Heating, Refrigeration and Air-Conditioning Engineers) Standards

and it is assumed to be airtight having air leakage values per unit area of 0.10 cfm/ft^2 [17]. However, through the years the envelope has been adjusting to different factors, such as extreme weather conditions, earth movements, external vibrations, etc. and its tightness has been modified from the original design.

The most suitable areas for air infiltration are throughout fenestration systems, affecting occupant comfort and energy consumption. These systems are usually replaced or maintained until they completely fail or when their low performance is evident to the tenants. Instantaneous energy performance indices (U-factor, solar heat gain coefficient, air leakage, etc.) are typically used to compare fenestration systems under a fixed set of conditions. However, the absolute and relative effect of these indices on the building's heating and cooling load can fluctuate as environmental conditions change. As a result, these indices alone are not good indicators of the annual energy performance attributable to the fenestration. Furthermore, such energy performance is difficult to quantify in and of itself because of numerous dynamic responses between the fenestration system and the total environment in which it has been installed [19]. Infiltration should not be confused with ventilation.

2.3. Lighting Systems

Lighting quality can have a dramatic influence on the attitude and performance of the occupants. In fact, different "moods" can be created by a lighting system. Although occupant behaviour is linked to interior design and other factors, lighting quality represents a significant influence. Occupants perceive and react to a space's light color. It is important that the lighting designer be able to recognize and create the subtle aspects of an environment that defines the theme of the space. Occupants can be influenced to work

more effectively if they are in an environment that promotes a "work-life" atmosphere [32]. The goal of the lighting design is to provide the appropriate quality of light for a particular task to create the right environment. Occupants' comfort and performance are worth more than energy savings. Figure 2.5 depicts illumination design on the first and second floors atrium.

Figure 2.5 Interior lighting design

BHC's lighting functions at 277V, where the ballasts are electronic instant start for a three lamp T8 32W fluorescent fixtures. This type of lamp produces an initial 2950

lumens and is predominant through the building. It also has a lumen depreciation of 5%, which accounts for the lamps not been replaced at 24,000 to 30,000 hours of operation. The following lighting criteria have been established by the Illuminating Engineering Society (IES) and the University's historical data. See Table 2.1

Table 2.1 Recommended lighting levels

Functional Area	Light Level (FC)	Functional Area	Light Level (FC)
Auditorium	30	Gymnasium General	30
Classrooms	45	Exhibitions/Matches	50
Standard	50	Library Reading Area	50
High Task – Drafting	70	Stacks	30
Science Labs	50-70	Check in/out	75
Home Economics	50-70	Lecture Halls	30
Industrial Arts	50-70	Offices Private	50
Locker Rooms	15	Open w/task lighting	35
Lounges	15	Computer Work	30
Cafeteria Eating Area	15	Rest Rooms	15
Food Preparation	75	Elevators	20
Computer Rooms	35	Hallways	15
Conference Rooms	35	Lobbies	15

However, based on the original design most of the areas at BHC are over lit being approximately 30% beyond the standard [15]. All offices on the west wall have wall occupancy sensor switches. Photocells are utilized in the atrium of the first and second floors for atrium lighting. The building utilizes Johnson Controls Metasys building automation system (BAS) for all corridor lighting schedules. Emergency/Egress lighting is on 24/7.

2.4. HVAC System

The BHC is served by the central heating steam power plant and cooling chilled water plants for campus as shown in figure 2.6.
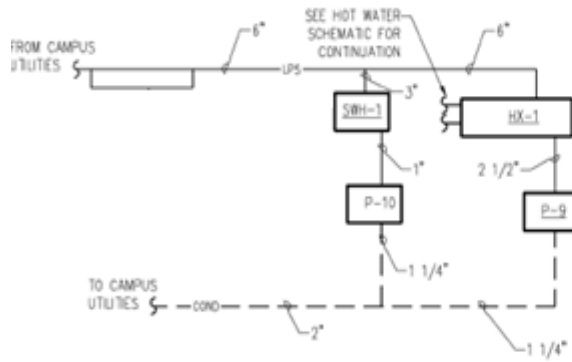
Steam Schematic
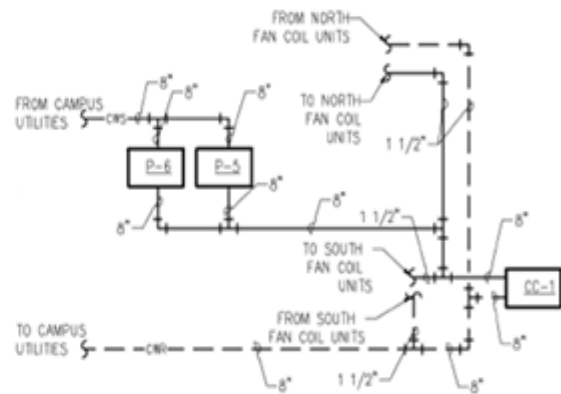
Chilled Water Schematic

Figure 2.6 Steam and chilled water schematic

Low pressure steam enters the building from steam tunnels and is converted to hot water inside the building using a heat exchanger unit. The converted hot water is then pumped by a pair of 7.5 HP pumps that are controlled via variable frequency drives (VFD) based on differential hot water pressure. Hot water is provided all year round. From the same steam line domestic hot water is supplied in to the hot water loop which supplies potable heated water to kitchens, bathrooms, showers, etc. A single 1 HP pump, with 70 ft. of head and 15 gpm flow recirculates the water inside the loop.

The chilled water is pumped through the building by a pair of 10 HP pumps that are controlled via VFD's based on differential chilled water pressure. Both sets of pumps are lead/lag. The control valves in the building are 2-way.

Heating ventilation and air conditioning is distributed throughout the facility by a single central station air handling unit (AHU). This unit is variable air volume and is supplied with outside-return mixed air, air filters, a preheating coil to protect the chilled water coil from freezing, a reheat coil for humidity control, a variable flow supply air and return fan to stabilize the negative pressure in the mixing box. Figure 2.7 presents a schematic of the building's HVAC system.
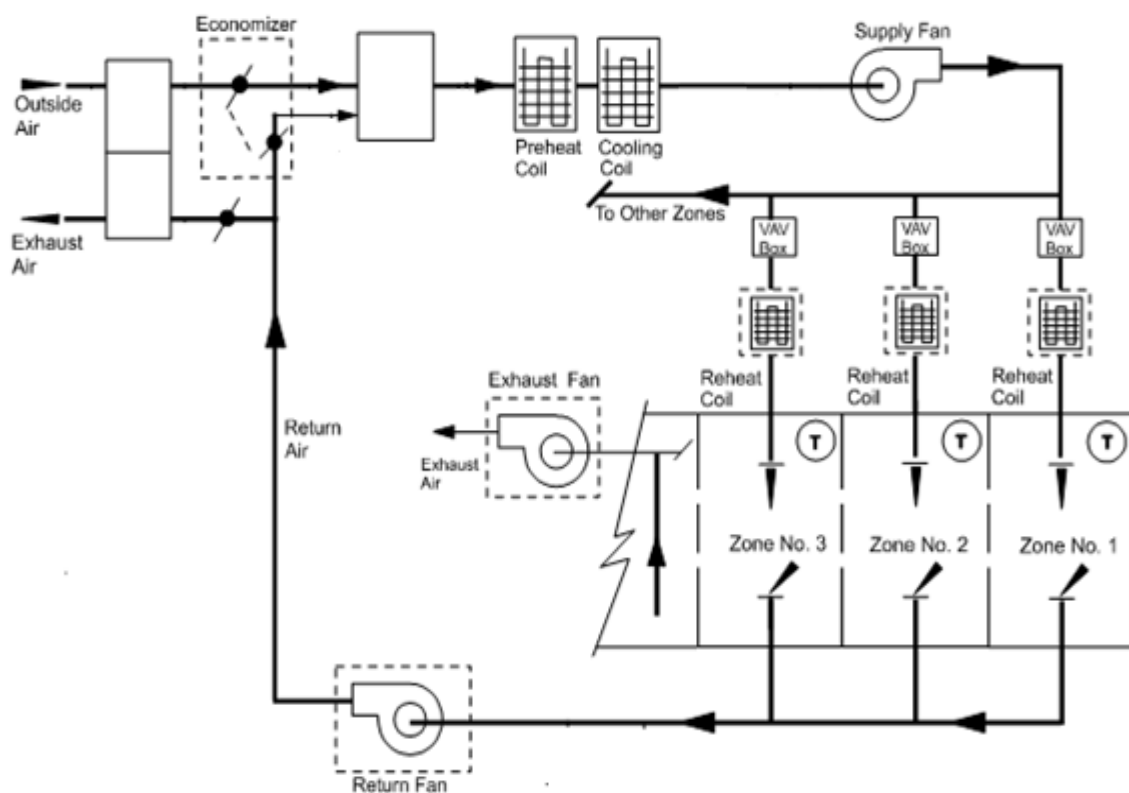
Figure 2.7 BHC schematic HVAC systems

The AHU total airflow capacity is 57,250 cfm and minimum outside airflow of 16,000 cfm. It is located in the basement with a network of variable air volume (VAV) boxes with reheat coils located throughout the building. The AHU fans are on variable

speed drive based on duct static pressure, which is supplied at a fan total system pressure of 4.95 in. of water.

The unit is cooling only discharging constant air temperature at 55 °F, ensuring that moisture removal leaving the cooling coil meets design specifications. This unit has full airside economizer and when operating in cold weather, a small rise in discharge air temperature sensed by the supply air controllers, will force the economizer to modulate open. On a further rise the cooling coil modulates to full open and the economizer closes once outdoor conditions are unfavorable. The economizer type is a dry bulb and the setpoint 68 °F outside temperature. The preheating coil operates independently of the supply air controller to prevent freeze-up of the cooling coil. The AHU preheating coil holds the supply temperature if the air leaving the cooling coils is colder than desired due to a maximum humidity requirement. The HVAC system is scheduled occupied/unoccupied by zone according to function as shown in table 2.2.

Table 2.2 Occupancy schedules by space type

Primary Occupancy 8am-6pm

Space Type	Building Schedule		HVAC Schedule		Lighting Hours of Operation
	Open	Closed	On	Off	
Classroom	8:00 AM	6:00 PM	6:00 AM	12:00 PM	9
Corridor	6:00 AM	12:00 PM	6:00 AM	12:00 PM	16
Library/Study	6:00 AM	12:00 PM	6:00 AM	12:00 PM	16
Storage	8:00 AM	6:00 PM	6:00 AM	12:00 PM	16
Bathroom	6:00 AM	12:00 PM	6:00 AM	12:00 PM	16

Primary Occupancy 8am-6pm

Space Type	Building Schedule		HVAC Schedule		Lighting Hours of Operation
	Open	Closed	On	Off	
Private Offices	8:00 AM	6:00 PM	6:00 AM	12:00 PM	9
Open Offices	8:00 AM	6:00 PM	6:00 AM	12:00 PM	16
Conference/Meeting	8:00 AM	6:00 PM	6:00 AM	12:00 PM	9

At the zone level each zone is controlled by variable air volume boxes with reheat coil. As the zone temperature drops below the cooling setpoint, the VAV dampers modulate closed until they are at their minimum flow ratio. As the zone temperature approaches the heating setpoint, the reheat coil begins to modulate open to prevent the zone temperature from dropping any further.

<p style="text-align:center">2.5. Building Automation System</p>

Control systems are an integral part of many energy related processes. Control systems can be as simple as a single thermostat, to very complex computer controlled systems for multiple buildings, to industrial processes control.

BHC is connected to a Johnson Controls Metasys building automation system controls that regulates the HVAC and hydronic equipment throughout the facility. The system is fully direct digital control (DDC), web based and connected to the central University of Iowa energy management system.

This control strategy uses microprocessors to provide control. A big advantage to DDC system is the fact that changes are often made with software and do not automatically require physical changes and cost like other technologies [36].

The Metasys building management system ensures comfort controls; lighting, fire safety and equipment operate together in harmony. Multiple smaller controllers are communicated upstream to a supervisory operator workstation and a single failure point will just affect a much smaller area increasing the overall process reliability. A schematic of the building automation system is presented in figure 2.8.
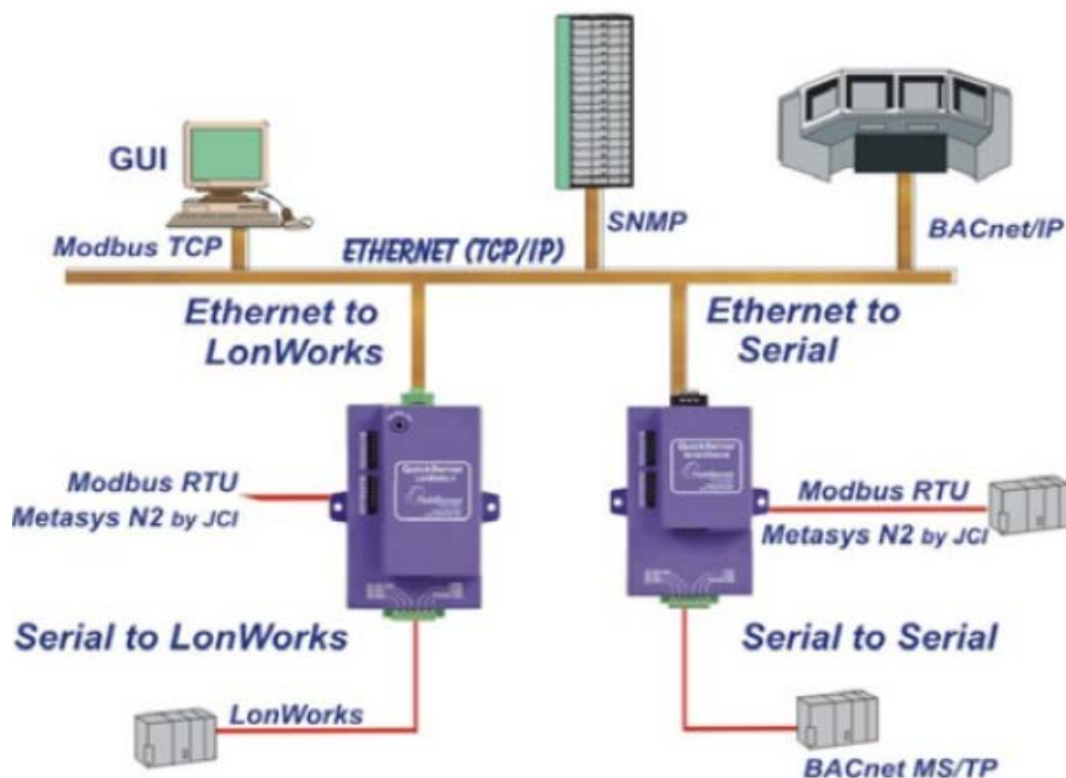
Figure 2.8 Schematic of the building automation system communications

2.6. Energy trends

The utility consumption data from fiscal year 2005 to fiscal year 2011 is provided from the University of Iowa Utilities and Energy Management [50]. The overall use (in kbtu/sf) for 2011 was 136, which is 43% higher than a Midwest average building with the same characteristics. In 2003, the United States Energy Information Administration conducted a Commercial Building Energy Consumption Survey (CBECS). This provides basic information about energy consumption and energy related characteristics of buildings throughout the United States.

According to the CBECS data, the average energy use for a building of greater than 50,000 square foot in the Midwest is approximately 95 kbtu/sf [71]. In figure 2.9 is

shown that the energy consumption had a big increase during fiscal year 2006 and 2007 and in 2008 dropped drastically to remain consistent to the present year.
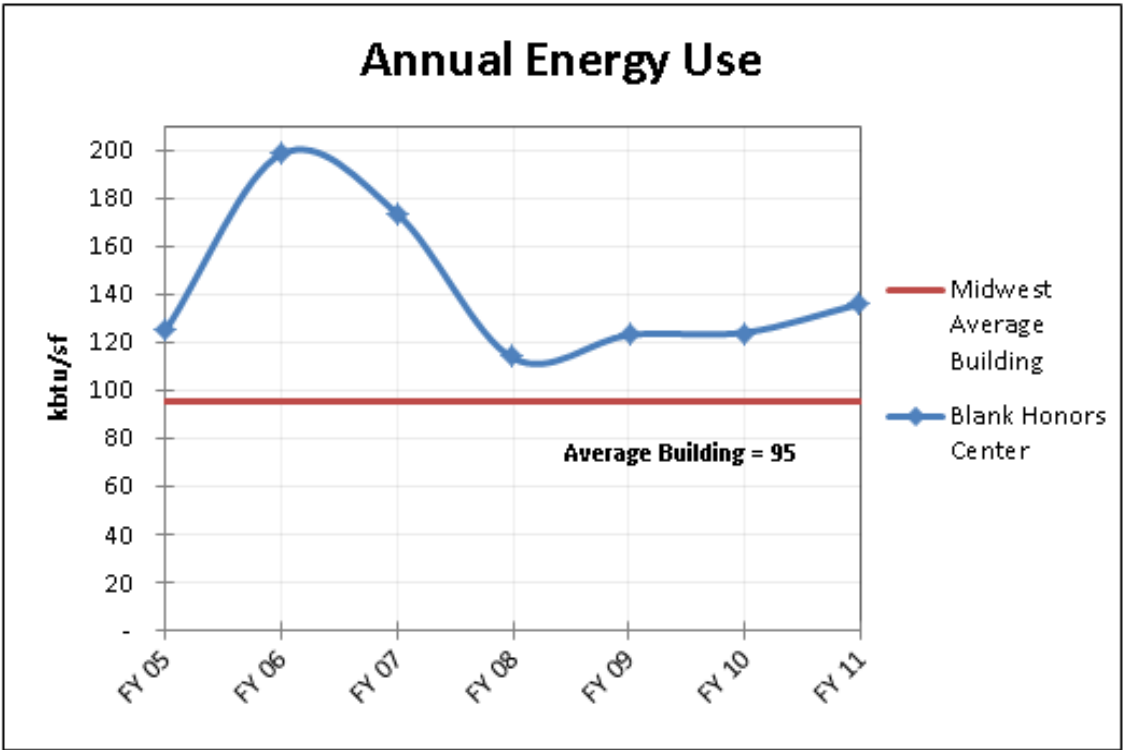
Figure 2.9 Annual energy use

While the energy consumption of BHC has remained relatively constant, energy costs have increased considerably over the last several years. In 2011, the total utility cost at BHC was nearly $171,000 ($2.76/sf). Figure 2.10 shows a clear upward trend of about 52% since fiscal year 2005.
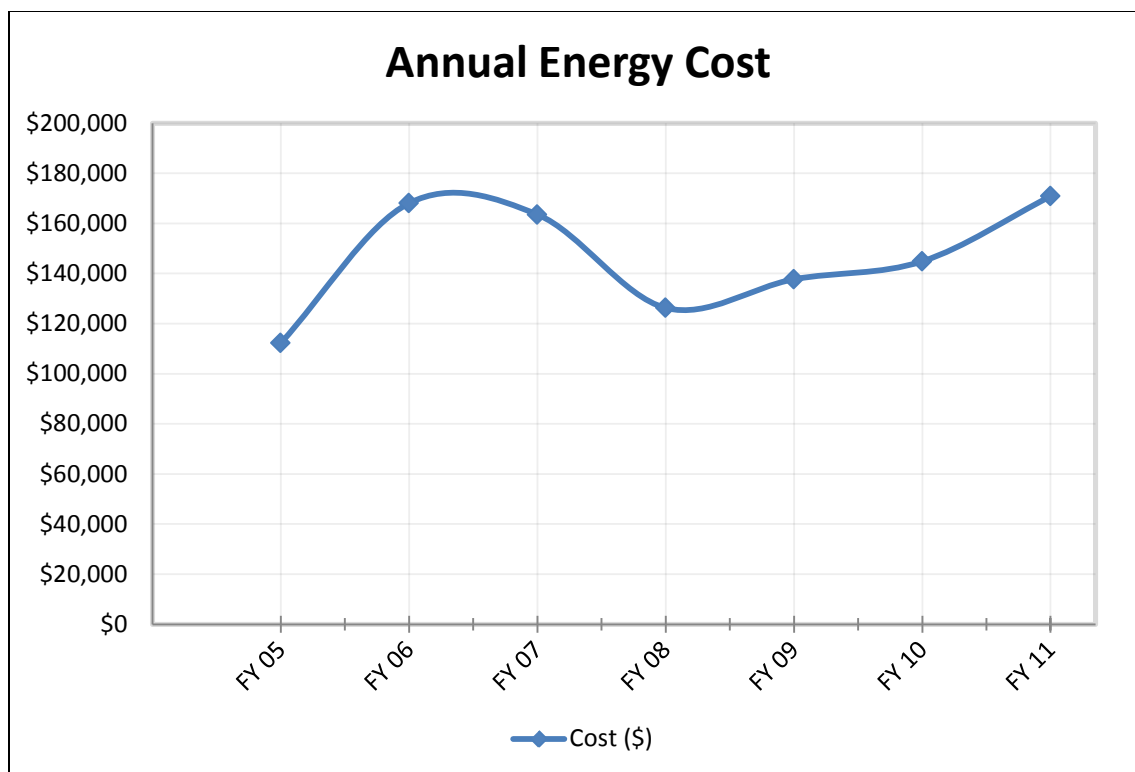
Figure 2.10 Annual energy cost

The annual utility consumption and cost are divided into electrical, steam and chilled water usage as presented in figures 2.11, 2.12 and 2.13 [50]. The chilled water use has been leveled from fiscal year 2005 until fiscal year 2007, when it began a sharp decrease that extended to the most recent data. Over this time period the unit cost of chilled water has increased substantially.

This big increment in cost has resulted in a 130% increase in annual chilled water cost from fiscal year 2005 to fiscal year 2011. In, 2005 chilled water cost accounted for approximately 33% of the BHC's annual utility cost, however, in 2011 even with the substantial reduction in chilled water usage the percentage remain 30% of the annual utility cost.
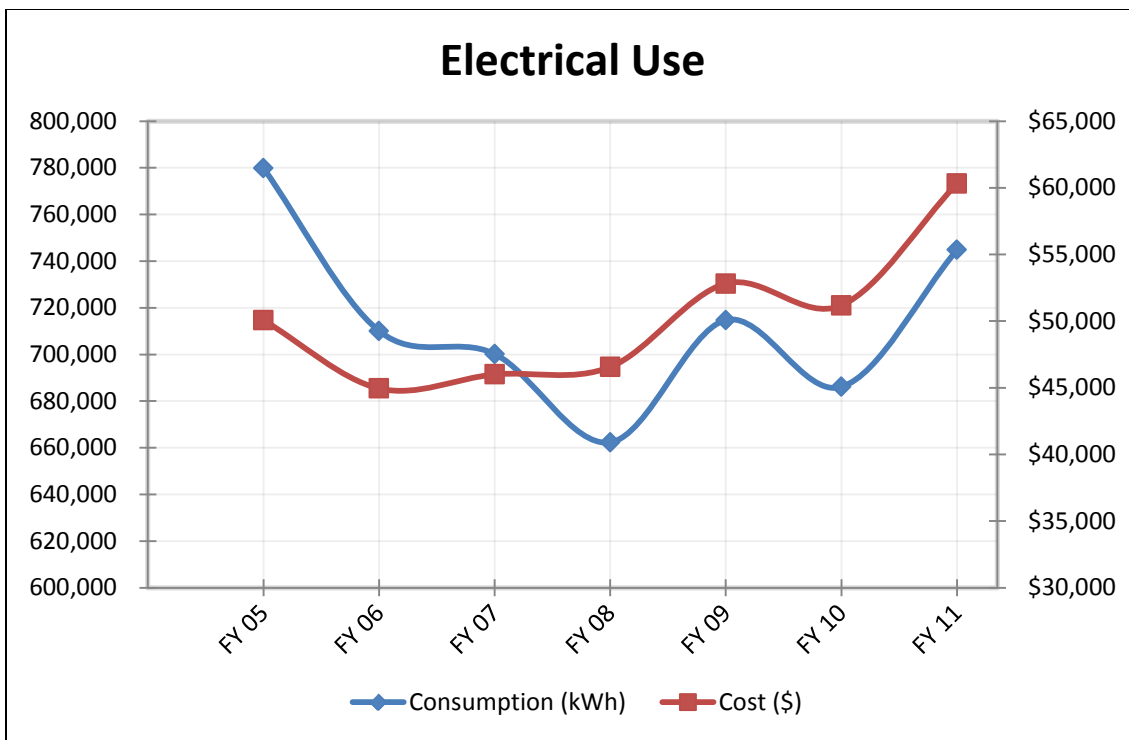
Figure 2.11 Annual electrical consumption and cost
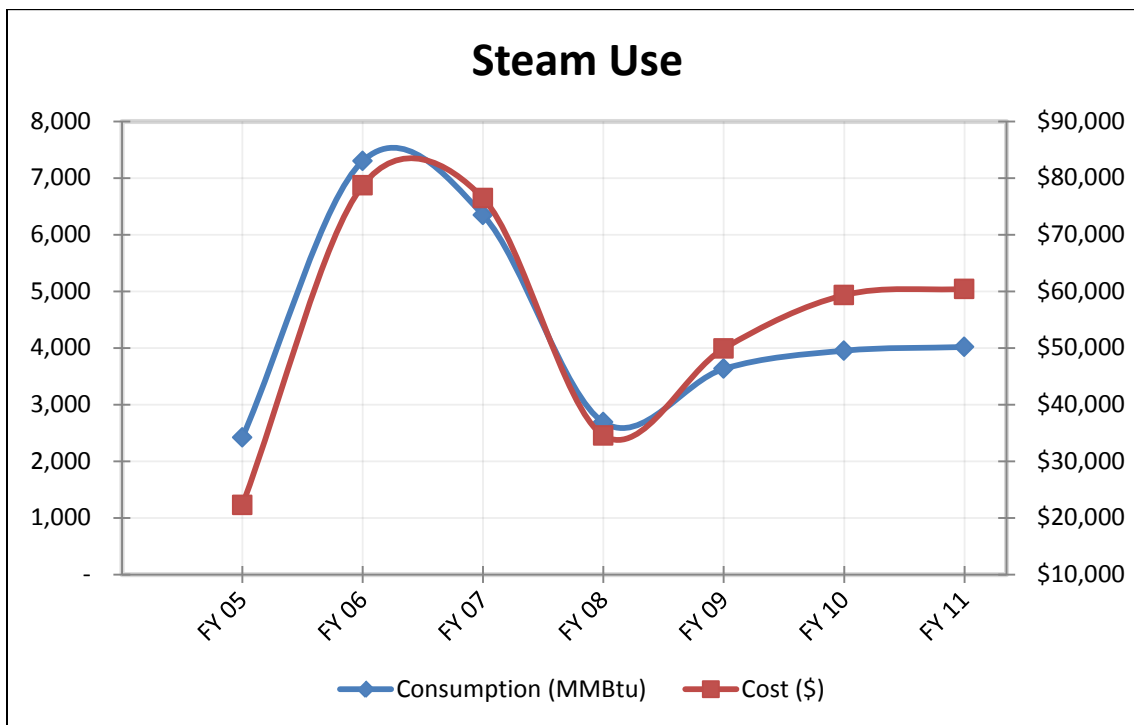
Figure 2.12 Annual steam consumption and cost
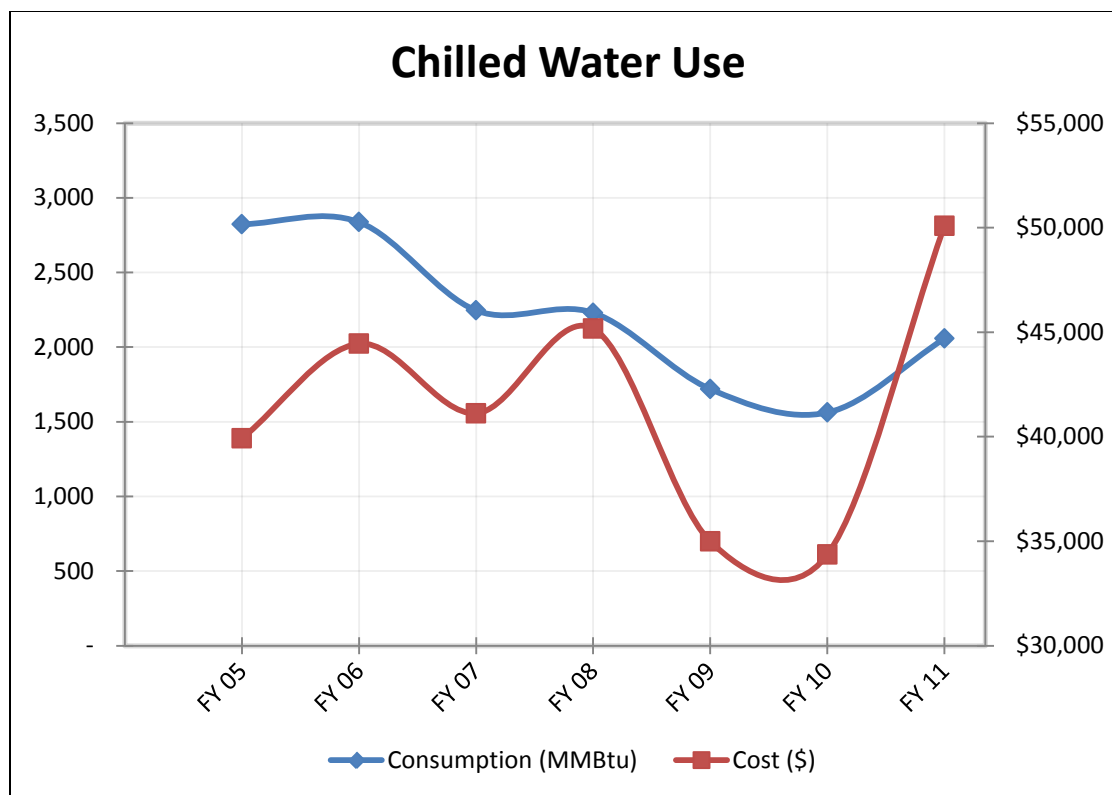
Figure 2.13 Annual chilled water consumption and cost

The steam use has varied drastically from fiscal year 2005 until fiscal year 2009 when it leveled and remained fairly consistent to the most recent data. The drastic oscillation in consumption and use could be attributed to many different factors, however based on information collected from the building maintenance people the cause of the increase on steam use was due to failed steam traps. These devices were later repaired once their location was identified as well as when the budget and time were available to perform this task.

The combination of increased use and increased cost has resulted in a 300% increase in annual steam cost from fiscal year 2005 to fiscal year 2011. In 2005, steam cost accounted for 20% of the BHC's annual utility cost. This percentage rose to 35% of the annual utility cost in fiscal year 2011.

2.6.1 Summer Energy Consumption and Cost

During the summer, most of the energy used at BHC is to provide space cooling. Approximately thirty three percent of the total annual energy cost is generated during this season of the year. A comparison of energy use, annual cost vs. summer cost, is presented in figure 2.14.

From the annual utility information is clear that chilled water is the main contributor to the utility energy cost due to its elevated price per unit. This research is focused on exploring energy consumption during the summer season and to optimize discharge air temperature and fan supply static pressure set points to provide substantial energy savings. A breakdown of the utility consumption and cost of electrical, steam and chilled water usage is shown in figures 2.15, 2.16 and 2.17 respectively.
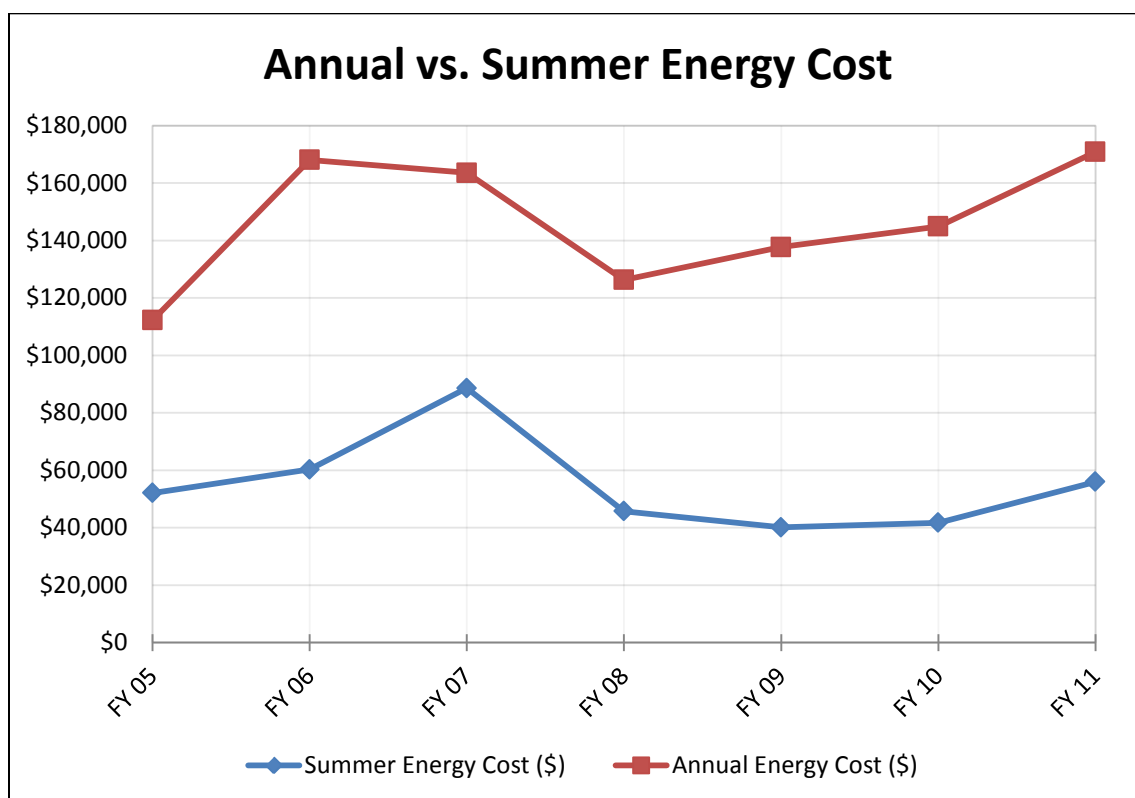
Figure 2.14 Summer vs. Annual energy cost
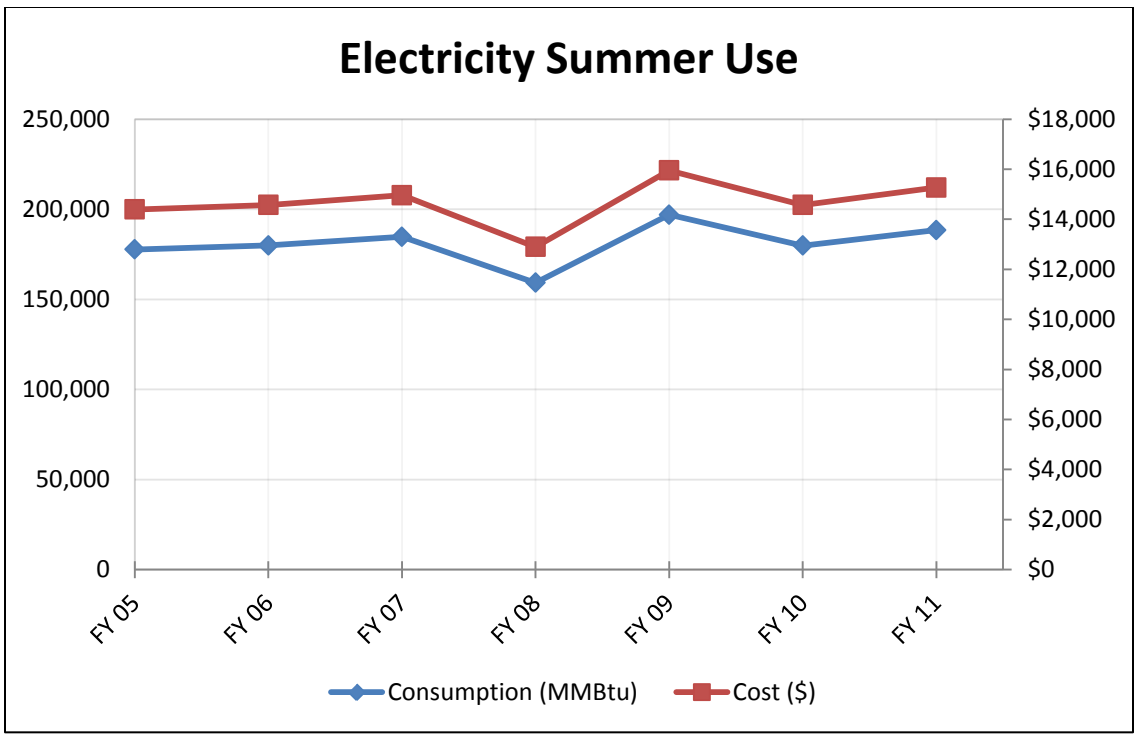
Figure 2.15 Summer electrical consumption and cost
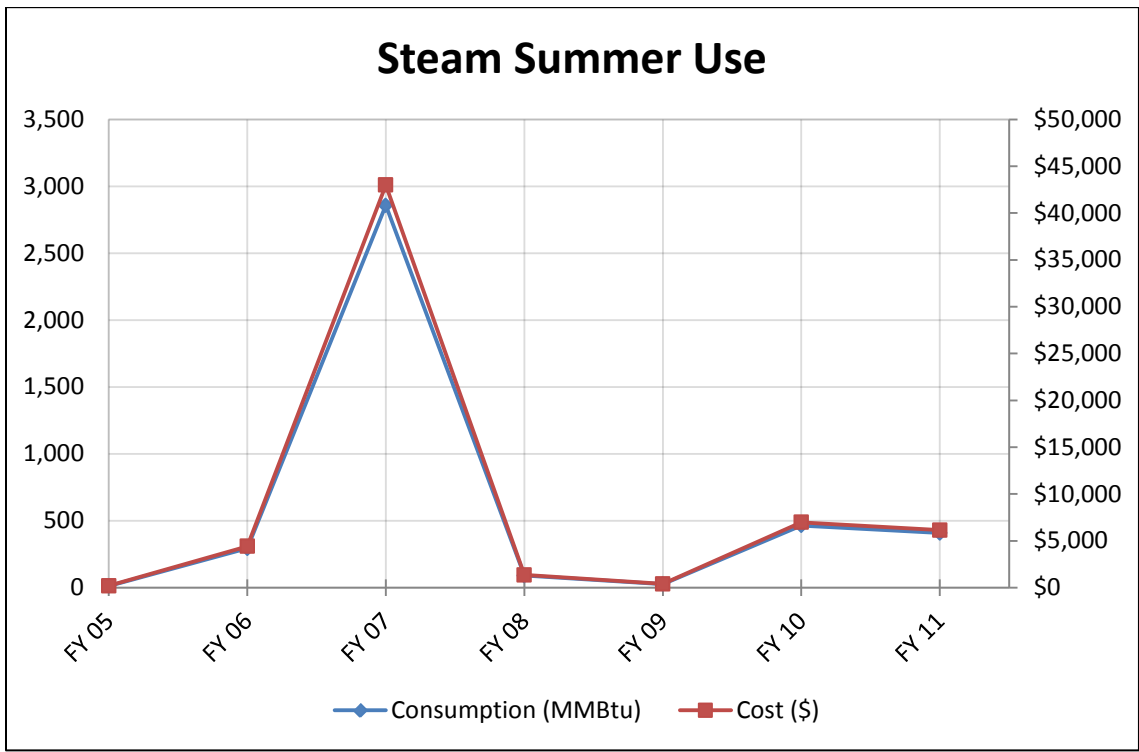
Figure 2.16 Summer steam consumption and cost
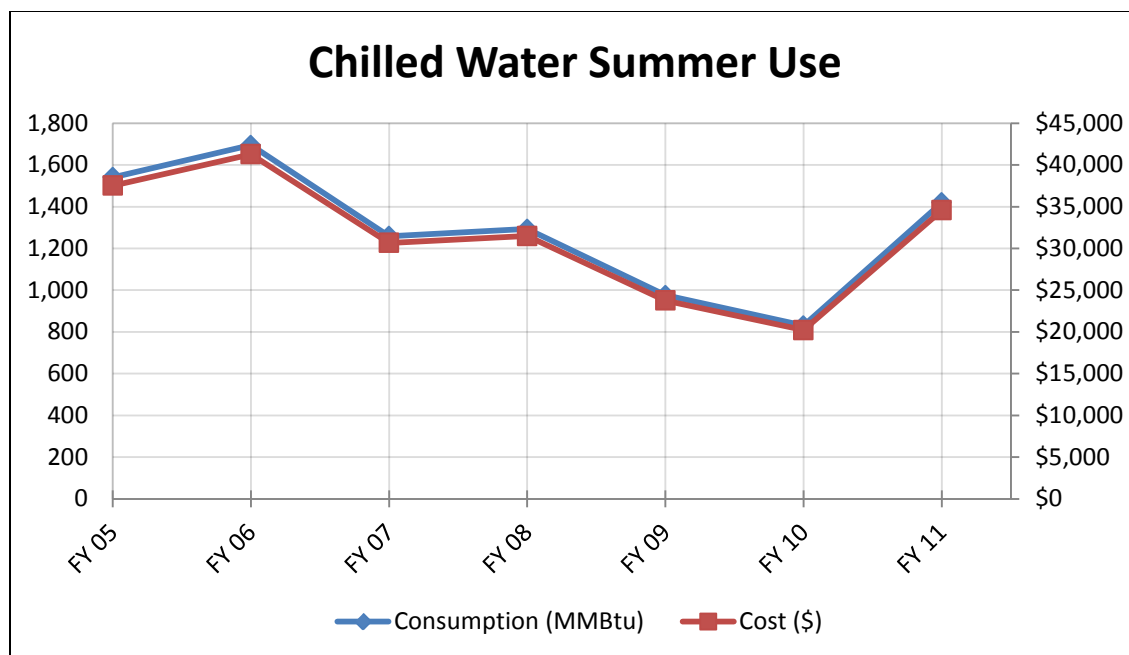
Figure 2.17 Summer chilled water consumption and cost

Even though steam is provided all year round, its consumption is very low during the summer. It is important to note that in fiscal 2007 there was a big spike in steam consumption. As mentioned previously this situation was originated due to a failure into the system. This research examines a fully functional-occupied facility, where ideal situations don't exist and maintenance issues need to be taken into account when building the simulation model.

2.7. Summary

Detailed description of the building main usage and components such as envelope, tightness, infiltration, HVAC, lighting and control systems are described and used to assess and understand its annual energy consumption. A seven-year average utility bill is used for the assessment. The fluctuation in energy consumption and cost is perceptible for a fully occupied multipurpose facility, where systems are not maintained

in ideal conditions and malfunctioning systems are likely to exist. The summer season is pointed as the major energy contributor to the annual utility cost. Space cooling is noted as the major source of energy consumption during this time of the year.

CHAPTER 3

COMPUTATIONAL ENERGY MODELING USING eQUEST

3.1. Introduction

Forty-year long development of building performance simulation tools has resulted in a wide range of currently available products [20, 22]. The different products' complexities range from a single spreadsheet to more advanced simulation tools, where some of them can handle a single aspect of a building's design or a more advance approach that integrates multiple aspects [35].

Computer-based simulation is now accepted as a tool for calculating building energy use[40, 51]. There are many different types of computer-based simulation tools that are available for performing building simulation.

The application DOE-2 is the most widely recognized and respected building energy analysis program use in today. Although DOE-2 was first released in the late 1970's, it was used as a starting point in early simulation tools and methods developed and funded by ASHRAE, NASA, the U.S. Postal Service, and the electric and gas utility industries [62].

During the first half of the 1980's, it was continued under the Department of Energy (DOE) sponsorship, but decreasing national concern about energy created the need for industry support, which became its principal source of funding through much of the 1990's.

The eQUEST engine expands and extends DOE-2's capabilities in several important ways, including: interactive operation, dynamic/intelligent defaults, and improvements to numerous long-standing shortcomings of DOE-2 older versions.

3.2. eQUEST

This simulation engine provides a sophisticated, yet easy-to-use building energy analysis tool, powerful enough to address every design domain but simple enough to permit a collaborative effort addressing every single aspect of the building design [24]. eQUEST calculates hour-by-hour building energy consumption over a whole year (8760 hours) using hourly weather data for the location under consideration. The energy consumption time period can be manually entered based on the user's needs.

Input to the program consists of a detailed description of the building, including hourly scheduling of occupants, lighting, equipment and thermostat settings.

This powerful tool provides very accurate simulation of building features such as shading, fenestration, interior building mass, envelope building mass, and the dynamic response of differing heating and air conditioning systems types and controls.

eQUEST also contains a dynamic daylighing model to assess the effect of natural lighting on thermal and lighting demands.

3.3. Building Data and Information Collection

The simulation process begins by collecting data of the building based on building plans, specifications and shop drawings. A baseline building model that assumes a minimum level of efficiency is then developed to provide the base from which energy savings are estimated. Figure 3.1 presents a flow chart where the logic in which the data is processed by the building simulator is described.
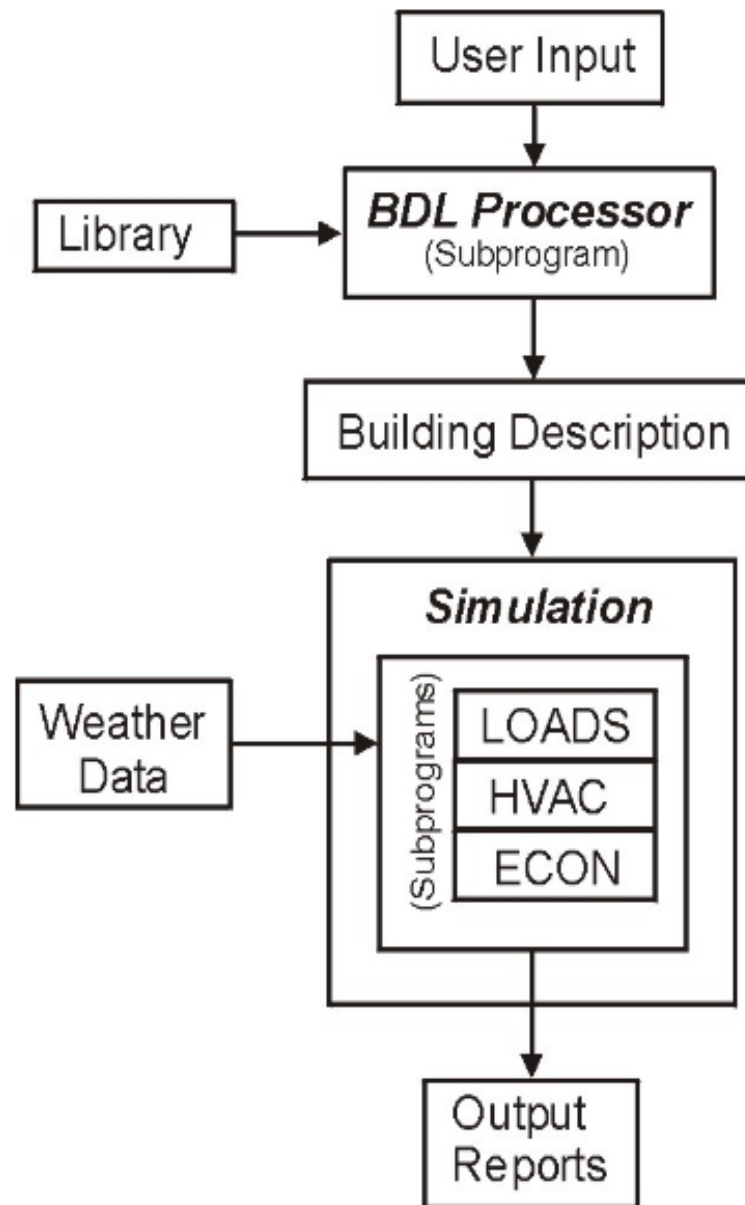
Figure 3.1 eQUEST flow chart

3.3.1. Site Information

Building site characteristics include latitude, longitude and elevation. Information

about adjacent structures or elevations capable of casting significant shadows should be

taken into account when providing the geometrical configuration and cardinal location of the facility.

3.3.2. Weather Data

Typical meteorological year (TMY) data set based on the location of the facility is provided into the model. These data sets are widely used for modeling. The TMY data is composed of twelve typical meteorological months (January through December) that are concatenated essentially without modification to form a single year with a serially complete twelve-year data record for primary measurements [65].

The twelve selected typical months are selected considering five elements: global horizontal radiation, direct normal radiation, dry bulb temperature, dew point temperature and wind speed. The latest version of the TMY is TMY3 [55], which data was created based on the procedures developed by Sandia National Laboratories, Hall et al. 1978 [31].

3.3.3. Building Configuration, Shell and Materials

Roof, walls and floors of the building are an essential part of the simulation and should be inputted into the model as they represent the mechanisms of how heat is transferred into or stored in the structure. The geometry, floor dimensions, and construction materials of each of the surfaces are essential. This includes glass properties of windows and the dimensions of any window shades, as well as external doors.

3.3.4. Building Operation and Scheduling

A clear understanding of the schedule of operation of the existing building is important to the overall accuracy of the simulation model. This includes information

about when building occupancy begins and ends (time of the week, and seasonal variations), occupied indoor thermostat setpoints, and HVAC and internal equipment operations schedules.

3.3.5. Internal Loads

Heat gain from internal loads, people, lights, equipment etc., constitutes a significant portion of the utility requirements, both from their direct power requirements and the indirect effect they have on cooling and heating requirements. The performance is impacted either directly or indirectly by the amount of internal load within the building [11].

3.3.6. HVAC Equipment and Performance

Few model components will have as much influence on overall building energy use and the performance as the HVAC equipment. Good information about these systems' efficiency will be crucial to the accuracy of any energy simulation used. Detailed equipment performance is obtained from design documents and shop drawings provided after construction was completed.

3.3.7. Utility Rates

Full details of the applicable utility rates can be coupled with the ability of eQUEST to predict hourly energy demand profiles. The result is the calculation of total energy cost per energy source.

Additional information is gathered on the field interviewing building maintenance personnel to ensure that the data collected is current and in accordance with the existing building conditions. The building automation system, Metasys from Johnson Controls, is

another source for building operation data, as well as the sequence of operation documents contained in the user's building operation and maintenance manual.

<p style="text-align:center"><u>3.4. Creation of a 3D Model Envelope</u></p>

Unnecessary detail and complexity in the simulation model are eliminated. On the west face of the building, from third floor to sixth floor, an additional shading structure is eliminated due to its complexity and difficult implementation into the simulation model. Shading factors and heat gain related to the structure are later compensated over the wall components.
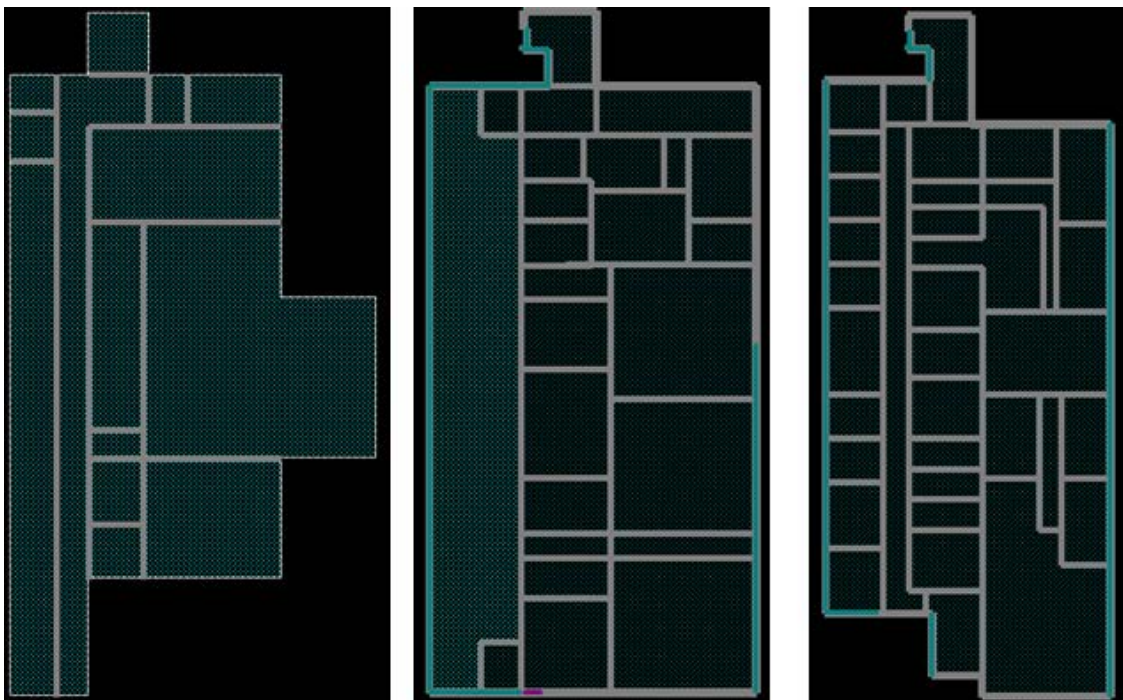
Figure 3.2 Thermal zones distribution for lower, 1st and 4th floors

The footprint and floor distribution are created to scale 1/8 inch = 1 foot, using AutoCAD 2012 [13]. The architectural as-built drawings are used to provide dimensions to build each individual floor and to layout the floor distribution according to the diverse

uses of the spaces. Once the models for each floor are completed, they have to be imported into eQUEST in a *.dwg* format as shown in figure 3.2 and 3.3.
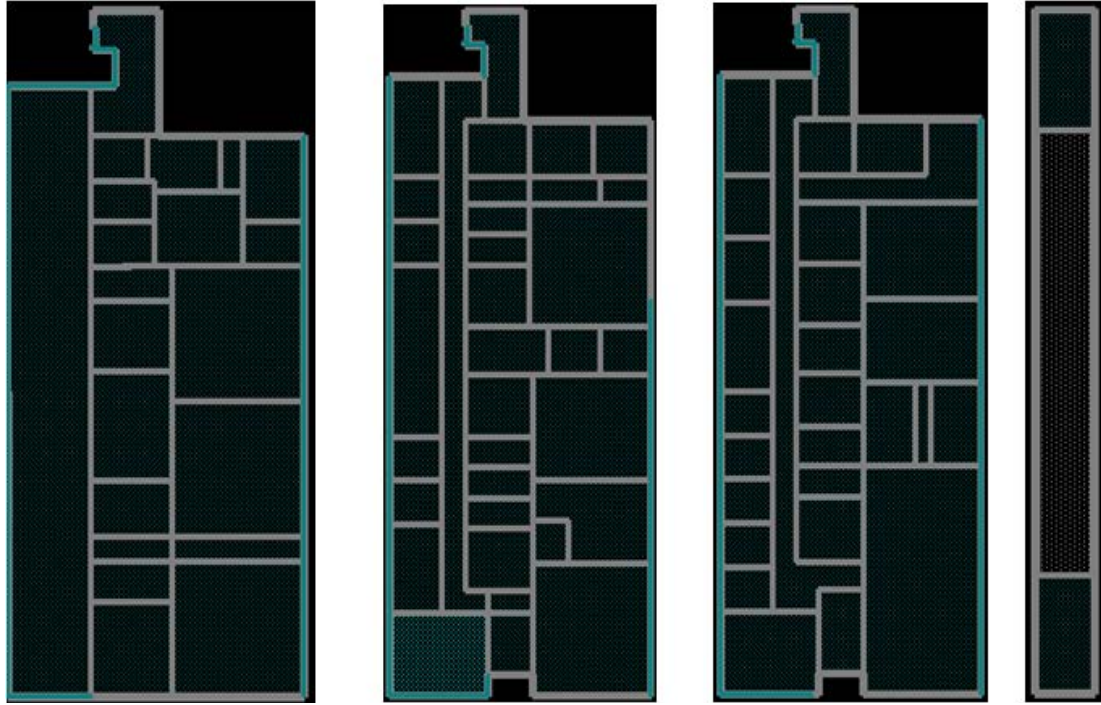
Figure 3.3 Thermal zones distribution for 2nd, 3rd and $5/6^{th}$ floors and penthouse

An initial pre-processing on the imported documents is done to define floors footprint dimensions and zoning patterns. Zone names and characteristics are inputted and the perimeter and core areas are defined. It is also in this stage where building orientation is defined, as well as floor heights (floor-to-floor and floor-to-ceiling). Once the floor height is defined, eQUEST will automatically create a plenum space that will be later used as part of the HVAC air-side return air system. The HVAC system will later identify the different zones defined into the model to create load profiles. For this reason the different zones are grouped together into the same categories and use, this will create higher accuracy into the model once the simulation is run. [21].

3.4.1 Building Envelope Constructions

Before a three-dimensional structure is created, detailed information about the building envelop constructions is inputted and it is divided as follows:

- Roof Surfaces – roof construction type represents the predominant roof construction used in the. Choices for roof construction include wood advanced frame, wood standard frame, and metal frame, concrete and adiabatic (no exterior exposure).

- Above grade walls – exterior wall construction type represents the predominant construction used in the exterior walls of the building. Choices for exterior wall construction are wood frame, metal frame, concrete, concrete masonry units (CMU), heavy weight concrete, stress skin, double standard wood frame and double advanced wood frame.

- Ground floor – floor exposure represents the predominant exposure used in the model. Choices for ground exposure are earth contact and over conditioned space.

- Infiltration and shell tightness – this value corresponds to the tightness of the building envelope to prevent air infiltration. Infiltration is very difficult to estimate for simulation purposes; however eQUEST presents different options such as loose construction, tight construction and unusually tight construction for selection.

For areas where roofs and walls present different types of material, eQUEST presents a custom, layer-by- layer option.

3.4.2 Building Interior Constructions

The next step into the model creation process to define the building construction interior components is as follows:

- Ceilings – ceiling type represents the predominant interior ceiling construction type used in the model. There are three choices for interior ceiling construction and they are lay-in-acoustic tile, drywall finish and plaster finish. Additional interior ceiling is provided if applicable to the model, allowing us to specify above ceiling insulation.

- Vertical walls – interior wall construction type represents the predominant interior wall construction used in the model. There are three choices for interior wall construction and they are air (none), frame and mass. Interior walls construction frame and mass contribute to the weighting factors of the building.

- Floors – it best represents the construction characteristics for the interior floor construction type. Only the most common types of interior floors are provided by eQUEST.

3.4.3 Building openings

Building openings constitute a thermal discontinuity point in a building's envelope. Energy transfer by openings via conduction and convection is usually a detriment and, therefore, it should be specified in the model. Energy transfer through radiation could be utilized in the winter for heating by solar radiation. The openings in a building are usually windows and doors and are a break in its external thermal envelope.

Inward and outward transfer of energy happens quicker through the openings than through the opaque envelope itself and occurs via convection, conduction and radiation.

eQUEST provides the capability to specify the areas where windows and doors are located within the building. It also allows inputting the type of material, height, sill and frame for each individual system.

The different ways these distributions can be achieved in the program are by selecting the percentage of net wall area (floor to ceiling), the percentage of gross wall area (floor to floor) or using a custom window/door placement tool, where exact coordinates and dimensions are inputted.
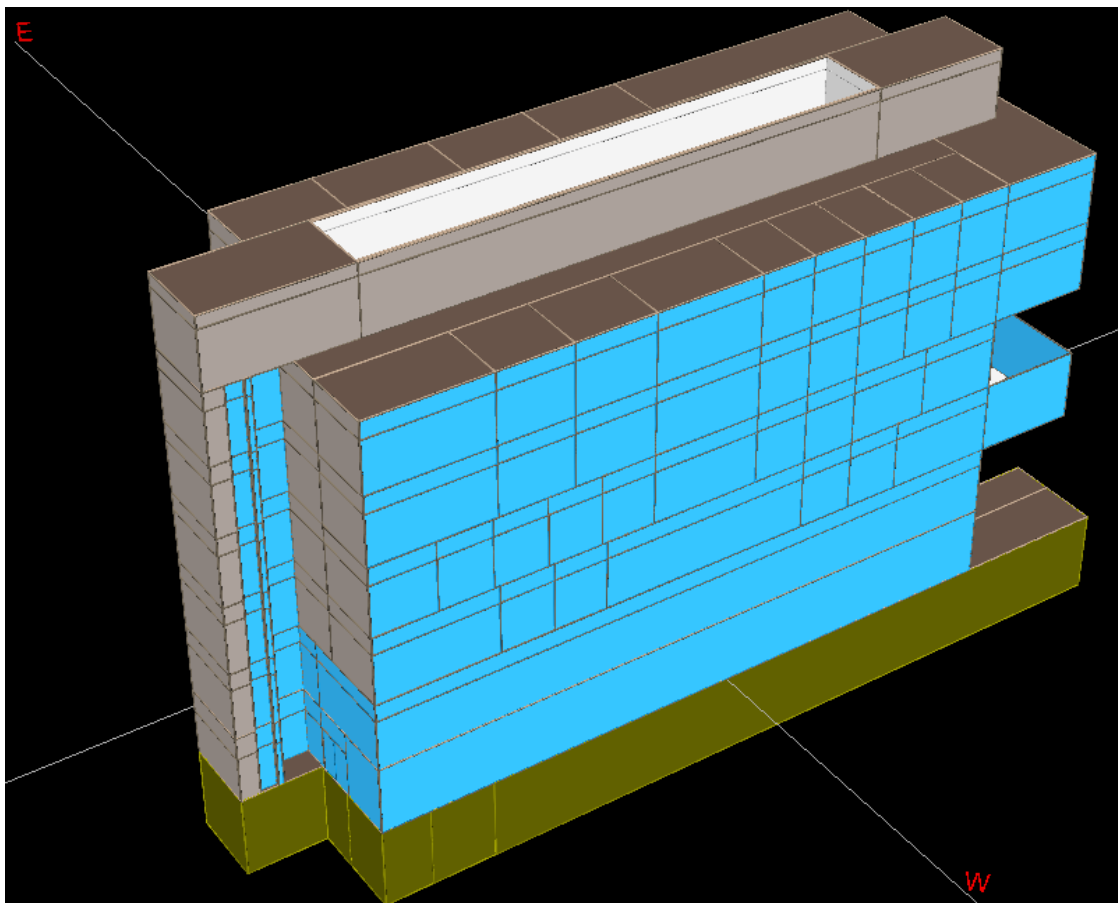
Figure 3.4 Northwest view geometric representation

The importance of precisely defining the openings into the model is reflected in the increase of energy consumption during the different seasons. During the winter loss of energy from the interior outwards by conduction, convection and radiation will force the building to cool off and it to invest energy in heating. In the summer it will be similar with the difference that energy will be invested in cooling.

Interior windows shades and blinds are added to the model and there are three choices, which are none, top floor only and all windows.

After all the building structural details are provided, the next step is to create the 3D model representation of BHC using eQUEST building rendering tools. The model representation seen from three differ angles is presented in figures 3.4, 3.5 and 3.6.
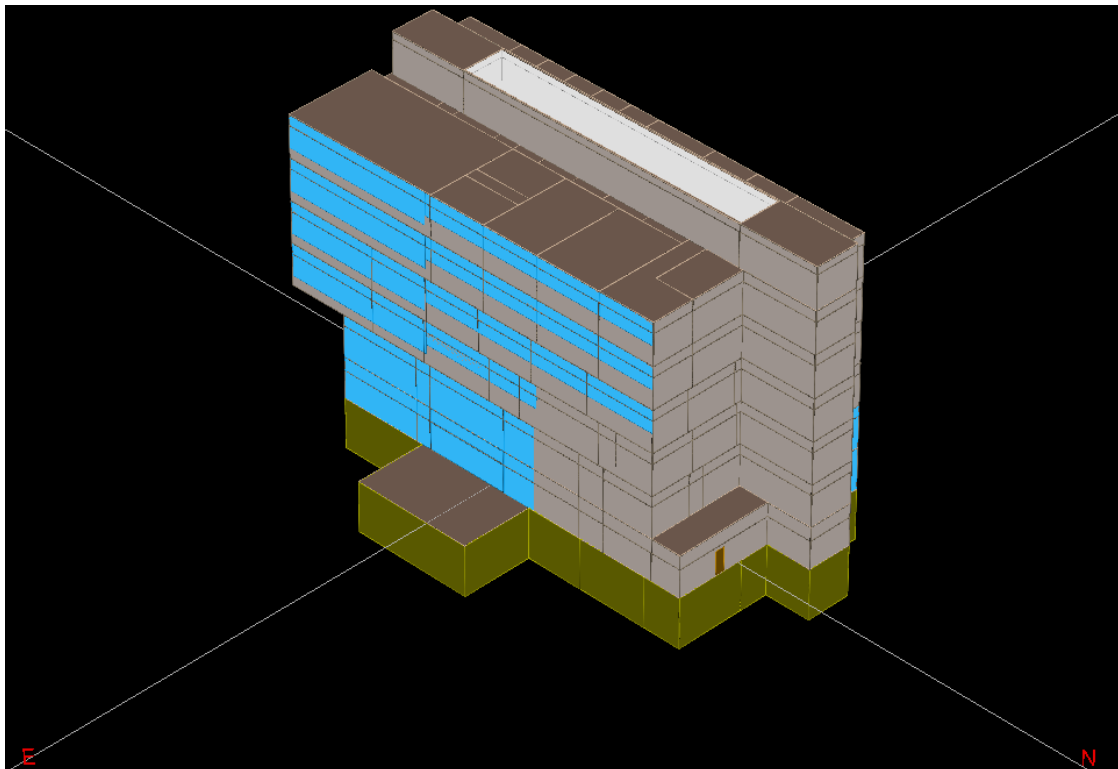
Figure 3.5 Northeast view geometric representation
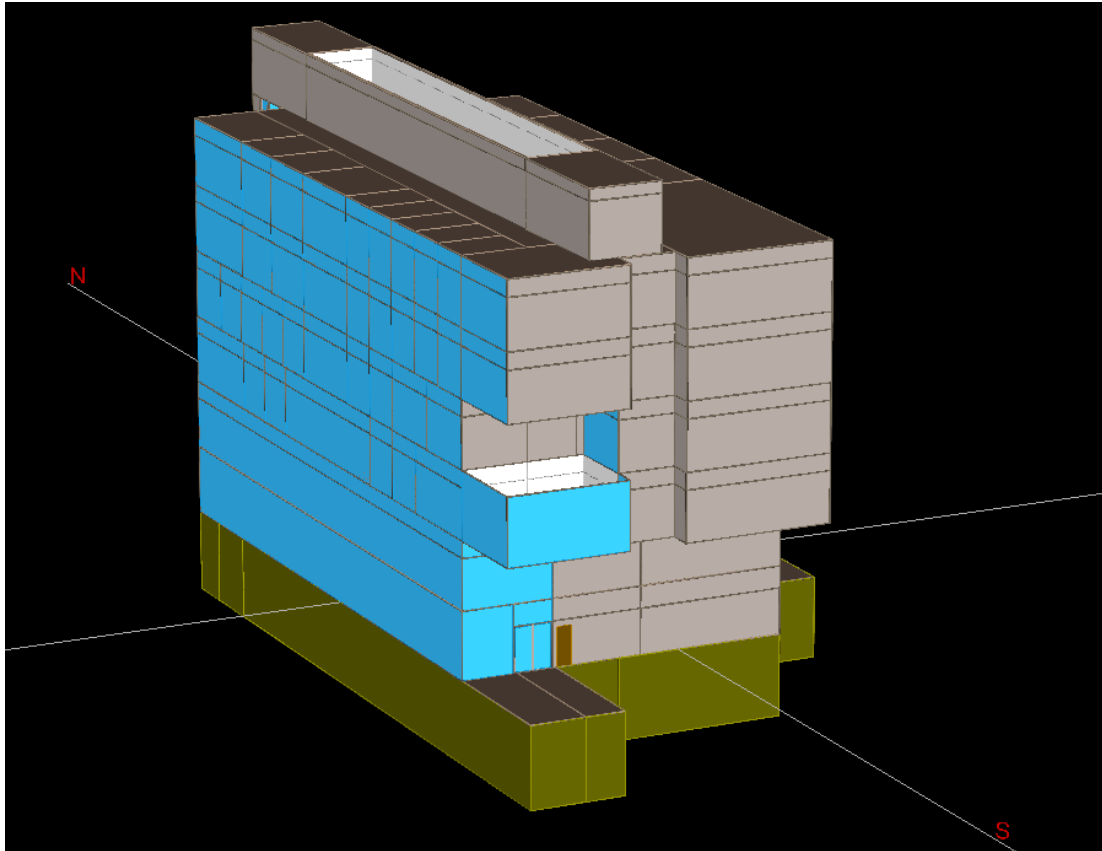
Figure 3.6 Southwest view geometric representation

3.5. HVAC System

The mechanical heating and cooling load in the building are dependent upon the various heat gains and losses experienced by the building including solar and internal heat gains and heat gains or losses due to transmission through the building envelope and infiltration of outside air. The primary purpose of the HVAC system is to regulate the dry-bulb air temperature, humidity and air quality by adding or removing heat energy [9].

HVAC equipment is typically classified as heating equipment, cooling equipment and air distribution equipment primarily including the AHU and fans. The size of the HVAC equipment is determined into the model based on the information gathered from the building documentation.

3.5.1 Cooling Primary Equipment

Cooling primary equipment – the chilled water is provided from the main chilled water plant to the building. Once on-site, a series of pumps working on VFD's pump the water into the AHU's cooling coils to cool the discharge air. The chilled water plant is simulated into the model by attaching a chilled water meter to the chilled water loop interface.

The parameters for the meter are defined using the information from the chilled water plant. The source-site-efficiency, which is the ratio between the energy delivered to the building site and the source energy, is automatically calculated by eQUEST. The design chilled water temperature, which is the temperature of the chilled water that can be delivered into the building's chilled water loop, is inputted into the model. This is the designed temperature used for components that reject heat to the loop.
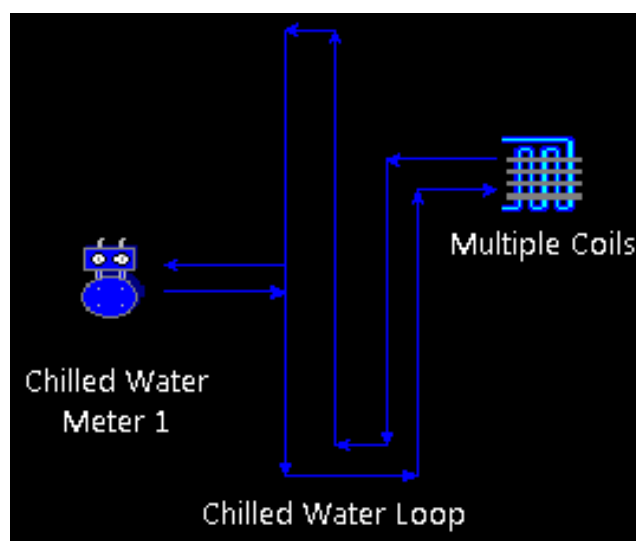
Figure 3.7 Schematic of the chilled water loop

The design temperature change of the loop is used in calculating the flow when the loop is sized based on the primary equipment. Chilled water pumps will define the

operating parameters of the pump attached to the chilled water circulation loop. The model will operate two 10 HP pumps with 50 ft. of head and a flow of 380 gpm. Capacity controls that modulate operation of the pump based on flow demand and motor class that specifies the efficiency of the pump motor are assigned. Motor efficiency is defined as standard, high and premium efficiency. Figure 3.7 presents a schematic representation of the chilled water loop.

3.5.2 Hot Water Plant Equipment

Steam is provided from the main steam power plant to the building. Once on-site, steam is converted into hot water on a heat exchanger and a series of pumps working on VFD's pump the hot water into the AHU's preheating coils to heat the discharge air. The steam power plant is simulated into the model by attaching a steam meter to the hot water loop interface. The parameters for the meter are defined using the information from the steam power plant. The source-site-efficiency, which is the ratio between the energy delivered to the building site and the source energy, is automatically calculated by eQUEST.

The design hot water temperature, which is the temperature of hot water that can be delivered into the building's hot water loop, is inputted into the model. This is the designed temperature used for components that draw heat from the loop. The design temperature change of the loop is used in calculating the flow when the loop is sized based on the primary equipment. Hot water pumps will define the operating parameters of the pump that is attached to the hot water circulation loop. The model operate two 7.5 HP pumps with 50 ft. of head and a flow of 355 gpm. Capacity controls that modulate operation of the pump based on flow demand and motor class that specifies the efficiency

of the pump motor are assigned. Motor efficiency is defined as standard, high and premium efficiency. Figure 3.8 presents a schematic representation of the hot water loop.
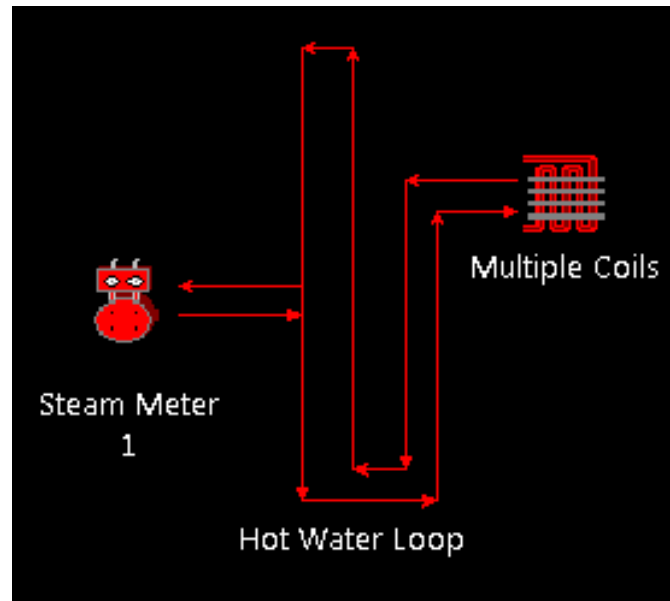
Figure 3.8 Schematic of the hot water loop

3.5.3 Domestic Hot Water Equipment

A domestic hot water loop supplies potable heated water to kitchens, bathrooms, etc. This water is provided by the steam power plant and converted in domestic hot water heat exchanger. The steam power plant is simulated into the model by attaching a second steam meter to the domestic hot water loop interface.

The parameters for the meter are defined using the information from the steam power plant. The source-site-efficiency, which is the ratio between the energy delivered to the building site and the source energy, is automatically calculated by eQUEST. A single 1HP pump with 70 ft. of head and 15 gpm flow recirculates the water inside the loop. Figure 3.9 presents a schematic representation of the domestic hot water loop.
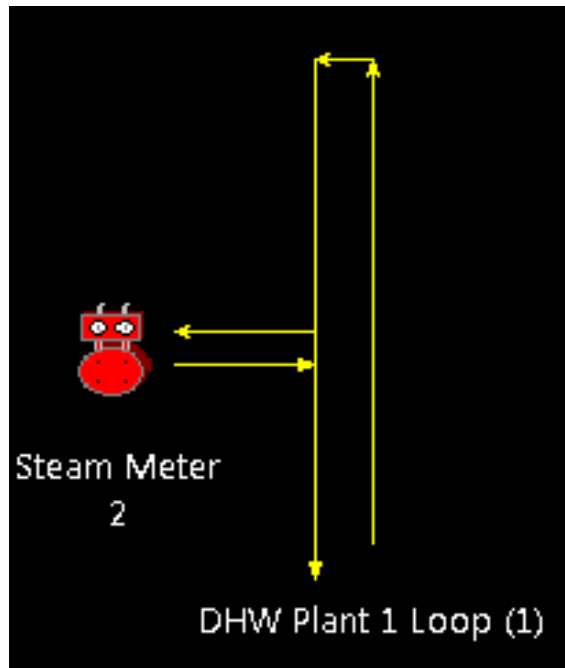
Figure 3.9 Cooling and heating equipment

3.5.4 Air-Side System

Heating ventilation and air conditioning is distributed throughout the facility by a single central station air handling unit (AHU). This unit is variable air volume and is simulated into the model with outside-return mixed air, air filters, a preheating coil to protect the chilled water coil from freezing, a reheat coil for humidity control, a variable flow supply air and return fan to stabilize the negative pressure in the mixing box. The AHU total airflow capacity is 57,250 cfm and minimum outside airflow of 16,000 cfm with a network of variable air volume (VAV) boxes with reheat coils located throughout the building. The plenum is the return air path to the AHU. The AHU fans are on variable speed drive based on duct static pressure, which is supplied at a fan total system pressure of 4.95 in. of water. Figure 3.10 presents a schematic representation of the air-side system.
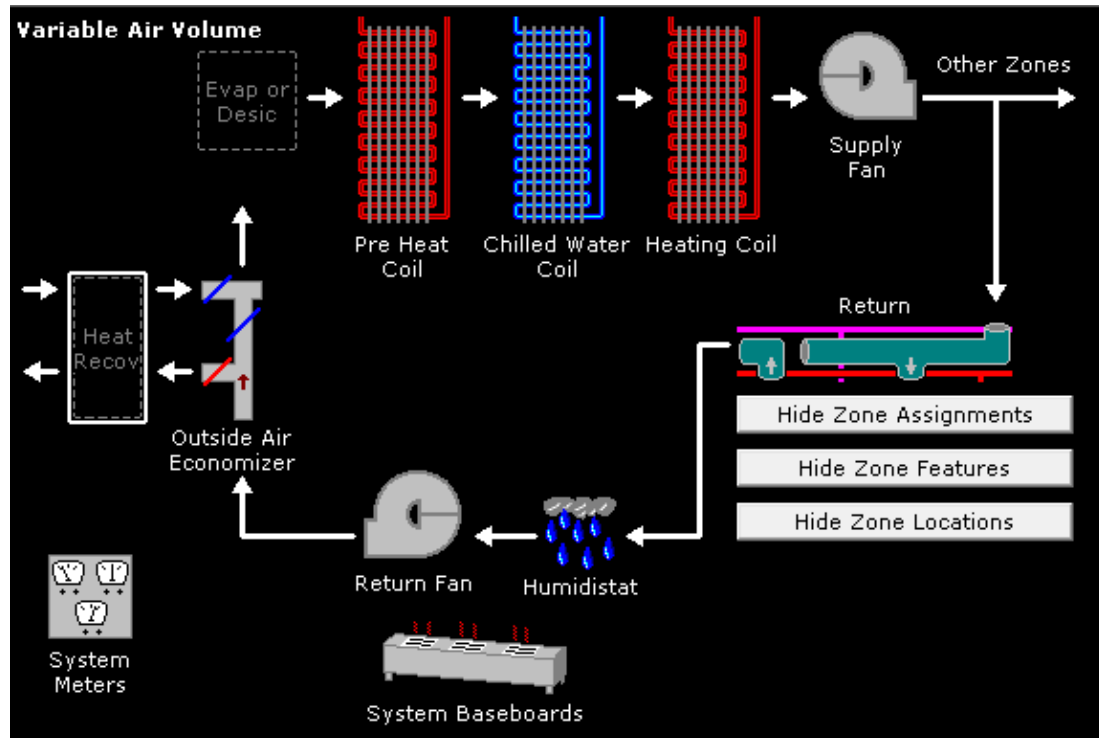
Figure 3.10 Schematic of the air-side system

At the zone level each zone is controlled by variable air volume boxes with reheat coil. As the zone temperature drops below the cooling setpoint, the VAV dampers modulate closed until they are at their minimum flow ratio. As the zone temperature approaches the heating setpoint, the reheat coil begins to modulate open to prevent the zone temperature from dropping any further. The HVAC system is scheduled occupied/unoccupied by zone according to function and seasons.

3.6. Model Assessment

The model was assessed based on seven-year average utility data energy consumption. One year is not enough information to accurately assess a simulation model. Sometimes weather conditions vary considerably from one year to the other and that can affect the annual energy usage. On the same hand, external factors such as

failures in the system, major renovation projects can skew the information [12]. The annual energy consumption by end-use is obtained from the simulation and broken down into the three main sources of energy (electricity, steam and chilled water). A pie chart of the annual electricity consumption by end-use is presented in figure 3.11.
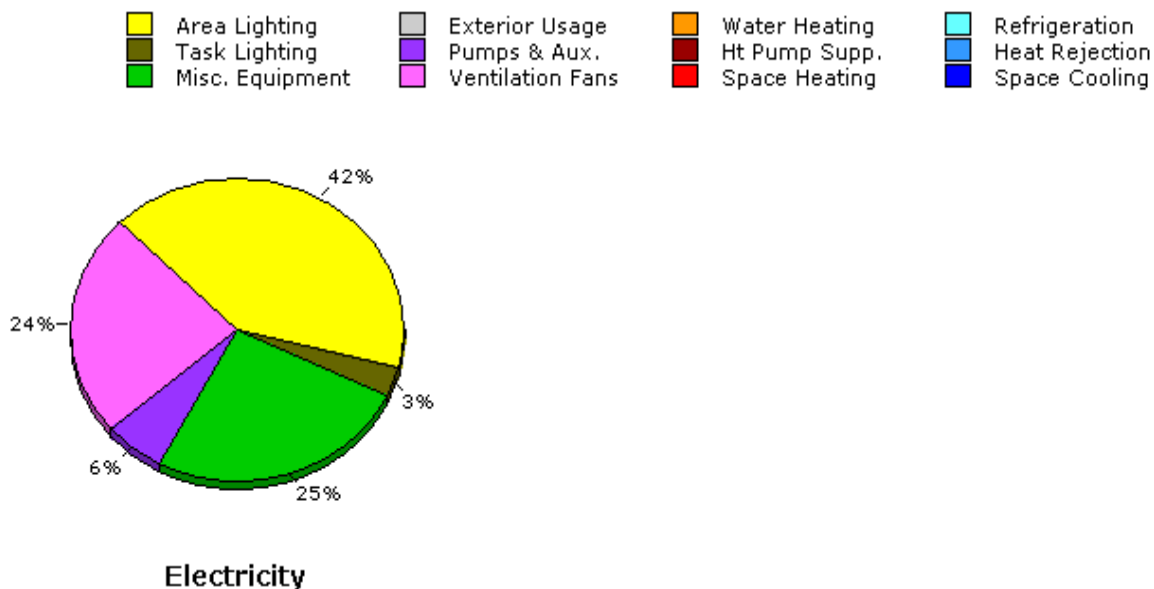
Figure 3.11 Annual electricity consumption by end-use

A pie chart of the annual steam and chilled water consumption by end-use is presented in figure 3.12, where chilled water is mainly used for space cooling.

Steam is converted into hot water and domestic hot water throughout heat exchangers. One portion of the steam converted is directed to the hot water loop to provide space heating. The other portion is used for domestic hot water.
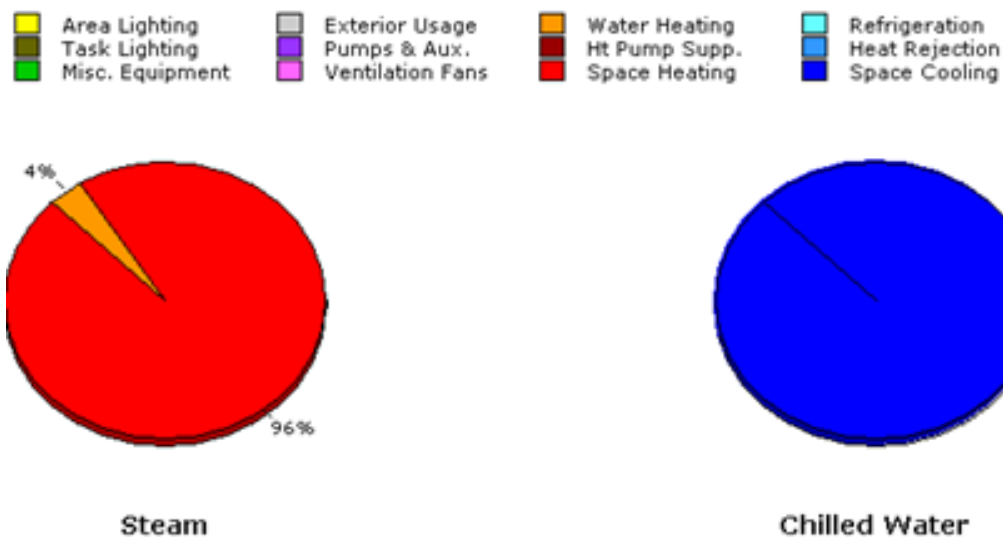
Figure 3.12 Annual steam and chilled water consumption by end-use

The accuracy of the simulation results for the three different sources of annual energy is shown in table 3.1.

Table 3.1 Annual energy data model assessment

	Electricity (kWh)	Steam (Mbtu)	Chilled Water (Mbtu)
Baseline	714028	4336.0	2074.0
Simulation	719180	4529.7	1993.8
Difference	5152.0	193.7	80.2
Error %	**0.72%**	**4.47%**	**3.87%**

It is observed that the model presents the higher percentage of error on the steam consumption. This percentage of error could be attributed to different factors such as weather file information, design based performance vs. actual performance, the model does not take into consideration malfunctioning devices and assumes fully functional systems, efficiency and performance of equipment, etc.

The level of accuracy of the model is within +/- five percent of error. Based on information from the Iowa Office of Energy independence (OEI), the energy regulatory organization in the state of Iowa, this level of accuracy exceeds by fifty percent their requirements. Their technical engineering analysis requires +/- 10% to authenticate the accuracy of any simulation perform [33].

3.7. Summary

eQUEST was used to create and replicate all the different aspects and systems of the building selected for this research. It was presented the importance of the different parameters that conform the building such as the envelope, HVAC, lighting and control systems. Simulation results were compared versus a seven-year average utility data. The results of the assessment provided an acceptable baseline with a margin of error within +/- five percent. From the baseline the annual energy consumed by the HVAC system was obtained. The next step was to focus on the summer season energy consumption, a new run was performed and results were obtained. Summer simulation results will be later compared against the results from the predictive model as a tool to reiterate and emphasize the effectiveness and accuracy of both approaches.

CHAPTER 4

PROPOSED DATA MINING TECHNIQUE AND OPTIMIZATION APPROACH

4.1. Introduction

Reducing the energy consumption of heating, ventilating and air-conditioning (HVAC) systems is essential due to the upheavals of energy cost in recent years. Operations efficiency of the HVAC system becomes more and more significant.

The performance of the HVAC system can be significantly improved by optimization of controllable set points. In the past years more research has been done in modeling and optimizing the performance of the overall HVAC system as well as local devices at the zone level.

Zheng et al [28] formulated the thermal process in a variable air volume (VAV) box with constraints on zone humidity. Nassif et al [56, 57] applied evolutionary algorithms to one-objective and two-objective optimization of an HVAC system, and the supervisory control strategies resulted in energy savings. Kusiak et al [3] applied a strength multi-objective particle swarm algorithm to optimize HVAC systems.

An HVAC system is a complex, nonlinear, discrete system containing numerous variables and constraints. Therefore, the modeling and optimization of an HVAC system is a challenge for traditional mathematical models [14] and simulation approaches [25]. In this thesis, a multi-objective particle swarm optimization algorithm is proposed for generating optimal control strategies of an existing fully occupied multipurpose HVAC system.

<center>4.2. Experiment and Data Description</center>

The data set in this research was obtained from an experiment at Blank Honors Center at The University of Iowa. The experiment aimed to assess the relationship between the states of the HVAC system, such as energy consumption and indoor temperature, as well as two of its controllable set points:

– Supply air static pressure set point (SA-SPSPT)

– Discharge air temperature set point (DAT-SPT).

The values for SA-SPSPT are modified from 1.9 in. WG to 2.8 in. WG with 0.1 in. WG increments; whereas DAT-SPT varied from 55°F to 65 °F at 1 °F increments over the course of the experiment.

The data was collected from July 6th to August 4th, 2011. Table 4.1 presents the experimental data in detail used to make the prediction. The data set used in this research uses a 15-min sampling interval.

<center>Table 4.1 Experiment period and data set instances</center>

No.	Data Set Type	Time Period	Number of Instances
1	Data set	07/06/2011-08/04/2011	2300
2	Training data set	Randomly selected from data set 1	1900
3	Test data set	Randomly selected from data set 1	400

<center>4.3. Parameter Selection</center>

Parameter selection is critical in the construction of data-driven models. A typical HVAC system contains hundreds of parameters. Some of the parameters collected are relevant to the output, while others are irrelevant or in some cases redundant.

The presence of irrelevant or redundant parameters may mask the primary patterns discovered in data mining [58]. These types of parameters duplicate the information contained in other parameters, making the model more complex and less accurate. Eliminating redundant or less important parameters improves the accuracy, scalability, and comprehensibility of the predicting model [41].

The parameter selection is performed using a boosting tree algorithm [34, 67, 60]. The boosting three algorithm shares advantages of the decision tree induction and tends to be robust in the removal of irrelevant parameters. In addition literature review and common domain knowledge were used as part of this process.

Eighteen parameters were selected and divided into three major groups:

- Adjusted input parameters.

- Uncontrollable input parameters.

- System outputs.

The adjusted input parameters are the variables to be modified during the optimization process and for the purpose of the simulation they are:

- AHU discharge air temperature

- Supply air duct static pressure

The uncontrollable parameters such as outside air temperature, chilled mixed air temperature to mention some, were highly correlated to the AHU energy cost and indoor temperature. Their effect on the output is considerable and had a large effect on the results. The system output parameters are the total energy cost and the indoor air temperature. We would like to make sure we get the highest savings without sacrificing occupants comfort. Table 4.2 presents all the different parameters and their divisions.

Table 4.2 Parameter selection by domain knowledge

Parameter Type	Parameter Name	Description	Unit
Adjusted input parameter	DAT-SPT	AHU discharge air temperature set point	°F (°C)
	SFDSP-SPT	Supply fan duct static pressure set point	in. WG (kPa)
Uncontrollable input parameter	CHWS-TEMP	Chilled water supply temperature	°F (°C)
	CC-TEMP	Coiling coil temperature	°F (°C)
	CC-VLV	Cooling coil valve position	%Open
	DAT	AHU discharge air temperature	°F (°C)
	HC-TEMP	Heating coil temperature	°F (°C)
	MA-DEMP	Mixed air damper position	%Open
	MA-TEMP	Mixed air temperature	°F (°C)
	RA-TEMP	Return air temperature	°F (°C)
	RA-CFM	Return fan air flow rate	CFM
	SA-CFM	Supply fan air flow rate	CFM
	SF-DSP	Supply fan duct static pressure	in. WG (kPa)
	OA-TEMP	Outside air temperature	°F (°C)
	RA-HUMD	Return air humidity	%RH
	OA-HUMD	Outside air humidity	%RH
System output	Total cost	Total cost of the energy consumption	$
	RM-TEMP	Indoor temperature	°F (°C)

In order to analyze the sensitivity of the parameters and select the ones with the highest impact on the prediction of the output values, the selection of uncontrollable parameters was performed using the boosting tree algorithm. Because of the different characteristics of the outputs, the input parameters used to build predictive models were ranked by their order of importance.

The parameters with a value of one are the most influential in the predictive model, meanwhile values smaller than one are less relevant. Typically values with a level of importance higher than fifty percent are desired for an accurate predictive model.

SF-CFM , RF-CFM and CC-VLV are presented as to be the most influential for the creation of the total cost predictive model. The results from the boosting tree algorithm are shown in Tables 4.3

Table 4.3 Total cost predictive model parameters rank

	Variable - Rank	Importance
SF-CFM	100	1.000000
RF-CFM	96	0.955825
CC-VLV	96	0.955594
CHWS-TEMP	71	0.706076
DAT	69	0.690989
CC-TEMP	66	0.661674
MA-TEMP	63	0.626951
OA-TEMP	63	0.626640
HC-TEMP	62	0.622464
RA-TEMP	59	0.594485
DAT_SPT	41	0.411404
SFDSP_SPT	38	0.376310
OA-HUMD	29	0.289981
SFDSP_SPT	22	0.224039
MA-DAMP	18	0.180393
RA-HUMD	0	0.000000

RA-TEMP, DAT, CC-TEMP, RF-CFM and SF-CFM are presented as to be the most influential for the creation of the indoor temperature predictive model. The results are shown in Tables 4.4.

It is important to emphasize that building thermal comfort and air quality should not be compromised in achivieng energy savings. A good predictive model for total

energy cost and indoor temperature is very important to be able to create and accurate correlation of both variables.

Table 4.4 Indoor temperature predictive model parameters rank

	Variable - Rank	Importance
RA-TEMP	100	1.000000
DAT	86	0.859791
CC-TEMP	85	0.846567
RF-CFM	85	0.845250
SF-CFM	83	0.834942
CHWS-TEMP	73	0.725499
OA-HUMD	72	0.717477
SFDSP	58	0.582579
CC-VLV	51	0.511859
MA-TEMP	51	0.508240
HC-TEMP	47	0.465776
DAT_SPT	45	0.447787
SFDSP_SPT	39	0.393586
OA-TEMP	38	0.377207
MA-DAMP	16	0.155805
RA-HUMD	0	0.000000

Because of the dynamic characteristics of the HVAC system, the time series' property of the collected data was considered to build the predictive models. Using time series allow getting the future value by adding the past values. In other words, the current value for the most relevant parameters go back in time $t - 1$ and collect the data to later create the future value $t + 1$. The parameters that are not as influential in the prediction process use their actual values only. The parameters for the two predictive models selected are presented in tables 4.5 and 4.6 respectively.

Table 4.5 Selected parameters total cost model

Parameter	Parameter Name	Description
$y_1(t)$	RM-TEMP	Total cost at time t
$y_1(t-1)$	RM-TEMP	Total cost at time t – 1
$v_{y1}(t)$	SF-CFM	Supply fan air flow rate at time t
$v_{11}(t-1)$	SF-CFM	Supply fan air flow rate at time t - 1
$v_{12}(t)$	RF-CFM	Return fan air flow rate at time t
$v_{12}(t-1)$	RF-CFM	Return fan air flow rate at time t - 1
$v_{13}(t)$	CC-VLV	Cooling coil valve position at time t
$v_{13}(t-1)$	CC-VLV	Cooling coil valve position at time t - 1
$v_{14}(t)$	CHWS-TEMP	Chilled water supply temperature at time t
$v_{15}(t)$	DAT	Discharge air temperature at time t
$v_{16}(t)$	CC-TEMP	Cooling coil temperature at time t
$v_{17}(t)$	MA-TEMP	Mixed air temperature at time t
$v_{18}(t)$	OA-TEMP	Outside air temperature at time t
$v_{19}(t)$	HC-TEMP	Heating coil temperature at time t
$x_1(t+1)$	DAT-SPT	Discharge air temperature set point at time t + 1
$x_2(t+1)$	SFDSP-SPT	Supply fan duct static pressure set point at time t + 1

Table 4.6 Selected parameters indoor temperature model

Parameter	Parameter Name	Description
$y_2(t)$	Indoor temperature	Indoor temperature at time t
$y_2(t-1)$	Indoor temperature	Indoor temperature at time t - 1
$v_{21}(t)$	RA-TEMP	Return air temperature at time t
$v_{21}(t-1)$	RA-TEMP	Return air temperature at time t - 1
$v_{22}(t)$	DAT	Discharge air temperature at time t
$v_{23}(t)$	CC-TEMP	Cooling coil temperature at time t
$v_{24}(t)$	RF-CFM	Return fan air flow rate at time t
$v_{25}(t)$	SF-CFM	Supply fan air flow rate at time t
$v_{26}(t)$	CHWS-TEMP	Chilled water supply temperature at time t
$v_{27}(t)$	OA-HUMD	Outside air humidity at time t
$x_1(t+1)$	DAT-SPT	Discharge air temperature set point at time t + 1
$x_2(t+1)$	SFDSP-SPT	Supply fan duct static pressure set point at time t + 1

4.4. Model Creation and Validation

Once the parameters are selected and time series used, the models are created. The derived model $f_i(\cdot)\ (i = 1, 2)$ for total cost and indoor temperature predictive models are shown in equations 1 and 2, where $y_1(t + 1)$ is the total cost, $y_2(t + 1)$ the indoor temperature and $c_1(t + 1)$ and $c_2(t + 1)$ the discharge air temperature set point and the supply air duct static pressure set point respectively.

$$y_1(t+1) = f_1(y_1(t), y_1(t-1), v_{11}(t), v_{11}(t-1), v_{12}(t), v_{12}(t-1), v_{13}(t), v_{13}(t-1),$$
$$v_{14}(t), v_{15}(t), v_{16}(t), v_{17}(t), v_{18}(t), v_{19}(t), x_1(t+1), x_2(t+1)) \tag{1}$$

$$y_2(t+1) = f_2(y_2(t), y_2(t-1), v_{21}(t), v_{21}(t-1), v_{22}(t), v_{23}(t),$$
$$v_{24}(t), v_{25}(t), v_{26}(t), v_{27}(t), x_1(t+1), x_2(t+1)) \tag{2}$$

The data set was divided into two parts: two-thirds for training data set and one-third testing data set and four metrics, the mean absolute error (MAE), the mean absolute percentage error (MAPE), the standard deviation of absolute error (Std_AE), and the standard deviation of absolute percentage error (Std_APE) are employed to evaluate performance of the predictive models generated by the multi-layer perceptron (MLP) algorithm [10]. Equations (3) through (6) present these metrics.

$$MAE = \frac{\sum_{i=1}^{N} \left| \hat{y}_i - y_i \right|}{N} \tag{3}$$

$$MAPE = \frac{1}{N} \sum_{i=1}^{N} \left| \frac{\hat{y}_i - y_i}{y_i} \right| \tag{4}$$

$$Std\_AE = \sqrt{\frac{1}{N} \sum_{i=1}^{N} (\left| \hat{y}_i - y_i \right| - \frac{1}{N} \sum_{i=1}^{N} \left| \hat{y}_i - y_i \right|)^2} \tag{5}$$

$$Std \_ APE = \sqrt{\frac{1}{N}\sum_{i=1}^{N}(\left|\frac{\hat{y}_i - y_i}{y_i}\right| - \frac{1}{N}\sum_{i=1}^{N}\left|\frac{\hat{y}_i - y_i}{y_i}\right|)^2}$$

(6)

The performance of the predictive models is presented in table 4.7. There accuracy is ninety six percent and above. The level of accuracy of the model indicates that it can be used for optimization.

Table 4.7 Performance of predictive models

Objective	Data Set	MAE	MAPE	Std_MAE	Std_MAPE
Total cost	Training	0.10	0.03	0.12	0.04
	Test	0.13	0.04	0.16	0.07
Room temperature	Training	0.07	0.001	0.07	0.001
	Test	0.07	0.001	0.08	0.001

Predictive model for total cost is compared versus actual observed values and presented in figure 4.1
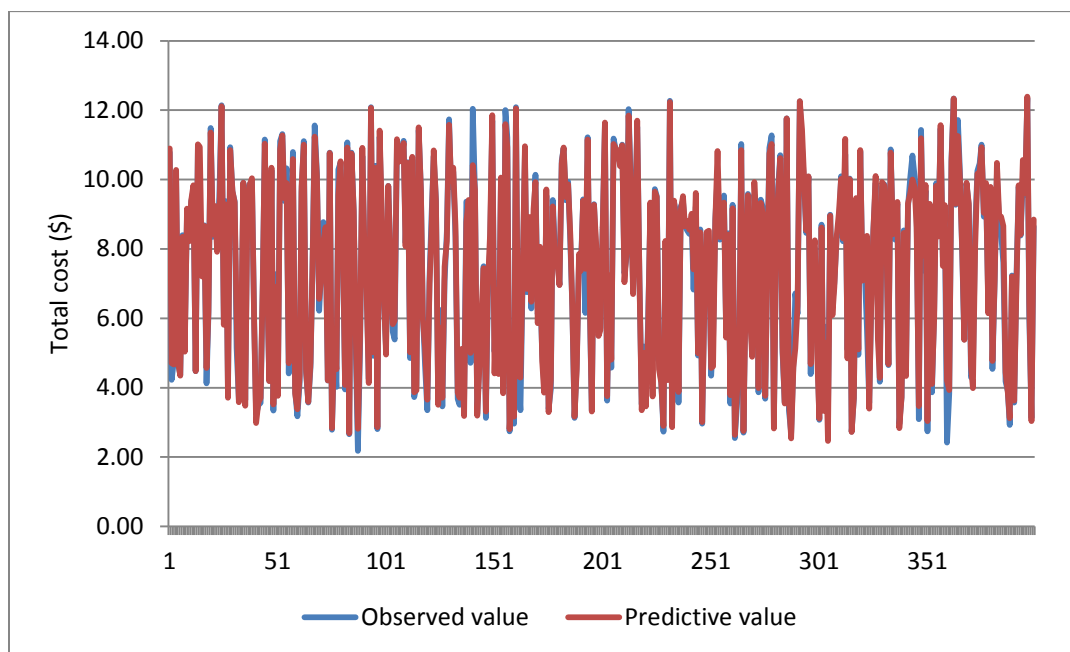
Figure 4.1 Predictive vs. observed total cost

Predictive model for indoor temperature is compared versus actual observed values and presented in figure 4.2
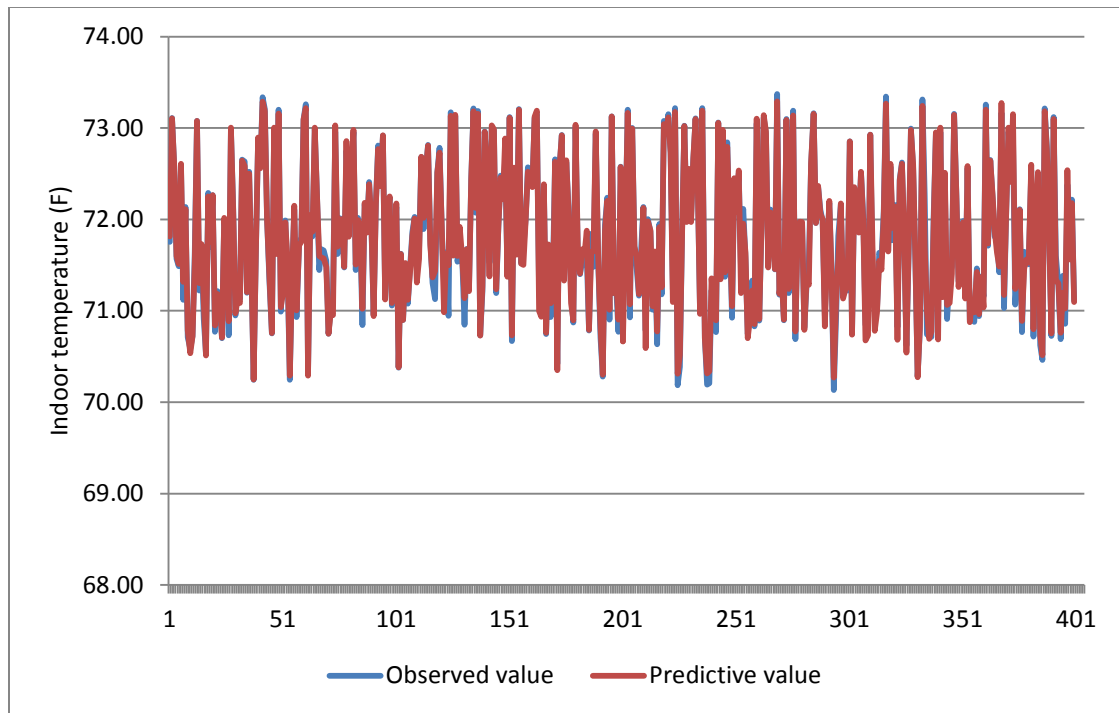
Figure 4.2 Predictive vs. observed indoor temperature

From the above graphs shown in figure 4.1 and 4.2 it is observed that the parameter selection was well done and as a result the prediction model fit the observed value in a very accurate manner.

4.5. Model Optimization

4.5.1 Optimization Model Formulation

Now that the prediction model has been validated, the next step is to optimize it. The prediction model is used to construct the optimization model and to minimize the total energy cost of the HVAC system. The constraints of the model are identified and the

limits of the control parameters for room temperature are set. The optimization model is formulated in equation 7.

$$\min_{x_1(t+1), x_2(t+1)} y_1(t+1)$$

$$\text{subject to:}$$

$$y_1(t+1) = f_1(y_1(t), y_1(t-1), v_{11}(t), v_{11}(t-1), v_{12}(t), v_{12}(t-1), v_{13}(t), v_{13}(t-1), v_{14}(t), v_{15}(t), v_{16}(t), v_{17}(t), v_{18}(t), v_{19}(t), x_1(t+1), x_2(t+1))$$

$$y_2(t+1) = f_2(y_2(t), y_2(t-1), v_{21}(t), v_{21}(t-1), v_{22}(t), v_{23}(t), v_{24}(t), v_{25}(t), v_{26}(t), v_{27}(t), x_1(t+1), x_2(t+1))$$

$$55 \leq x_1(t+1) \leq 66$$

$$1.9 \leq x_2(t+1) \leq 2.8$$

$$68 \leq y_2(t+1) \leq 72$$

$$(7)$$

The optimization model is then converted into a bi-objective optimization model using the following objective functions shown in equations 8 and 9.

$$Obj1 = y_1(t+1) \tag{8}$$

$$Obj2 = \max\{0, 68 - y_2(t+1)\} + \max\{0, y_2(t+1) - 72\} \tag{9}$$

The bi-objective optimization model is presented in equation 10

$$\min_{x_1(t+1), x_2(t+1)}(Obj1, Obj2)$$

$$\text{subject to:}$$

$$y_1(t+1) = f_1(y_1(t), y_1(t-1), v_{11}(t), v_{11}(t-1), v_{12}(t), v_{12}(t-1), v_{13}(t), v_{13}(t-1), v_{14}(t), v_{15}(t), v_{16}(t), v_{17}(t), v_{18}(t), v_{19}(t), x_1(t+1), x_2(t+1))$$

$$y_2(t+1) = f_2(y_2(t), y_2(t-1), v_{21}(t), v_{21}(t-1), v_{22}(t), v_{23}(t), v_{24}(t), v_{25}(t), v_{26}(t), v_{27}(t), x_1(t+1), x_2(t+1))$$

$$55 \leq x_1(t+1) \leq 66$$

$$1.9 \leq x_2(t+1) \leq 2.8$$

$$(10)$$

4.5.2 Multi-objective particle swarm optimization algorithm

The optimization model derived from the MLP is complex and the gradients cannot be practically calculated using traditional algorithms, therefore particle swarm optimization (PSO) is used. Some other algorithms are suitable for the application however, for the purpose of this research PSO is considered as a good fit for optimization based on previous literature review. Even though there are different variants of PSO, the traditional PSO algorithm is used and presented below [38]:

Step 1: Initialize a group of particles with random positions $x_i \in R^D$ and velocities $v_i \in R^D$ in the problem space. Perform the next step until the pre-set requirements are satisfied.

Step 2: For each particle compute fitness by using function $f(\cdot)$.

Step 3: Compare each particle's fitness with its $pbest_i$. If current value is better than $pbest_i$, then use current value instead of $pbest_i$ and update $p_i \in R^D$ with current location x_i. Compare all of the particles' $pbest_i$ and find the best one assigned as $gbest$ and set its current location as $p_g \in R^D$.

Step 4: Update the particles' velocities and positions based on the following equation:

$$
\begin{aligned}
v_i &\leftarrow v_i + U(0,\varphi_1)\cdot(p_i - x_i) + U(0,\varphi_2)\cdot(p_g - x_i) \\
x_i &\leftarrow x_i + v_i
\end{aligned}
\tag{11}
$$

Step 5: If the stop criterion is satisfied, p_g is the final solution and $gbest$ is the final optimal fitness.

Stopping criteria is usually a sufficiently good fitness or a maximum number of iteration generations. A flow chart describing steps for the algorithm is shown in figure 4.3. The PSO presented consists on changing the velocity (acceleration) of each particle toward its $pbest_i$ and $gbest$ locations, acceleration is weighted by separate random numbers for the acceleration towards the $pbest_i$ and $gbest$ positions, fitness comparisons are made against the $pbest_i$ which is replaced with higher fitness values and finally particles are flown to their new location.
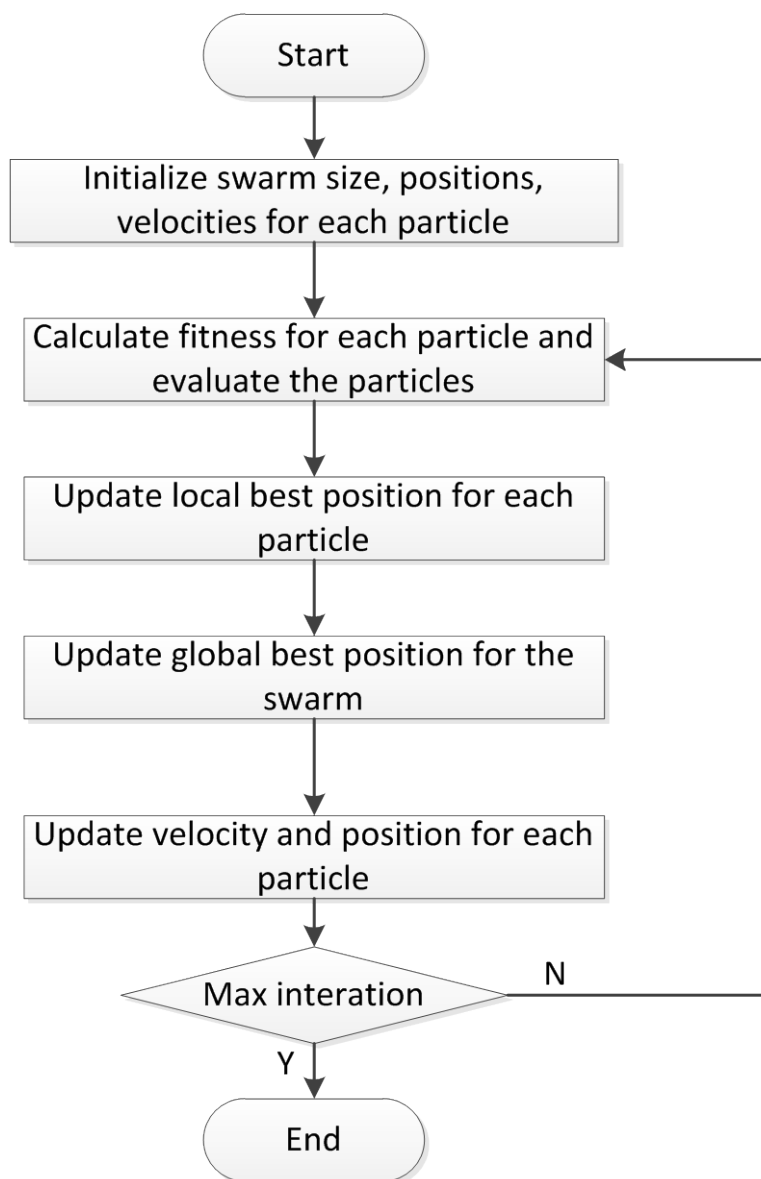
Figure 4.3 PSO algorithm flow chart

To adopt the above algorithm for solving a multi-objective optimization model, the following modifications are made according to Abido et al [6].

Modification 1: Create a set S_i to store the non-dominated solutions for i^{th} particle up to the current time.

Modification 2: Create a set G to store the non-dominated solutions from all S_i at each iteration.

Modification 3: Create an external set E to store the non-dominated solutions from G at each iteration.

Modification 4: Process to update S_i : At each iteration, compare the current particle solution with the stored solutions. Dominated solutions are removed while non-dominated solutions are kept.

Modification 5: Process to update G: At each iteration, copy all to G where dominated solutions are removed.

Modification 6: Process to update external non-dominated set E: at each iteration copy solutions from G to E and remove the dominated solutions from E.

Modification 7: Process to generate local and global best solution: For each particle's iteration, the Euclidean distances among solutions from the corresponding local non-dominated set and global non-dominated set are measured. The pair with minimum distance in the search space is selected as the local and global best for this particle in under-taking the later velocity and position updating process.

4.6. Optimization Results

The testing data set mentioned in Table 4. 1 was randomly selected from the experiment obtained from July 6th to August 4th, 2011. The optimization algorithm is applied to find the most suitable values of supply air static pressure and discharge air temperature set points for energy savings. Since the optimization problem is bi-objective, the final optimal solution is selected from the elite set based on the weighted normalized objective function presented in equation 12.

$$Obj = w_1 \frac{Obj1 - Obj1_{min}}{Obj1_{max} - Obj1_{min}} + w_2 \frac{Obj2 - Obj2_{min}}{Obj2_{max} - Obj2_{min}}$$

(12)

Where w_1 and w_2 are the user-defined weights indicating the preference of the corresponding objective, and $Obj1_{max}$ and $Obj1_{min}$ are the maximum and the minimum values of $Obj1$ in the final elite set. Similar notation is used for $Obj2_{max}$ and $Obj2_{min}$. Note that $w_1 + w_2 = 1$, with w_1 and w_2 being either constants or functions of other objectives.

Table 4.8 presents three scenarios that represent different preferences to the objectives.

Table 4.8 Three scenarios involving different weight values

Scenario	Weights	Description
1	$w_1 = 1, w_2 = 0$	No room temperature constraints when select elite set
2	$w_1 = 0, w_2 = 1$	Consider room temperature constraints when select elite set
3	$w_1 = \begin{cases} 1 & if \ y_2 \in [68,72] \\ 0.5 & otherwise \end{cases}, w_2 = \begin{cases} 0 & if \ y_2 \in [68,72] \\ 0.5 & otherwise \end{cases}$	Consider indoor room temperature as constraint when select elite set

Table 4.9 shows the optimized set points over the testing data set in three different scenarios.

Table 4.9 Optimized set points for three scenarios

Scenario	Supply air duct static pressure (in. WG)	Discharge air temperature (°F)
1	1.94	65.99
2	2.37	65.99
3	2.24	65.99

Figures 4.4 and 4.5 show the total cost and energy savings for the three scenarios, as well as a comparison against the observed value.
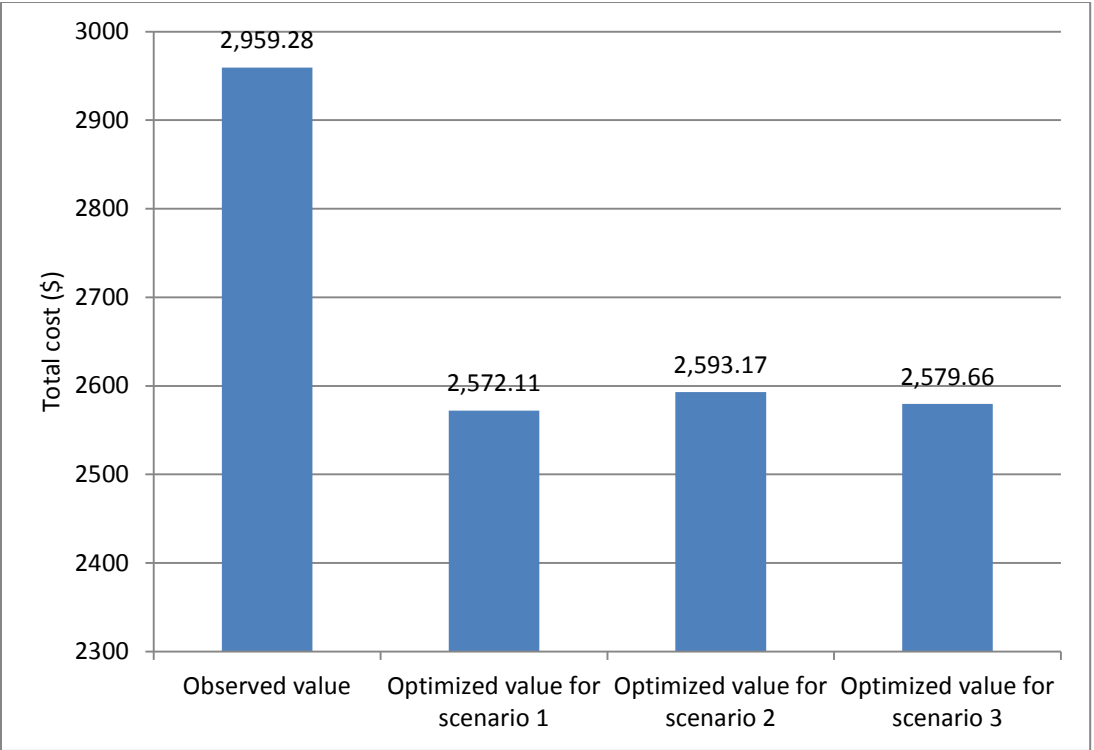
Figure 4.4 Observed vs. optimized total cost in the three scenarios
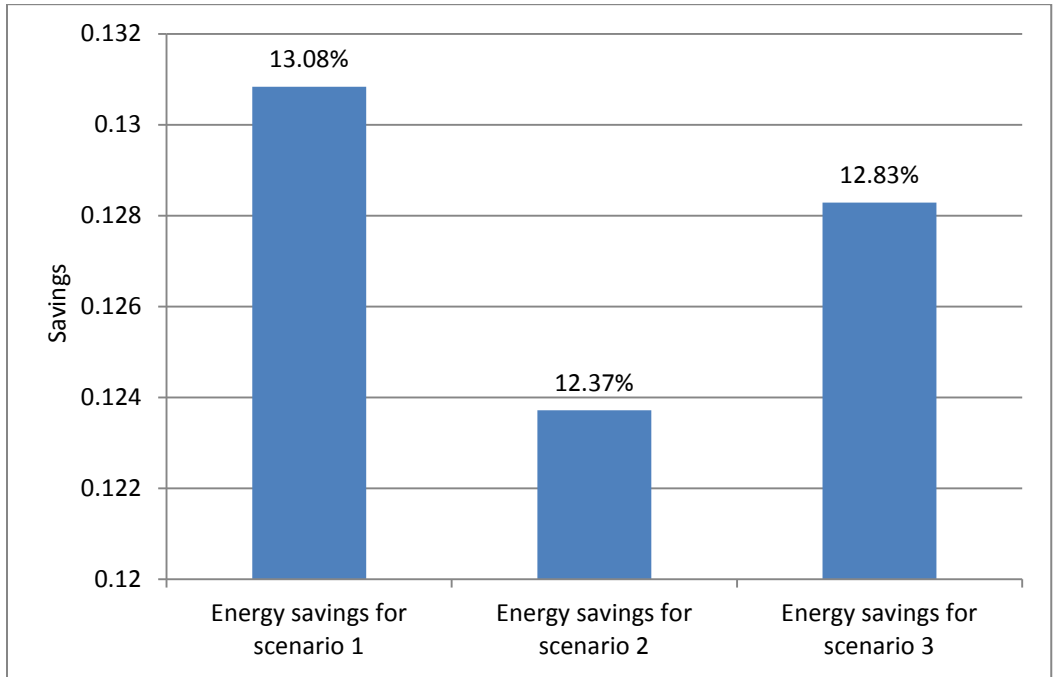
Figure 4.5 Energy savings in three scenarios

4.7. Summary

The data set obtained from the experiment run from July 6th to August 4th, 2011 was pre-processed and the parameters were selected and ranked using a boosting tree algorithm and a wrapper. The predictive models were trained and tested using a multi-layer perceptron algorithm. The accuracy of these models was corroborated versus the observed model. It was proved that their error percentage is within +/- four percent.

The predictive models were converted into a bi-objective model and later optimized. After a series of runs, the optimized set points were obtained to minimize building HVAC energy consumption by maximizing its efficiency during the summer season. Different control strategies are given by weighting the objective functions to satisfy the preference on management operations. The energy usage and indoor space temperature required for actual operations were predicted and optimized. The energy savings obtained from the optimized model will be validated using eQUEST.

CHAPTER 5

IMPLEMENTATION AND VALIDATION ANALYSIS

5.1. Introduction

With emphasis on efficient energy management of the existing building components, a building simulation tool is useful for and in-depth investigation and validation, particularly for complex projects. The use of a hybrid model allows the enhancement of building simulation and optimization algorithm capabilities and validation. This approach, able to handle discrete, non-linear and highly constrained building' parameters, provides optimum settings with potential savings. For this research eQUEST and the traditional PSO technique coupling are used for that purposed.

The building simulation baseline built in Chapter 3 accounts for all the different aspects of the building including envelope, lighting and HVAC systems. Therefore, as HVAC systems accounts for most of the energy consumed in a facility [46], the optimization and implementation analysis focuses on it.

5.2. Parametric Runs Using Optimized Set Points

The ultimate objective of this approach is to maintain occupants indoor thermal comfort and at the same time save energy. This maximization of the indoor thermal comfort is done by establishing a heat balance between occupants and their environment. Since the body can exchange heat energy with its environment by conduction, convection and radiation, it is necessary to look at the factors which affect these heat transfer processes along with the body's ability to cool itself by the evaporation of perspiration.

In addition to the air temperature, humidity air motion and the surface temperature of the surroundings, all have significant influence on the rate at which the human body can dissipate heat [8]. In general terms, thermal comfort can be achieved at air temperatures between 68 °F and 80°F, and relative humidity between 20% and 70% under variable air velocities and radiant surface temperatures.

Optimized set points and their results from the optimization model and eQUEST are presented in table 5.1. The test period for this first run was July 6th to August 1st, 2011.

Table 5.1 PSO vs. eQUEST energy savings July 6th to August 1st

Optimized Set Points					Energy Savings	
Discharge Air Temperature (°F)	Supply Fan Static Pressure (w.in)	Actual	Run	Diff	eQUEST	PSO
65.99	4.688	12,864.10	10,951.18	1,912.92	15%	13.08%

A small difference in energy savings is observed between both models, where eQUEST presents the highest saving by two percent. The accuracy of the optimized model is validated as well as the importance of the parameters selected for it creation.

The same optimized set points are applied for the summer season using eQUEST and compared with the original optimized model. Higher energy savings are observed as shown in table 5.2.

Table 5.2 PSO testing period vs. eQUEST summer season savings

Optimized Set Points					Energy Savings	
Discharge Air Temperature (°F)	Supply Fan Static Pressure (w.in)	Actual	Run	Diff	eQUEST	PSO
65.99	4.688	35,795.34	29,349.73	6,445.61	18%	13.08%

Based on the result obtained, the initial time period used for the optimization model is assumed to be representative of the summer season. As mentioned in previous chapters, energy savings are not allowed to be achieved sacrificing indoor thermal comfort. The next step is to take random samples of zones per floor and verify that the optimized set points keep the indoor air temperature within comfortable levels.

The building automation system (BAS) is used to obtain data for the different zones tested and for the period of time when the building simulation model is run. The BAS collects data on a 15-minutes interval period, meanwhile the simulation model runs hourly reports. In order to correlate these results the observed values from the BAS will be divided by four. The areas of higher traffic and demand are selected to perform the assessment.

5.2.1. Assessment First Floor

First floor is conformed mainly by three main classrooms on the east side and a main lobby on the West which is the point of reunion and transition inside the building. This area is heavily occupied by University students, staff and visitors that come to the facility.

For this assessment the main lobby was selected due to its heavy use, as well as its location. On the west, this area has a big glass wall (curtain wall) that allows the sun rays to penetrate and add heat into the space. This situation, in addition to its heavy use makes this area a perfect target for hot spots and uncomfortable indoor temperature parameters if the proper optimization set points are not selected properly. Figure 5.1 presents peak indoor temperatures which oscillate between 75 °F and 85 °F. The number of summer hours that this space is observed to be between 80 °F and 85 °F is 5 hours.
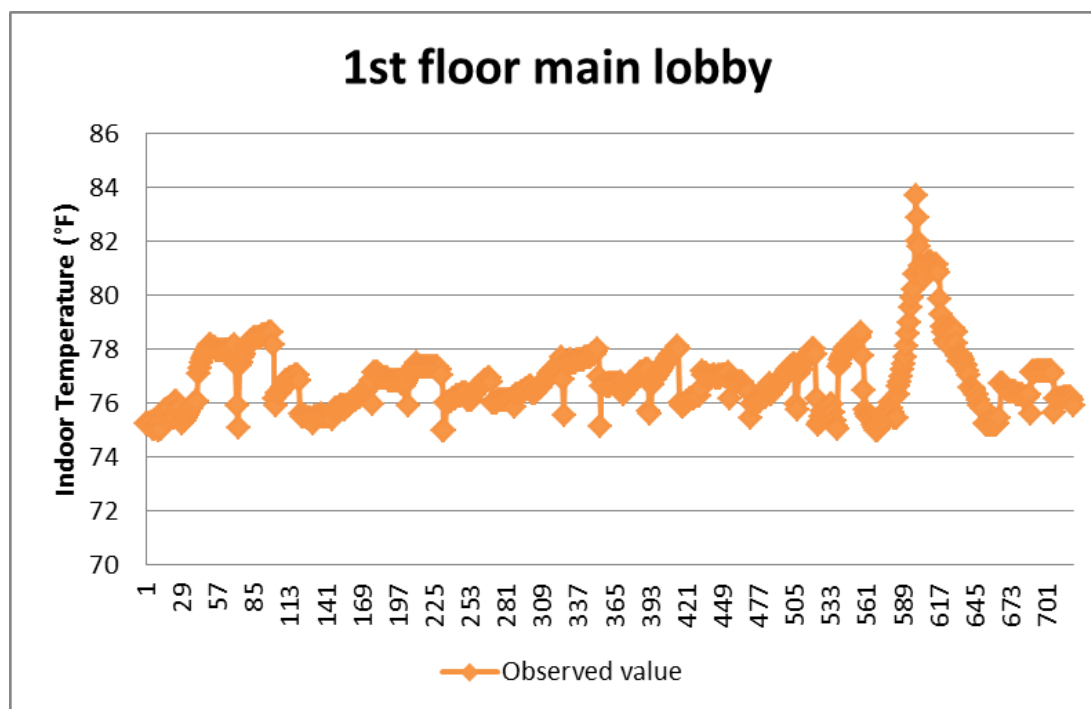
Figure 5.1 Observed indoor temperatures – main lobby

Figure 5.2 presents the results from the building simulation, where the model predicts four hours of summer with indoor air temperatures between 80 °F and 85 °F.

```
                              TOTAL HOURS AT TEMPERATURE LEVEL AND TIME OF DAY

          HOUR    1AM  2    3    4    5    6    7    8    9   10   11   12   1PM  2    3    4    5    6    7    8    9   10   11   12   TOTAL
          ---  --- --- --- --- --- --- --- --- --- --- --- --- --- --- --- --- --- --- --- --- --- --- --- ---   -----

ABOVE 85     0    0    0    0    0    0    0    0    0    0    0    0    0    0    0    0    0    0    0    0    0    0    0    0       0

80-85        0    0    0    0    0    0    0    0    0    0    0    0    0    0    0    0    2    2    0    0    0    0    0    0       4

75-80        0    0    0    0    0    0    0    0    0    0    0    0    0    0   14   28   35   22    9    0    0    0    0    0     108

70-75        0    0    0    0    0   49   49   49   49   49   49   49   49   55   46   32   21   35   45   50   49   49   49    0     823

65-70        1    1    2    2    1    1    2    7   11   12   13   14   14    8    3    2    4    2    2    1    2    3    4    2     114

60-65        2    3    4    5    7    9   11    7    4    3    2    1    1    1    1    1    0    0    0    2    2    3    4    3      76

BELOW 60     0    0    0    0    0    0    0    0    0    0    0    0    0    0    0    0    0    0    0    0    0    0    0    0       0

          === === === === === === === === === === === === === === === === === === === === === === === ===   =====
```

Figure 5.2 Simulation baseline indoor temperatures – main lobby

Figure 5.3 presents results from the optimized set points implemented into the simulation model. It is observed that the number of hours within the observed ranges increased and did not exceed these values.

```
                      TOTAL HOURS AT TEMPERATURE LEVEL AND TIME OF DAY

          HOUR    1AM  2   3   4   5   6   7   8   9  10  11  12  1PM  2   3   4   5   6   7   8   9  10  11  12   TOTAL
                  ---  --- --- --- --- --- --- --- --- --- --- --- --- --- --- --- --- --- --- --- --- --- --- ---  -----
ABOVE 85            0   0   0   0   0   0   0   0   0   0   0   0   0   0   0   0   0   0   0   0   0   0   0   0     0

80-85               0   0   0   0   0   0   0   0   0   0   0   0   0   0   8  17  26  16   7   0   0   0   0   0    74

75-80               0   0   0   0   0   0   0   0   0   2   6   6  10  27  33  27  16  21  21  17  10   2   1   0   199

70-75               0   0   0   1   1  44  44  50  58  55  51  54  48  31  16  12  14  17  20  26  29  33  39   0   643

65-70               0   0   0   0   0   1   2   2   3   2   1   1   1   1   1   1   0   0   0   0   0   0   0   0    16

60-65               0   0   0   0   0   0   0   0   0   0   0   0   0   0   0   0   0   0   0   0   0   0   0   0     0

BELOW 60            0   0   0   0   0   0   0   0   0   0   0   0   0   0   0   0   0   0   0   0   0   0   0   0     0

                  === === === === === === === === === === === === === === === === === === === === === === === ===  =====
```

Figure 5.3 Simulation optimized indoor temperatures – main lobby

Table 5.3 presents a summary of the summer peak indoor temperature hours. The values from the observed and simulation models are campared against the optimized results.

Table 5.3 Main lobby indoor temperature summary

Main Lobby (Summer 2160hrs)			
Indoor Temperature	BAS	Simulation	Optimized
80 °F - 85 °F	5hrs	4hrs	68hrs
75 °F - 80 °F	170hrs	108hrs	188hrs
70 °F - 75 °F			

Indoor temperatures using optimized set points did not violate existing observed conditions, however they increased the amount of hours and temperatures the space will be around 80 °F and 85 °F. The amount of hours the indoor temperature for the optimized model will be around these values represent three percent of the total summer hours.

5.2.2. Assessment Second Floor

On the second floor classroom 214 was selected to perform the analysis. This space is heavily used during week days, figure 5.4 presents peak indoor temperatures

between 70 °F and 75 °F. The total summer hours that the space is maintained within these temperatures are 1458 hours.
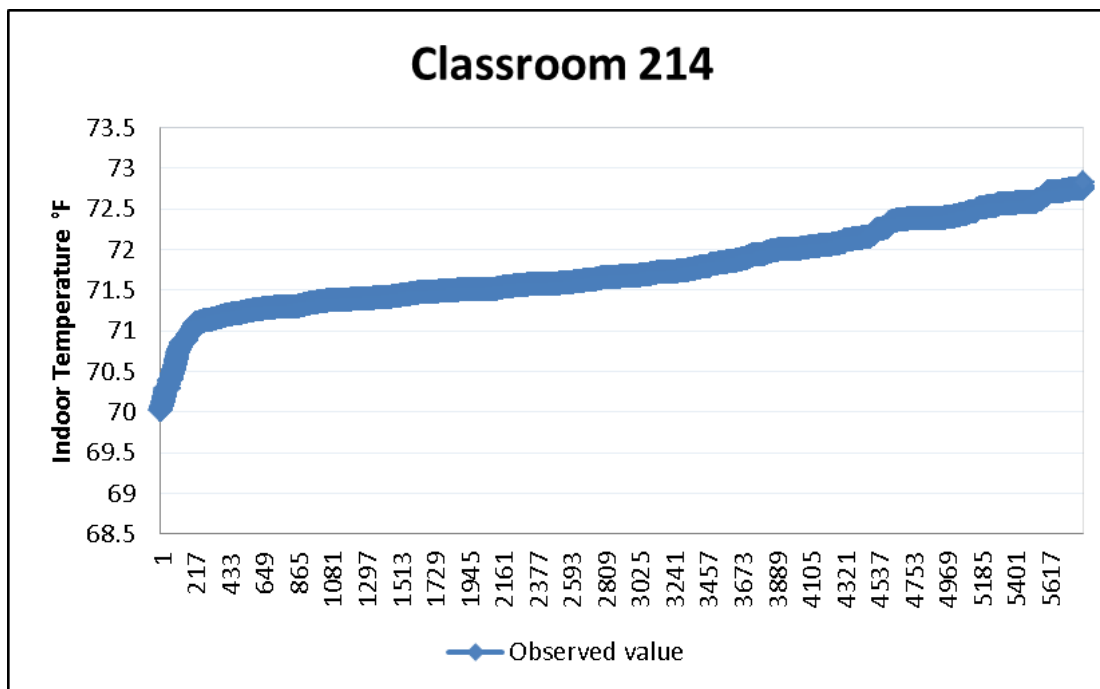
Figure 5.4 Observed indoor temperatures – classroom 214

Baseline simulation results show 882 hours of indoor temperature between 70 °F and 75 °F. The results from the simulation model are presented in figure 5.5.

```
                        TOTAL HOURS AT TEMPERATURE LEVEL AND TIME OF DAY

          HOUR   1AM  2   3   4   5   6   7   8   9  10  11  12  1PM  2   3   4   5   6   7   8   9  10  11  12   TOTAL
                 ---  --- --- --- --- --- --- --- --- --- --- --- --- --- --- --- --- --- --- --- --- --- --- ---  -----

ABOVE 85          0   0   0   0   0   0   0   0   0   0   0   0   0   0   0   0   0   0   0   0   0   0   0   0     0

80-85             0   0   0   0   0   0   0   0   0   0   0   0   0   0   0   0   0   0   0   0   0   0   0   0     0

75-80             0   0   0   0   0   0   0   0   0   0   0   0   0   0   0   0   0   0   0   0   0   0   0   0     0

70-75             0   0   0   0   0  49  49  49  49  49  49  49  49  49  49  49  49  49  49  49  49  49  49   0    882

65-70             0   0   3   3   2   2   3   5   9   9   9   6   2   2   2   2   1   1   0   0   0   0   0   1     62

60-65            12  12   9   9  10  11  12  10   6   6   6   9  13  13  13  13  14  14  15  15  15  15  14  11    277

BELOW 60          0   0   0   0   0   0   0   0   0   0   0   0   0   0   0   0   0   0   0   0   0   0   0   0     0

                 === === === === === === === === === === === === === === === === === === === === === === === ===  =====
```

Figure 5.5 Simulation baseline indoor temperatures – classroom 214

In figure 5.6 the results from the implemented optimized set points is presented. The indoor temperature values increased to temperatures between 75 °F and 80 °F.

```
                         TOTAL HOURS AT TEMPERATURE LEVEL AND TIME OF DAY

          HOUR    1AM 2   3   4   5   6   7   8   9  10  11  12   1PM 2   3   4   5   6   7   8   9  10  11  12   TOTAL
                  --- --- --- --- --- --- --- --- --- --- --- ---  --- --- --- --- --- --- --- --- --- --- --- ---  -----

ABOVE 85           0   0   0   0   0   0   0   0   0   0   0   0    0   0   0   0   0   0   0   0   0   0   0   0     0

80-85              0   0   0   0   0   0   0   0   0   0   0   0    0   0   0   0   0   0   0   0   0   0   0   0     0

75-80              0   0   0   0   0   0   1   8  16  21  18  14   12  11  10   8   4   3   2   0   0   0   0   0   128

70-75              0   0   0   0   0  42  42  40  36  35  36  43   45  47  49  49  53  49  45  41  43  44  47   0   786

65-70              2   2   2   1   2   3   3   2   4   4   5   4    5   5   4   5   5   5   5   3   2   3   4   3    83

60-65              0   0   0   0   0   0   0   0   0   0   0   0    0   0   0   0   0   0   0   0   0   0   0   0     0

BELOW 60           0   0   0   0   0   0   0   0   0   0   0   0    0   0   0   0   0   0   0   0   0   0   0   0     0

                  === === === === === === === === === === === ===  === === === === === === === === === === === ===  =====
```

Figure 5.6 Simulation optimized indoor temperatures – classroom 234

Table 5.4 presents a summary of the summer peak indoor temperature hours. The values from the observed and simulation models are campared against the optimized results.

Table 5.4 Classroom 214 indoor temperature summary

Classroom 214 (Summer 2160hrs)			
Indoor Temperature	BAS	Simulation	Optimized
80 °F - 85 °F			
75 °F - 80 °F			128hrs
70 °F - 75 °F	1458hrs	882hrs	786hrs

Indoor temperatures using optimized set points increased to 75 °F and 80 °F. The new values increased in temperature, however they did not violate comfort levels. The amount of hours the indoor temperature for the optimized model will be around these values represent six percent of summer time.

5.2.3. Assessment Third Floor

On the third floor a study room-301 on the west side and a computer room-318 on the east side were selected to perform the assessment. Third floor is a heavily used area and connects to the dormitories. Its hours of operation are extensive and occupants comfort is a must.

The effects of the glass west wall into the space temperature were observed and figure 5.7 presents the observed temperature peak values between 75 °F and 80 °F, which result in 104 hours of the summer.

Figure 5.7 Observed indoor temperatures – study room 301

Baseline simulation results show lower hours of indoor temperature between 75 °F and 80 °F with a total of 92, however, the model presents 1 hour of the summer between temperatures of 80 °F and 85 °F as shown in figure 5.8.

```
                    TOTAL HOURS AT TEMPERATURE LEVEL AND TIME OF DAY

         HOUR   1AM 2   3   4   5   6   7   8   9  10  11  12   1PM 2   3   4   5   6   7   8   9  10  11  12   TOTAL
                --- --- --- --- --- --- --- --- --- --- --- ---  --- --- --- --- --- --- --- --- --- --- --- ---  -----

ABOVE 85         0   0   0   0   0   0   0   0   0   0   0   0    0   0   0   0   0   0   0   0   0   0   0   0     0

80-85            0   0   0   0   0   0   0   0   0   0   0   0    0   0   0   0   0   0   1   0   0   0   0   0     1

75-80            0   0   0   0   0   0   0   0   0   0   0   0    0   0   0   4  19  30  24  12   3   0   0   0    92

70-75            0   0   0   0   0  49  49  49  49  49  49  49   49  49  52  39  29  35  43  50  50  49  49   1   838

65-70           12  11   9   7   6   3   2   2   4   7  10  11   13  14   6   3   4   2   2   1   2   9   9  10   159

60-65            2   4   6   8   9  12  13  13  11   8   5   4    2   1   1   1   0   0   0   1   2   2   4   3   112
```

Figure 5.8 Simulation baseline indoor temperatures – study room 301

Figure 5.9 presents results from the optimized set points implemented into the simulation model. The existing indoor temperature values are exceed and indoor comfort temperature is violeted adding a total of 81 hours between 80 °F and 85 °F.

.
```
                    TOTAL HOURS AT TEMPERATURE LEVEL AND TIME OF DAY

         HOUR   1AM 2   3   4   5   6   7   8   9  10  11  12   1PM 2   3   4   5   6   7   8   9  10  11  12   TOTAL
                --- --- --- --- --- --- --- --- --- --- --- ---  --- --- --- --- --- --- --- --- --- --- --- ---  -----

ABOVE 85         0   0   0   0   0   0   0   0   0   0   0   0    0   0   0   0   0   0   0   0   0   0   0   0     0

80-85            0   0   0   0   0   0   0   0   0   0   0   0    0   0   1  12  27  25  14   2   0   0   0   0    81

75-80            0   0   0   0   0   0   0   0   0   2   5   6   12  28  41  36  23  24  29  27  16   7   8   0   264

70-75            1   3   3   2   1  50  50  50  50  48  46  49   47  30  17  13  10  10  12  19  22  30  38   0   601

65-70            2   4   9  12  14  14  14  13  13  10   6   4    1   1   1   1   1   0   0   0   0   0   1   1   122

60-65            0   0   0   0   0   0   0   0   0   0   0   0    0   0   0   0   0   0   0   0   0   0   0   0     0
BELOW 60         0   0   0   0   0   0   0   0   0   0   0   0    0   0   0   0   0   0   0   0   0   0   0   0     0
```

Figure 5.9 Simulation optimized indoor temperatures – study room 301

Table 5.5 presents a summary of the summer peak indoor temperature hours. The values from the observed and simulation models are campared against the optimized results.

Table 5.5 Study room 301 indoor temperature summary

Study room 301 (Summer 2160hrs)			
Indoor Temperature	BAS	Simulation	Optimized
80 °F - 85 °F		1hr	73hrs
75 °F - 80 °F	104hrs	92hrs	255hrs

Indoor temperatures using optimized set points increased to 80 °F and 85 °F. The new values exceed observed parameters and violate comfort levels. The amount of hours the indoor temperature for the optimized model will be around these values represent three percent of summer time.

Computer room 318 represents a hot spot and as a result more cool air is required to keep the indoor temperature within comfortable levels. Computer equipment is one of the major sources of heat generation in a facility. It has been observed through the building automation system data that indoor peak temperature values range between 75 °F and 80 °F. Figure 5.10 presents the observed temperature peak values between 75 °F and 80 °F, which result in 208 hours of the summer.
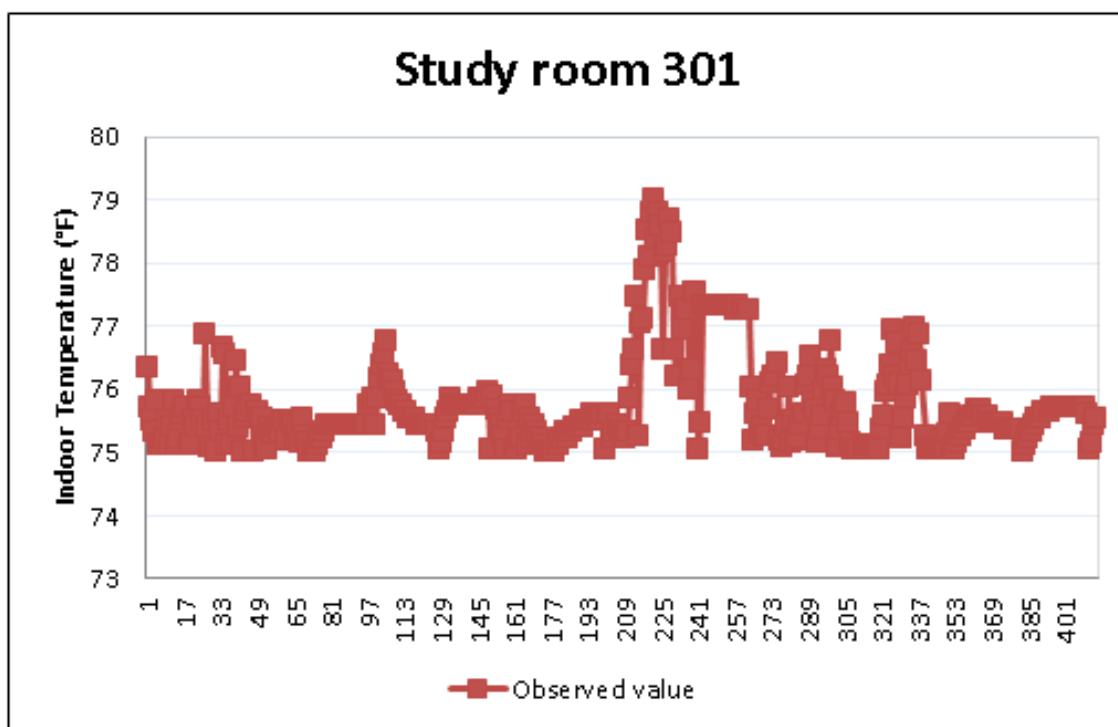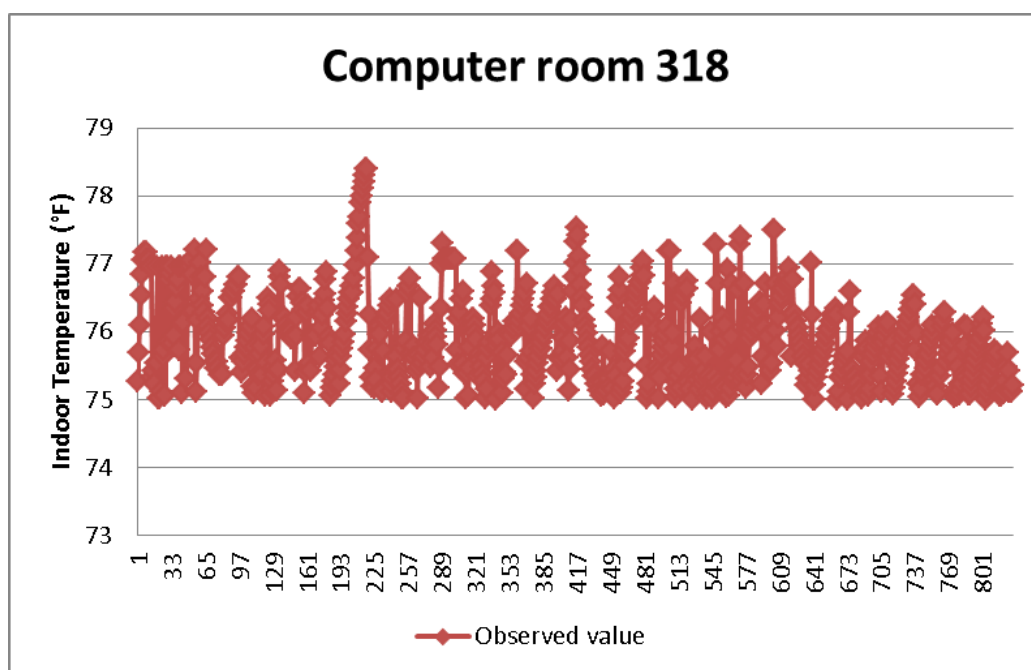

Figure 5.10 Observed indoor temperatures – computer room 318

Baseline simulation results present lower hours of indoor temperature between 75 °F and 80 °F with a total of 45 hours as shown in figure 5.11.

```
                        TOTAL HOURS AT TEMPERATURE LEVEL AND TIME OF DAY

         HOUR    1AM 2   3   4   5   6   7   8   9  10  11  12  1PM 2   3   4   5   6   7   8   9  10  11  12   TOTAL
         ---  --- --- --- --- --- --- --- --- --- --- --- --- --- --- --- --- --- --- --- --- --- --- --- ---  -----

ABOVE 85          0   0   0   0   0   0   0   0   0   0   0   0   0   0   0   0   0   0   0   0   0   0   0   0     0

80-85             0   0   0   0   0   0   0   0   0   0   0   0   0   0   0   0   0   0   0   0   0   0   0   0     0

75-80             0   0   0   0   0   0   0   0   9  12  12   6   0   0   1   1   1   1   1   1   0   0   0   0    45

70-75             0   0   0   0   0  49  49  49  40  37  37  43  49  49  47  47  47  47  48  48  49  49  49   0   833

65-70             0   0   0   0   0   0   0   1   7   9   9   6   4   0   0   0   0   0   0   0   0   0   0   0    36

60-65            14  15  15  15  15  15  15  14   8   6   6   9  11  15  15  14  15  14   8   6   5  11  13  14   288
```

Figure 5.11 Simulation baseline indoor temperatures – computer room 318

Figure 5.12 presents results from the optimized set points implemented into the
baseline simulation model. Existing indoor temperature values are exceeded and
ocuppancy comfort violetedadding a total of 102 hours between 80 °F and 85 °F.

```
                        TOTAL HOURS AT TEMPERATURE LEVEL AND TIME OF DAY

         HOUR    1AM 2   3   4   5   6   7   8   9  10  11  12  1PM 2   3   4   5   6   7   8   9  10  11  12   TOTAL
         ---  --- --- --- --- --- --- --- --- --- --- --- --- --- --- --- --- --- --- --- --- --- --- --- ---  -----

ABOVE 85          0   0   0   0   0   0   0   0   0   0   0   0   0   0   0   0   0   0   0   0   0   0   0   0     0

80-85             0   0   0   0   0   0   0   2  10  14  14  13   8   7   7   7   7   7   5   1   0   0   0   0   102

75-80             0   0   0   0   0   8  17  25  25  22  21  23  32  33  37  38  36  33  34  33  22  15  13   0   467

70-75             0   0   0   0   0  41  32  22  18  18  17  18  13  10   7   8   9   9   9  11  16  22  32   0   312

65-70             3   7  12  12  11  13  15  14  10   6   5   5   7   9   9   9   9  10   7   3   0   0   2   1   179

60-65             0   0   0   2   4   2   0   0   0   0   0   0   0   0   0   0   0   0   0   0   0   0   0   0     8

BELOW 60          0   0   0   0   0   0   0   0   0   0   0   0   0   0   0   0   0   0   0   0   0   0   0   0     0
```

Figure 5.12 Simulation optimized indoor temperatures – computer room 318

Table 5.6 presents a summary of the summer peak indoor temperature hours.
The values from the observed and simulation models are campared against the optimized
results.

Table 5.6 Computer room 318 indoor temperature summary

Computer room 318 (Summer 2160hrs)			
Indoor Temperature	BAS	Simulation	Optimized
80 °F - 85 °F			102hrs
75 °F - 80 °F	208hrs	45hrs	467hrs

Indoor temperatures using optimized set points increased to 80 °F and 85 °F. The new indoor temperature exceed observed values and violates comfort levels. The amount of hours the indoor temperature for the optimized model will be around these values represent five percent of summer time.

5.2.4. Assessment Fourth Floor

Office room 413 is a typical office room located on the west side of the building. These offices are mainly occupied for university staff part of the honors program. Figure 5.13 presents observed indoor temperature data from the space during the summer. Approximately 35 hours of the summer, temperatures oscillate between 80 °F and 85 °F.
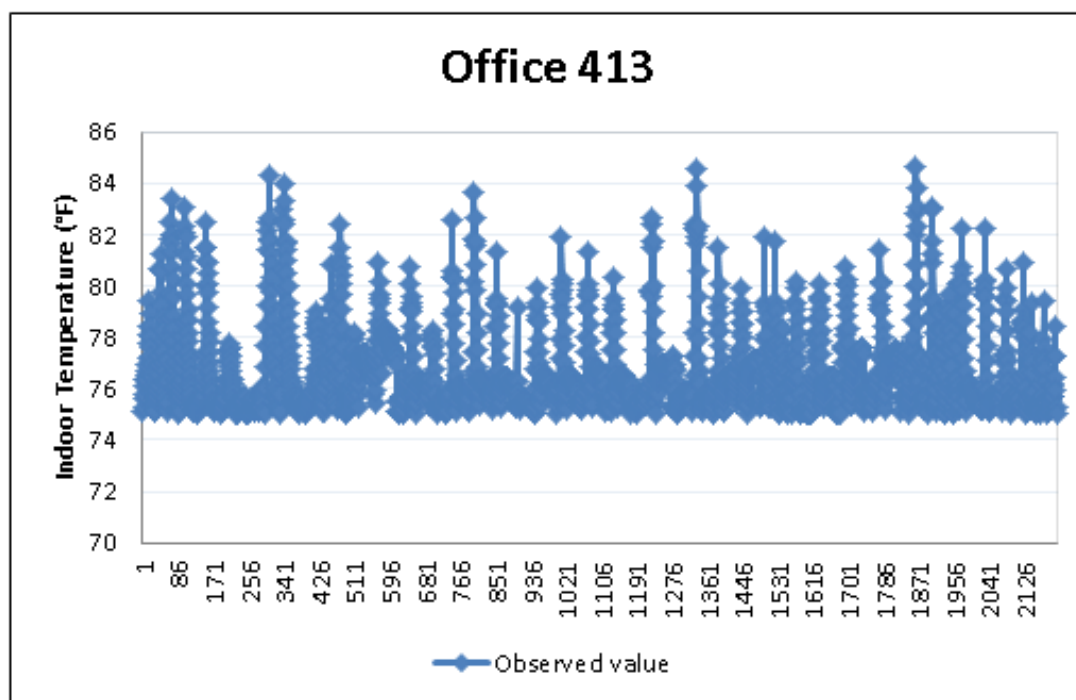
Figure 5.13 Observed indoor temperatures – office 413

Even though observed zone temperatures are above thermal comfort level, no complaints from the occupants are known that indicates otherwise [30]. Baseline

simulation results present four hours of indoor temperature above 85 °F and sixty nine hours between 80 °F and 85 °F. These temperatures doubled and exceed the range observed by the BAS. Figure 5.14 presents the results from the simulation model.

TOTAL HOURS AT TEMPERATURE LEVEL AND TIME OF DAY

HOUR	1AM	2	3	4	5	6	7	8	9	10	11	12	1PM	2	3	4	5	6	7	8	9	10	11	12	TOTAL
ABOVE 85	0	0	0	0	0	0	0	0	0	0	0	0	0	0	0	0	0	3	1	0	0	0	0	0	4
80-85	0	0	0	0	0	0	0	0	0	0	0	0	0	0	0	22	27	16	4	0	0	0	0	0	69
75-80	0	0	0	0	0	0	0	0	0	0	0	0	0	6	42	21	17	24	11	0	0	0	0	0	121
70-75	0	0	0	0	0	1	1	0	4	11	17	22	36	46	13	13	8	11	22	23	9	0	0	0	237
65-70	0	0	1	0	2	47	49	52	55	51	46	42	28	11	9	6	8	10	15	27	42	56	48	4	609
60-65	12	11	11	13	11	14	13	12	5	2	1	0	0	0	0	0	0	0	1	2	3	6	13	9	139
BELOW 60	1	2	2	2	2	0	0	0	0	0	0	0	0	0	0	0	0	0	0	0	0	0	0	1	10

Figure 5.14 Simulation baseline indoor temperatures – office 413

Figure 5.15 show results from the optimized set points implemented into the baseline simulation model. Observed indoor temperature values are violeted and extended, presenting a total of 117 hours above 85 °F.

TOTAL HOURS AT TEMPERATURE LEVEL AND TIME OF DAY

HOUR	1AM	2	3	4	5	6	7	8	9	10	11	12	1PM	2	3	4	5	6	7	8	9	10	11	12	TOTAL
ABOVE 85	0	0	0	0	0	0	0	0	0	0	0	0	0	0	7	32	41	30	7	0	0	0	0	0	117
80-85	0	0	0	0	0	0	0	0	0	0	0	0	0	16	37	15	7	15	20	6	0	0	0	0	116
75-80	0	0	0	0	0	0	0	0	4	16	22	36	44	35	12	10	9	10	16	24	17	8	2	0	265
70-75	0	0	0	1	1	30	30	27	41	29	25	12	11	5	2	1	3	2	10	12	18	21	26	0	307
65-70	2	3	4	6	5	15	10	9	3	2	1	1	0	0	0	0	0	0	1	1	4	7	12	1	87
60-65	0	0	2	2	2	0	0	0	0	0	0	0	0	0	0	0	0	0	0	0	0	0	0	0	6
BELOW 60	0	0	0	0	0	0	0	0	0	0	0	0	0	0	0	0	0	0	0	0	0	0	0	0	0

Figure 5.15 Simulation optimized indoor temperatures – office 413

Table 5.7 presents a summary of the summer peak indoor temperature hours. The values from the observed and simulation models are campared against the optimized results.

Table 5.7 Office 413 indoor temperature summary

Office 413 (Summer 2160hrs)			
Indoor Temperature	BAS	Simulation	Optimized
Above 85 °F		4hrs	117hrs
80 °F - 85 °F	35hrs	69hrs	116hrs
75 °F - 80 °F	516hrs	121hrs	265hrs

Indoor temperatures using optimized set points increased above 85 °F exceeding original values. The observed model indoor temperature violates comfort levels. The amount of hours the indoor temperature for the optimized model will be around these values represent eleven percent of summer time.

5.2.5. Assessment Fifth Floor

Fifth floor is mainly administrative offices and reception. Its hours of operation are from 8 a.m. to 4:30 p.m. during the week.
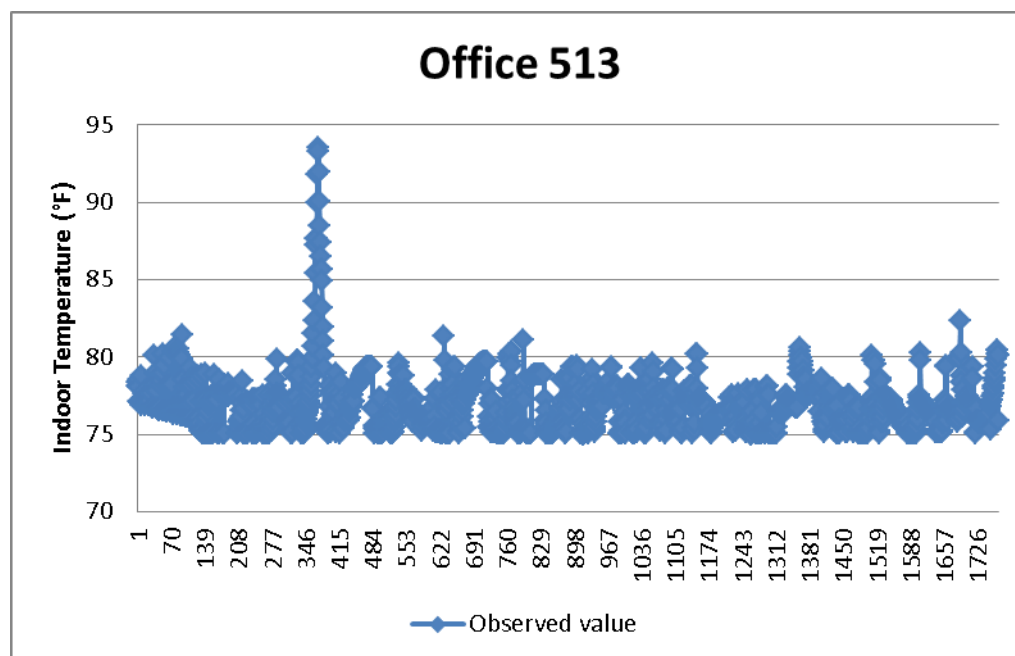
Figure 5.16 Simulation baseline indoor temperatures – office 413

Figure 5.16 presents trend from the BAS, where high indoor temperatures are observed. No complaints from tenants have been recorded even though indoor temperatures are above the standard comfortable limit. Baseline simulation results present four hours of indoor temperature above 85 °F and sixty nine hors between 80 °F and 85 °F. Temperature hours are doubled and exceed in the simulation. Figure 5.17 presents the results from the simulation model.

TOTAL HOURS AT TEMPERATURE LEVEL AND TIME OF DAY

HOUR	1AM	2	3	4	5	6	7	8	9	10	11	12	1PM	2	3	4	5	6	7	8	9	10	11	12	TOTAL
ABOVE 85	0	0	0	0	0	0	0	0	0	0	0	0	0	0	0	0	0	0	0	0	0	0	0	0	0
80-85	0	0	0	0	0	0	0	0	0	0	0	0	0	0	0	5	13	9	0	0	0	0	0	0	27
75-80	0	0	0	0	0	0	0	0	0	0	0	0	0	6	21	31	26	17	12	0	0	0	0	0	113
70-75	0	0	0	0	0	49	49	50	51	53	55	56	61	54	42	25	24	37	45	52	50	49	49	0	851
65-70	0	1	0	0	0	0	3	7	10	8	6	5	2	1	1	1	0	0	1	1	1	1	2	0	51
60-65	2	3	2	2	2	2	0	0	0	0	0	0	0	0	0	0	0	0	0	0	0	1	2	3	19
BELOW 60	0	0	0	0	0	0	0	0	0	0	0	0	0	0	0	0	0	0	0	0	0	0	0	0	0

Figure 5.17 Simulation baseline indoor temperatures – office 513

Figure 5.18 show results from the optimized set points implemented into the baseline simulation model. Observed indoor temperature values are violeted and extended, presenting a total of 117 hours above 85 °F.

.

TOTAL HOURS AT TEMPERATURE LEVEL AND TIME OF DAY

HOUR	1AM	2	3	4	5	6	7	8	9	10	11	12	1PM	2	3	4	5	6	7	8	9	10	11	12	TOTAL
ABOVE 85	0	0	0	0	0	0	0	0	0	0	0	0	0	0	0	0	6	1	0	0	0	0	0	0	7
80-85	0	0	0	0	0	0	0	0	0	0	0	0	0	1	26	37	34	25	11	0	0	0	0	0	134
75-80	0	0	0	0	0	0	0	1	3	6	8	9	14	41	26	16	13	21	15	6	0	0	0	0	179
70-75	0	0	0	0	0	35	28	28	37	36	37	39	41	12	6	6	7	9	26	34	33	33	34	0	481
65-70	0	0	0	0	0	0	0	0	0	0	0	0	0	0	0	0	0	0	0	0	0	0	0	0	0
60-65	0	0	0	0	0	0	0	0	0	0	0	0	0	0	0	0	0	0	0	0	0	0	0	0	0
BELOW 60	0	0	0	0	0	0	0	0	0	0	0	0	0	0	0	0	0	0	0	0	0	0	0	0	0

Figure 5.18 Simulation optimized indoor temperatures – office 513

82

Table 5.8 presents a summary of the summer peak indoor temperature hours. The values from the observed and simulation models are campared against the optimized results.

Table 5.8 Office 513 indoor temperature summary

Office 513 (Summer 2160hrs)			
Indoor Temperature	BAS	Simulation	Optimized
Above 85 °F	4hrs		7hrs
80 °F - 85 °F	9hrs	27hrs	134hrs
75 °F - 80 °F	431hrs	113hrs	179hrs

Indoor temperatures using optimized set points exceeded 85 °F. Both simulated and optimized models violate indoor temperature comfort levels. The amount of hours the indoor temperature for the optimized model will be around these values represent seven percent of summer time.

Reception 520 is the area where visitors and university community come for information about the honors program. Because of its high exposure to the public and heavy use, indoor temperature requirements are a mandatory to create a pleasant environment to whoever frequents this area.

Figure 5.19 presents the trend from the BAS, where indoor temperatures are shown. These values are located at the upper limit of the comfortable threshold and humidity levels are maintained to avoid complaints from the occupants due unpleasant indoor temperature conditions. Human heat is a big factor taken into consideration for the cooling of this space. Computational equipment and other devices that generate heat are not a main issue for the space.
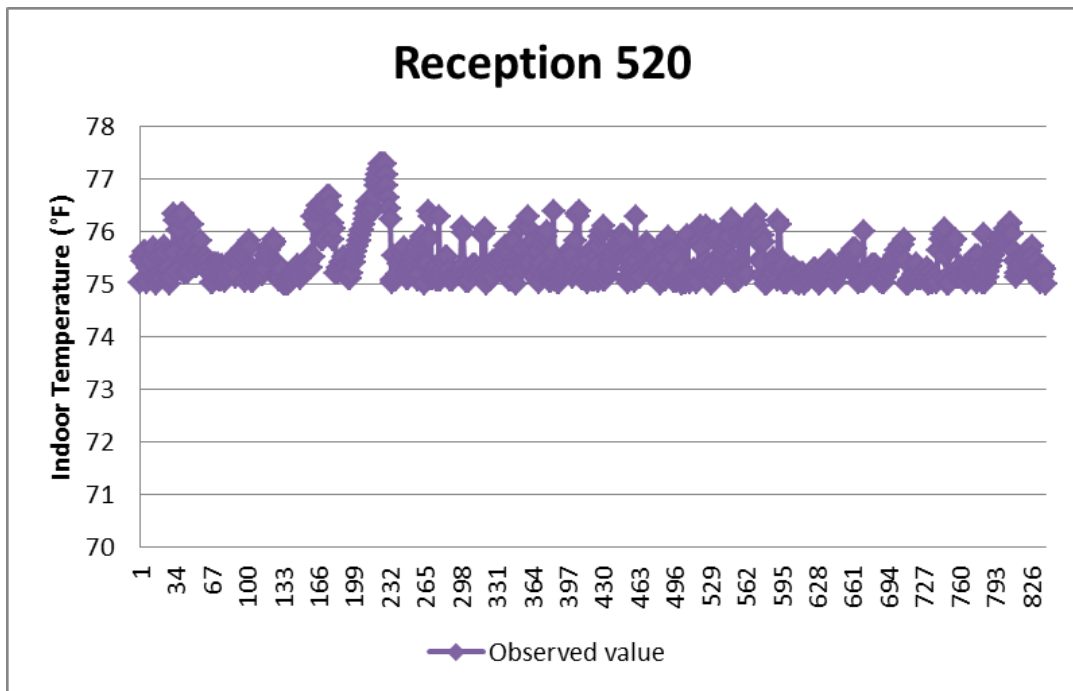
Figure 5.19 Simulation baseline indoor temperatures – reception 520

Baseline simulation results present fifty five hours of indoor temperature between 75 °F and 80 °F, this is 156 hours less than the observed model. Temperature hours are maintained within existing parameters. Figure 5.20 presents the results from the simulation model.

TOTAL HOURS AT TEMPERATURE LEVEL AND TIME OF DAY

HOUR	1AM	2	3	4	5	6	7	8	9	10	11	12	1PM	2	3	4	5	6	7	8	9	10	11	12	TOTAL
ABOVE 85	0	0	0	0	0	0	0	0	0	0	0	0	0	0	0	0	0	0	0	0	0	0	0	0	0
80-85	0	0	0	0	0	0	0	0	0	0	0	0	0	0	0	0	0	0	0	0	0	0	0	0	0
75-80	0	0	0	0	0	0	1	7	19	18	6	0	0	0	0	0	1	1	1	1	0	0	0	0	55
70-75	0	0	0	0	0	49	48	47	38	39	52	57	58	54	57	55	55	53	53	48	49	49	49	0	910
65-70	2	4	2	2	2	2	3	3	4	4	3	4	5	7	7	7	7	9	4	4	2	2	4	3	96
60-65	0	0	0	0	0	0	0	0	0	0	0	0	0	0	0	0	0	0	0	0	0	0	0	0	0
BELOW 60	0	0	0	0	0	0	0	0	0	0	0	0	0	0	0	0	0	0	0	0	0	0	0	0	0

Figure 5.20 Simulation baseline indoor temperatures – reception 520

Figure 5.21 show results from the optimized set points implemented into the baseline simulation model. Indoor temperature increased to 80 °F and 85 °F, exceeding occupant's comfortable threshold and providing thirty hours within this range.

```
                  TOTAL HOURS AT TEMPERATURE LEVEL AND TIME OF DAY
        HOUR    1AM 2   3   4   5   6   7   8   9  10  11  12  1PM 2   3   4   5   6   7   8   9  10  11  12   TOTAL
                --- --- --- --- --- --- --- --- --- --- --- --- --- --- --- --- --- --- --- --- --- --- --- ---  -----
ABOVE 85          0   0   0   0   0   0   0   0   0   0   0   0   0   0   0   0   0   0   0   0   0   0   0   0     0
80-85             0   0   0   0   0   0   0   2   9  12   7   0   0   0   0   0   0   0   0   0   0   0   0   0    30
75-80             0   0   0   0   0   1   8  16  23  21  33  41  46  48  52  53  52  51  43  28  15  10   4   0   545
70-75             0   0   0   0   0  34  20  11   8   9   5   7   9   6   6   6   8   5   9  12  18  23  30   0   226
65-70             0   0   0   0   0   0   0   0   0   0   0   0   0   0   0   0   0   0   0   0   0   0   0   0     0
60-65             0   0   0   0   0   0   0   0   0   0   0   0   0   0   0   0   0   0   0   0   0   0   0   0     0
BELOW 60          0   0   0   0   0   0   0   0   0   0   0   0   0   0   0   0   0   0   0   0   0   0   0   0     0
```

Figure 5.21 Simulation optimized indoor temperatures – reception 520

Table 5.9 presents a summary of the summer peak indoor temperature hours. The values from the observed and simulation models are campared against the optimized results.

Table 5.9 Reception 520 indoor temperature summary

Reception 520 (Summer 2160hrs)			
Indoor Temperature	BAS	Simulation	Optimized
Above 85 °F			
80 °F - 85 °F			30hrs
75 °F - 80 °F	211hrs	55hrs	545hrs

Indoor temperatures using optimized set points increased to 80 °F and 85 °F range exceeding original observed values. The optimized model indoor temperature violates comfort levels. The amount of hours the indoor temperature for the optimized model will be around these values represent one percent of summer time.

5.2.6. Assessment Sixth Floor

Office 647 is located on the southeast corner of the facility. It is a typical office space occupied for university staff that is part of the honors program.

Figure 5.22 presents observed data from this space during the summer season. Indoor peak temperatures observed from the BAS are above 85 °F. It represents four hours of the summer time and ninety eight hours between 80 °F and 85 °F.

Figure 5.22 Observed indoor temperatures – office 647
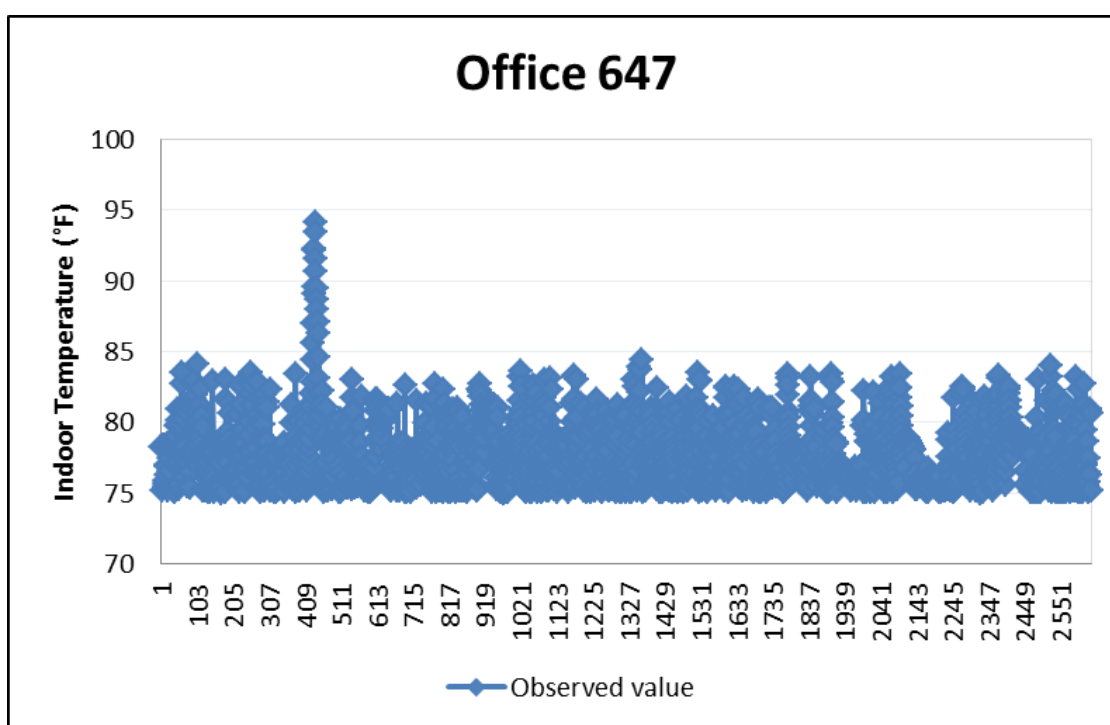
It is observed once again that an office space presents high indoor temperature values beyond occupancy comfort. No complaints from tenants have been recorded [30] indicating that this parameters are the cause of any discomfort in the area.

Baseline simulation results present lower hours of indoor temperatures above 85 °F and between 80 °F and 85 °F as shown in figure 5.23.

TOTAL HOURS AT TEMPERATURE LEVEL AND TIME OF DAY

HOUR	1AM	2	3	4	5	6	7	8	9	10	11	12	1PM	2	3	4	5	6	7	8	9	10	11	12	TOTAL
ABOVE 85	0	0	0	0	0	0	0	0	0	0	0	0	0	0	0	0	0	1	0	0	0	0	0	0	1
80-85	0	0	0	0	0	0	0	0	0	0	0	0	0	0	0	3	18	16	4	0	0	0	0	0	41
75-80	0	0	0	0	0	0	0	0	0	0	0	0	1	3	21	34	25	16	14	6	1	0	0	0	121
70-75	0	0	0	0	0	49	49	50	51	51	51	55	58	57	41	23	20	30	38	45	47	47	49	0	811
65-70	0	0	0	0	0	3	3	8	10	10	10	6	3	1	1	1	0	0	0	0	0	0	1	0	57
60-65	1	1	1	1	1	2	4	1	0	0	0	0	0	0	0	0	0	0	0	0	0	0	0	1	13
BELOW 60	0	0	0	0	0	0	0	0	0	0	0	0	0	0	0	0	0	0	0	0	0	0	0	0	0

Figure 5.23 Simulation baseline indoor temperatures – office 647

Figure 5.24 presents results from the optimized set points implemented into the baseline simulation model. Existing indoor temperature values, are not violated after implementaton, presenting a total of sixteen hours above 85 °F. This amount of hours is less than the observed ones within this range.

.

TOTAL HOURS AT TEMPERATURE LEVEL AND TIME OF DAY

HOUR	1AM	2	3	4	5	6	7	8	9	10	11	12	1PM	2	3	4	5	6	7	8	9	10	11	12	TOTAL
ABOVE 85	0	0	0	0	0	0	0	0	0	0	0	0	0	0	0	0	10	6	0	0	0	0	0	0	16
80-85	0	0	0	0	0	0	0	0	0	0	0	0	0	1	22	36	34	29	20	1	0	0	0	0	143
75-80	0	0	0	0	0	0	0	1	1	2	4	7	12	41	31	17	9	15	20	18	8	2	0	0	188
70-75	0	0	0	0	0	44	43	42	48	45	44	43	43	14	6	6	8	8	16	26	26	31	33	0	526
65-70	0	0	0	0	0	0	1	1	1	0	0	0	0	0	0	0	0	0	0	0	0	0	0	0	3
60-65	0	0	0	0	0	0	0	0	0	0	0	0	0	0	0	0	0	0	0	0	0	0	0	0	0
BELOW 60	0	0	0	0	0	0	0	0	0	0	0	0	0	0	0	0	0	0	0	0	0	0	0	0	0

Figure 5.24 Simulation optimized indoor temperatures – office 647

Table 5.10 presents a summary of the summer peak indoor temperature hours.

Table 5.10 Office 647 indoor temperature summary

Office 647 (Summer 2160hrs)			
Indoor Temperature	BAS	Simulation	Optimized
Above 85 °F	4hrs	1hr	16hrs
80 °F - 85 °F	98hrs	41hrs	143hrs
75 °F - 80 °F	558hrs	121hrs	188hrs

The values from the observed and simulation models are campared against the optimized results. Indoor temperatures using optimized set points increased original observed hours, however these parameters were never violated. The amount of hours the indoor temperature for the optimized model will be around these values represent seven percent of summer time.

5.3. Summary

An assessment of the most representative areas within the facility per floor is presented. The building simulation model has proved to provide reliable energy savings and values of zone temperature within the different areas when compared to the observed information provided by the building automation system. Discrepancies in the indoor temperature hours have been observed. These differences could be attributed to the fact that the building simulation model does not account for all the real-life parameters that an occupied building presents, such as wear-and-tear, maintenance issues among others. Energy savings obtained from the optimization algorithm and the building simulation models have shown consistency being in the fifteen percent savings range for the period testing period of July 6th to August 1st, 2011. When optimized set points were applied to the summer season higher savings of about eighteen percent were observed. The level of detailed and complexity of the building simulation model helps to account for factors not included into the optimization model and that seems to be the reason of the savings difference, however data mining PSO has proven to provide reliable results for modeling and optimizing HVAC energy consumption [5, 63]. The hybrid approach gives the flexibility to verified optimized results before implementation.

CHAPTER 6

CONCLUSION

This thesis is centered on using a hybrid computational approach for modeling and optimizing the HVAC system of a fully occupied university facility. With an emphasis on efficient energy management, computational simulation is ideal to explore and push the threshold on aggressive energy savings, while maintaining indoor temperature comfort.

The framework presented in this thesis contains four major parts. The first part (Chapter 2) introduces the facility and its annual energy usage is compared to similar buildings within the Midwest. Variations and impact on annual energy consumption are observed. Summer is found to be the season where the highest energy savings can be achieved. Due to the nature of the facility, ideal system conditions are not present.

The second part (Chapter 3) is centered on the creation of the model. The building envelope, systems, occupied/unoccupied schedules are defined and inputted. Simulation results are assessed to match current seven-year average utility data. Simulation baseline is created and accuracy of the model is set below +/- five percent margin of error.

The third part (Chapter 4) is centered on applying computational intelligence to optimize the baseline model. Optimization will be applied to the summer season using a representative data set of that period from a test run from July 6th to August 1st, 2011. Parameters are selected and ranked to determine their influence on energy cost as well as indoor air temperature. Neural networks are used to develop a predictive model of the AHU. Due to the non-linearity and complexity of the models a particle swarm optimization algorithm is considered to find optimal set points to provide the highest

energy savings and at the same time will maintain observed indoor temperature. Results from the optimized model presented savings of about thirteen percent. Discharge air temperature and supply fan static pressure were the set points optimized.

The fourth part (Chapter 5) implements and verify HVAC optimized values using the baseline created on Chapter 3. When optimized set points are implemented for the testing period of July 6th to August 1st, 2011, savings from the optimized model are verified. A small discrepancy of two percent is observed between simulation and optimization models and is attributed to the level of detail and parameter accounted into the simulation.

The optimized set points are evaluated for the summer season and savings of about eighteen percent are shown. In addition, some trade-offs between indoor air temperature and energy savings are observed. Based on the information provided from the BAS, existing conditions present high indoor temperature levels already. Relative humidity is maintained within thirty and seventy percent and it seems the reason that comfort is maintained even though the indoor temperature threshold is exceeded.

The future research will involve tuning of the existing model to narrow temperature zones hours between actual and building simulation model while still achieving eighteen percent savings. Another future research will involve the development of a dynamic interface between eQUEST and the optimization algorithm, to enhance the response capabilities of the simulation model.

REFERENCES

[1]   A.I. Dounis, C. Caraiscos. "Advanced control systems engineering for energy and comfort management in a building environment" Vol. 46, chap. 15-16, 2553-2565. Renewable and Sustainable Energy Reviews, 2005.

[2]   A. Kusiak, M.Y. Li. "Cooling output optimization of an air handling unit". Applied Energy. Vol. 87, pp. 901-909, 2010.

[3]   A. Kusiak, F. Tang, Guanglin Xu. "Optimization of HVAC system with a strength multi-objective particle swarm algorithm" Applied Energy, 2011.

[4]   A. Kusiak, F. Tang, and Guanglin Xu. "Multi-objective optimization of HVAC system with an evolutionary computation algorithm". Applied Energy, 2011.

[5]   A. Kusiak, L. Mingyang, F. Tang. "Modeling and optimization of HVAC energy consumption". Applied Energy, 2010.

[6]   American Society of Heating, Refrigeration and Air-Conditioning Engineers. "ASHRAE Handbook of Fundamentals". Chapter 18:5, Atlanta, GA, 2011.

[7]   American Society of Heating, Refrigeration and Air-Conditioning Engineers. "ASHRAE Handbook: Fundamentals". Chapter 16:28, Atlanta, GA, 2011.

[8]   American Society of Heating, Refrigeration and Air-Conditioning Engineers. "ASHRAE Handbook of Applications.". Atlanta, GA, 2010.

[9]   American Society of Heating, Refrigeration and Air-Conditioning Engineers, "ASHRAE Handbook: HVAC Systems and Equipment". Atlanta, GA: American Society of Heating, Refrigeration and Air-Conditioning Engineers Inc., 2010.

[10]   A.P. Engelbrecht, "Computational Intelligence". NJ, John Wiley & Sons Inc., 2007.

[11]   Arch Tracker, "University of Iowa Blank Honors Center – Substance Architecture". 2009. http://www.archtracker.com/university-of-iowa-blank-honors-center-substance-architecture.

[12]   Association of Energy Engineers, "AEE Energy Conservation and Management". 2011. http://www.aeecenter.org/i4a/pages/index.cfm?pageid=1

[13]   Autodesk Inc., "AutoCAD". 2011. http://usa.autodesk.com/autocad/.

[14]   B.H. Gebreslassie, G. Guillen-Gosalbaz, L. Jimenez, D. Jimenez, "Design of environmentally conscious absorption cooling systems via multi-objective optimization and life cycle assessment". Applied Energy. Vol. 86, No. 9, pp. 1712–22, 2005.

[15]   B. Kilgore, "General Install Occupancy Sensors". Feasibility Study, Roseville, MN: Sebesta Blomberg, 2010.

[16]   B. Tashtoush, M. Molhim, M. Al-Rousan. "Dynamic model of an HVAC system for control analysis". Energy 2005; 30(10):1729-45.

[17]   C.M. Fonseca, P.J. Fleming "An overview of evolutionary algorithms in multi objective optimization". Evolutionary Computation 1995;3(1):1-16.

[18]   Center Scientifique et Technique du Batiment, "SIMBAD: Building and HVAC Toolbox". 1999.

[19]   C.W. Turner, S. Doty, "Energy Management Handbook". Lilburn, GA, The Fairmont Press, Inc., pp. 221-146, 2006.

[20]   D.R. Clark, "HVACSIM+ Building system and equipment simulation program reference manual". Gaithersburg, MA: Natioanal Institute of Standard Technology, 1985.

[21]   D.V. Bush, J.L. Maestas. "Effective load management planning". Journal of the Association of Energy Engineers - Energy Conservation and Management, 2003: 70-80.

[22]   D.B. Crawley, J.W. Hand, M. Kummert, B.T. Griffith. "Contrasting the capabilities of building energy performance simulation programs". U.S. Department of Energy, 2005.

[23]   D&R International, Ltd. "2010 Buildings Energy Data Book". 10-29. U.S. Department of Energy, 2011.

[24]   Energy Design Resources, "Your Guide to Energy Efficient Design Practices" 2011.http://www.energydesignresources.com/Resources/Publications/DesighBrief.aspx.

[25]   E.H. Mathews, D.C. Arndt, C.B. Piani, E. Van Heerdan. "Developing cost efficient control strategies to ensure optimal energy use and sufficient indoor comfort". Applied Energy. Vol. 66, No. 2, pp. 135–59, 2000.

[26]   F. Rosenblatt, "Principles of Neurodynamics: Perceptrons and the Theory of Brain Mechanism". Washington, DC: Spartan Press, 1969.

[27]   G.P. Henze, D.E. Kalz, S. Liu, C. Felsmann. "Experimental analysis of model-based predictive optimal control for active and passive building thermal storage inventory". Vol. 11, chap. 2, 189-214. HVAC&R Research, 2005.

[28]   G.R. Zheng, M. Zaheer-Uddin. "Optimization of thermal processes in a variable volume HVAC system". Energy 21, no. 5 (1996): 407-420.

[29]   H.L. Zhou, "Optimization of ventilation system design and operation in office environment". 44(4):651-6. Building and Environment , 2009.

[30]   H. Moss, Area Mechanic, The University of Iowa Facilities Management Building and Landscape services.

[31]   I.J. Hall, "Generation of a typical meteorological year". Proceedings of the 1978 annual meeting of AS ISES. Denver, CO, 1978.

[32]   Illuminating Engineering Society, "IES". 2011. http://www.ies.org.

[33]   Iowa Office of Energy Independence, "Technical Engineering Analysis". 2011. http://www.state.ia.us/government/governor/energy/.

[34]   J. Friedman "Stochastic gradient boosting. Statistics Department". Stanford University; 1999.

[35]   J.A. Clarke, "Energy Simulation in Building Design". UK: Butteworth-Heinemann, 2001.

[36]   Johnson Controls, "Metasys® Building Automation and Control Systems". 2011. http://www.johnsoncontrols.com/publish/us/en/products/building_efficiency/building_management/metasys.html.

[37]   J.H. Holland, "Adaptatioin in Natural and Artificial Systems". Ann Arbor, MI: University of Michigan Press, 1975.

[38]   J. Kennedy and R.C. Eberhart. "Particle swarm optimization". Proceedings of international conference on neural networks. Piscataway, NJ: IEEE, 1995. 1942-1948.

[39]   J.F. Kreider, A. Rabl, "Heating and cooling of buildings: design for efficiency". NJ, McGraw-Hill; 1994.

[40]   J.P. M.S., "Computerized Building Simulation Handbook". Marcel Dekker, 2000.

[41]   J. Wang. "Data mining: opportunities and challenges". Hershey, PA: Idea Group Pub.; 2003.

[42]   K.F. Fong, V.I. Hanby, T.T. Chow. "HVAC system optimization for energy management by evolutionary programming". Applied Energy, 2005.

[43]   L.A. Zadeh, "Outline of a new approach to the analysis of complex systems and decision processes." IEEE Transaction on Systems, Man, and Cybernetics, 1973: 28-44.

[44]   L.J. Fogel, A.J. Owens, M.J. Walsh. "Artificial Intelligence through simulated evolution". Chichester, NJ. Wiley, 1966.

[45]   L. Magnier, H. Fariborz. "Multiobjective optimization of building design using TRNSYS simulations, genetic algorithms and artificial neural network". Applied Energy, 2009.

[46]   L. Perez-lombard, J. Ortiz, C.A. Pout. "A review on buildings energy consumption information". Energy and Buildings, 2008: 40(3):394-8.

[47]   M.A. Abido "Optimal Design of Power System Stabilazers: using particle swarm optimization". IEEE Transactions on Energy Conversion 2002; 17(3):406-13.

[48]   M.A. Abido, "Two-level of non-dominated solutions approach to multi-objective particle swarm optimization". Genetic and Evolutionary Computation Conference, 2007, pp. 726-733

[49]   M. Bida, J.F. Kreider "Monthly-averaged cooling load calculations-residential and small commercial buildings". ASME, 1987.

[50]   M.E. Donnelly, "Annual Utility Rates". Historical Data, Iowa City, IA: The University of Iowa Facilities Management, Utilities and Energy Management, 2011.

[51]   M.S. Al-Homoud, "Computer-aided building energy analysis techniques". 415-440. Building and Environment 36, 2001.

[52]   McGraw-Hilll Construction. "Energy Efficiency Trends in Residential and Commercial Buildings". 10-20. U.S Department of Energy, 2010.

[53]   M. Minsky, S. Pappert. "Perceptrons: An introduction to Computational Geometry". Cambridge, MA: MIT Press, 1969.

[54]   M. Turrin, P. Von Buelow, R. Stouffs. "Design explorations of performance driven geometry in architectural design using parametric modeling and genetic algorithms". Building and Environment, 2011.

[55]   National solar radiation data base, "1991- 2005 Update: Typical Meteorological Year 3". 2011. http://rredc.nrel.gov/solar/old_data/nsrdb/1991-2005/tmy3.

[56]   N. Nassif, S. Kajl, R. Sabourin. "Evolutionary algorithms for multi-objective optimization in HVAC system control strategy". Proceedings of NAFIPS, North American Fuzzy Information Processing Society, Alberta, Canada; 2004.

[57]   N. Nassif, S. Kajl, and R. Sabourin. "Optimization of HVAC control system strategy using two-objective genetic algorithm". HVAC&R Research. Vol. 11, No. 3, pp. 459-486, Jul 2005.

[58]   P.N. Tan, M. Steinbach, V. Kumar. "Introduction to data mining". New York: Addison Wesley, 2005.

[59]   R.J. Dossat. "Principles of Refrigeration". Wiley; 1991.

[60]   R. Kohavi, G.H. John, "Wrappers for feature subset selection". Artif Intell 1997; 97 (1-2):273-324.

[61]   R. Poli, W. Langdon, N.F. McPhee, J.R. Koza. "A Field Guide to Genetic Programming". 2008.

[62]   Simulation Research Group, Lawrence Berkley National Laboratory, "Overview of DOE 2.2". 2011. http:/www.doe2.com/.

[63]   S. Wang, X. Jin, "Model-based optimal control of VAV air-conditioning system using genetic algorithm". Building and Environment. Vol. 35, No. 6, pp. 471-487, 2000.

[64]   S. Wang, Z. Ma. "Supervisory and optimal control of building HVAC systems: A review". HVAC&R Research 14 (2008): 3-32.

[65]   S. Wilcox, W. Marion. "Users Manual for TMY3 Data Sets". Golden, CO: National Renewable Energy Laboratories, 2008.

[66]   S. Karatasou, M. Santamouris, V. Geros. "Modeling and predicting building's energy use with artificial neural networks Methods and results". Energy and Buildings. Vol. 38, No. 8, pp. 949-958, 2006.

[67]   T. Hastie, R. Tibshirani, J.H. Firedman. "The elements of statistical learning". New York: Springer; 2001.

[68]   The University of Iowa Facilitites Management, "FM Connection". 2011. http://www.facilities.uiowa.edu/.

[69]   The University of Iowa Facilities Management Planning, Design and Construction. "Design Standards & Procedures". pp. 84-91, 2009.

[70]   The University of Iowa Honors Program, 2011. http://honors.uiowa.edu.

[71]   U.S Energy Information Administration. "2003 Commercial Building Energy Consumption Survey". U.S. Department of Energy, 2011.

[72]   U.S. Department of Energy. "Building Energy Software Tools Directory", 2011. http://www.eere.energy.gov/.

[73]   U.S. Department of Energy, "Overview of DOE-2". 2011. http://gundog.lbl.gov/dirsoft/d2whatis.html

[74]   U.S. Department of Energy, "ENERGY.GOV". Washingtong, DC, 2011. http://energy.gov/.

[75]   Wisconsin, University of. "TRNSYS: A transient system simulation program". Reference Manual. Vol. 1. Madison, WI: Solar Energy Laboratory, 1996.

[76]   X. Yu, J. Wen, T. F. Smith. "A model for the dynamic response of a cooling coil". Energy and Buildings, Vol. 37, chap. 12, 1278-1289. 2005.

[77]   Y. Wang, W. Cau, Y. Soh, S. Li, L. Lu, L. Xie. "A simplified modeling of cooling coils for control and optimization of HVAC systems". Applied Energy, 2004.

[78]   Y. Zhang, V.I. Hanby. "Model-based control of renewable energy systems in buildings". Vol. 12, chap. 3, 739-760. HVAC&R Research, 2006.

[79]   Y. Zhu, "Applying computer-based simulation to energy auditing: A case study". Energy and Buildings, 2005.

[80]   Z. Cumali, "Global optimization of HVAC system operations in real time". Vol. 94, chap. 1, 1729-1744. ASHRAE Transaction, 1988.